https://ntrs.nasa.gov/search.jsp?R=19690001711 2020-03-12T06:08:34+00:00Z

General Disclaimer

One or more of the Following Statements may affect this Document

- This document has been reproduced from the best copy furnished by the organizational source. It is being released in the interest of making available as much information as possible.

- This document may contain data, which exceeds the sheet parameters. It was furnished in this condition by the organizational source and is the best copy available.

- This document may contain tone-on-tone or color graphs, charts and/or pictures, which have been reproduced in black and white.

- This document is paginated as submitted by the original source.

- Portions of this document are not fully legible due to the historical nature of some of the material. However, it is the best reproduction available from the original submission.

Produced by the NASA Center for Aerospace Information (CASI)

N 69-11042
(ACCESSION NUMBER) (THRU)
160 1
(PAGES) (CODE)
CR-98028 05
(NASA CR OR TMX OR AD NUMBER) (CATEGORY)
FACILITY FORM 602

SPACE SCIENCES INCORPORATED

301 BEAR HILL ROAD, WALTHAM, MASSACHUSETTS, 02154

A WHOLLY OWNED SUBSIDIARY OF WHITTAKER CORPORATION

BIOSYSTEMS (Chicago) Division
SPACE SCIENCES INCORPORATED
Whittaker Corporation

April, 1968

FINAL REPORT

VISION DURING MANNED BOOSTER OPERATION

by: Arne Troelstra
William O'Neill
Lawrence Stark

PURCHASING OFFICE
GEORGE C. MARSHALL SPACE FLIGHT CENTER
NATIONAL AERONAUTICS AND SPACE ADMINISTRATION
CONTRACT No. NAS8-20381

FINAL REPORT

VISION DURING MANNED BOOSTER OPERATION

Section 1. Introduction

2. Basic Macroscopic Anatomy of the Accommodation Mechanism of the Human Eye

3. The Human Eye as an Optical System

4. Image Characteristics

5. Fourier Analysis of Image Formation

6. Control Aspects of the Accommodation System
   a. Definition
   b. Function
   c. Dynamics
   d. Optimization

7. Utilization of Image Errors for Accommodation Control

8. Microscopic Anatomy of the Retina

9. Accommodation System Neurological Pathways

10. Instrumentation Review of Dynamic Optometers
    a. Scheiner Methods
    b. Non-Scheiner Methods

11. Multivariable Nature of Accommodation Tracking

12. Need for Optical Status Tester

13. Mission-Oriented Applications
    a. Normal Conditions Tests
    b. Simulated and Actual In-Flight Conditions Tests

14. Clinical Applications

--. References

SECTION 1

1. INTRODUCTION

In order to obtain a basic understanding of the processes involved in keeping a clear, unblurred, image on the retina, it is necessary to deal in some detail with the anatomical and physiological properties of the human eye lens and its environment. In addition, the optics of the image formation and the neurological aspects of the image evaluation must be considered.

The process, which enables a person to change the optical power of his eye lens, is usually referred to as accommodation. It is a highly complicated interacting control system that consists of optical and mechanical transducers and partly unknown connecting neural pathways. In principle, the following events can be distinguished. Suppose an out-of-focus image of an object is formed on the retina because the power of the eyelens differs from the value necessary to make the object plane and retina conjugate. The blurred image on the retina is detected and information concerning this blur is transmitted to higher brain centers. After evaluation, a signal is transmitted back to muscles which allow the lens to change its dioptric power and to improve the focussing of the retinal image. A simplified block diagram of this feedback process is shown in Fig. 1.1. [51]

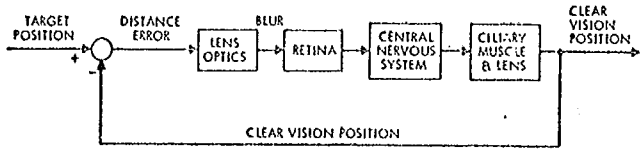

Automatic focusing system of human eye. Note geometric unity gain negative-feedback path.

Fig. 1.1

Under normal viewing conditions, the accommodative system is completely involuntary, i.e. adjustments in accommodation occur without any conscious effort or knowledge of the person himself. Its operation has the same effect as an automatic focussing device, well-known from sophisticated camera systems. In the subsequent sections, we will review the literature concerning the human eye lens and try to indicate some of the relevant characteristics of the various elements of this feedback system.

This report will present the latest available information regarding the anatomy, physiology and functional experimental procedures relative to the accommodative process of the human eye. Throughout the presentation quantitative aspects will be emphasized. In many instances this emphasis requires considerable attention be paid to past and present

methods of measuring accommodation because it was found that there does not exist a satisfactory means of measuring simultaneously and dynamically the near reflex ocular triad of accommodation, pupil diameter and convergence. The lack of such experimental equipment was not considered reason to neglect the theoretical considerations of accommodation. In particular considerable attention is given to image formation from both classical and spatial transformation viewpoints. In addition, the control-systems-theoretic analysis of the accommodative system is emphasized throughout the presentation and is culminated in a multi-variable block diagram of the system as it is thought to exist today.

Of considerable importance to experimentation is the instrument review of dynamic optometers which we feel illustrates the inadequacy of present instrumentation to fulfill the needs of a comprehensive study of accommodation and its associated systems. These needs are made explicit in a later section of the report.

The final two sections of the report outline briefly possible clinical and mission oriented applications of a proposed Optical Status Tester that we feel would fill the needs of monitoring the ocular near reflex under a wide range of environmental conditions.

SECTION 2

2. BASIC MACROSCOPIC ANATOMY OF THE ACCOMMODATION MECHANISM IN THE HUMAN EYE

A horizontal crossection of the human eye is shown in Fig. 2.1. The accommodative mechanism consists of the lens, the suspensary ligaments or zonule fibers, and the ciliary muscle. These components will be discussed in somewhat more detail in the next paragraphs

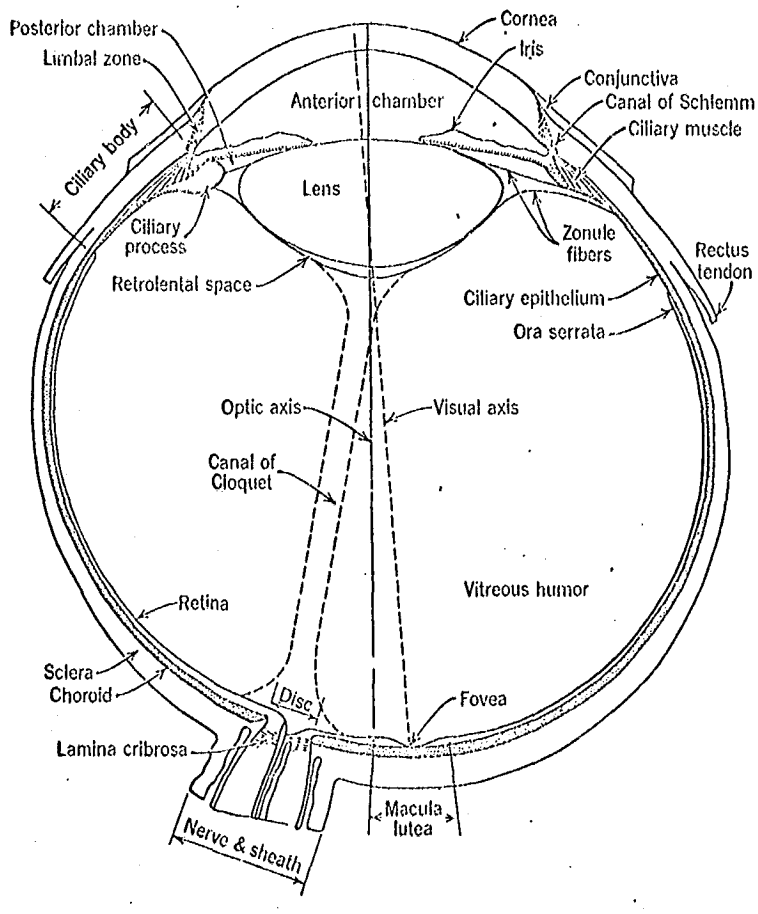

Horizontal section of the right human eye. (From Walls, 1942, as modified from Salzmann, 1912.)

Fig. 2.1

a. The Lens. The lens is a transparent structure of a biconvex shape with a rounded border or equator (Fig. 2.2).

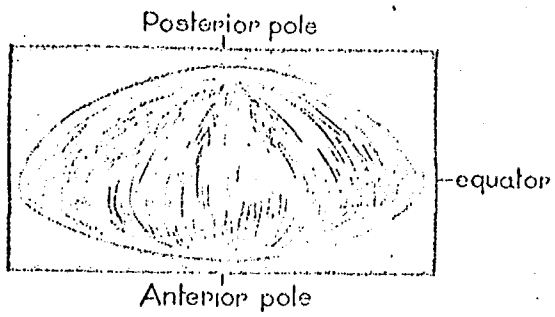

Fig. 2.2

The posterior surface is more highly curved than the anterior surface, with the curvatures culminating in the posterior and anterior poles respectively. The line between the two poles is called the axis. The lens is placed immediately behind the pupil, the iris resting on its anterior surface (Fig. 2.3).

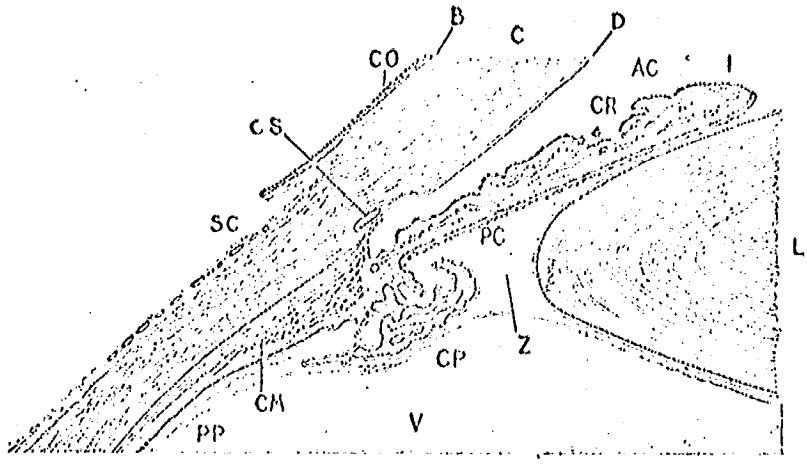

—The Region of the Angle of the Anterior Chamber.

AC.	Anterior chamber.	D.	Descemet's membrane.
B.	Bowman's membrane.	I.	Iris.
C.	Cornea.	L.	Lens.
CM.	Ciliary muscle.	PC.	Posterior chamber.
CO.	Corneal epithelium and conjunctiva.	PP.	Pars plana of ciliary body.
CP.	Ciliary processes.	SC.	Sclera.
CR.	Iris crypts.	V.	Vitreous.
CS.	Canal of Schlemm.	Z.	Zonule of Zinn.

Fig. 2.3

Its position is fairly vertical but not quite symmetrical, since its axis deviates from the visual axis by about 4° [17]. The lens is surrounded by a strong and highly elastic capsule through which it is supported from the ciliary body by the zonule fibers (suspensory ligaments). No quantitative measurements about the elasticity of the capsule have been made so far. Although seemingly structureless, the capsule is composed of two layers as can be shown by appropriate staining methods [41]. The outer of these two layers is called

the zonular lamella. In persons exposed to heat and glare the zonular lamella may become exfoliated, forming a type of opacity knowy as glass blower's cataract. The lens capsule is transparent and very resistant to pathological and chemical influences. Its thickness varies at different parts of the lens and increases gradually with increasing age. Fig 2.4 gives an idea of the relative change in thickness. The thinnest part (2 micron) is found at the posterior pole, and on both the anterior and posterior surfaces there is a circular zone of maximal thickness (23 micron) running round concentrically with the equator. These changes in thickness determine for a great part the shape of the lens.

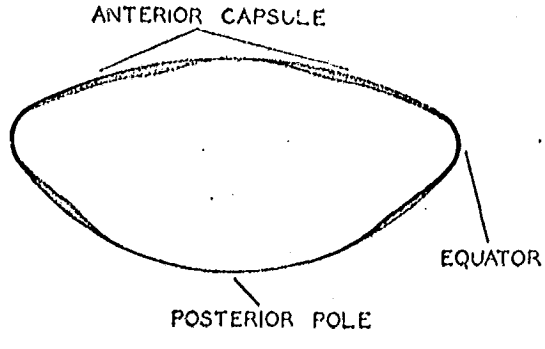

Diagram of the relative thickness of the capsule in various portions, as measured by Fincham.

Fig. 2.4

The lens epithelium extends as a single layer of cells under the anterior capsule as far as the equator. At the equator the epithelial cells develop into young lens fibers, which compose the lens substance. The lens substance is not elastic. If the lens capsule is removed, the lens will not return to its original shape after deformation by an external force. [1)]

The lens is a living structure and throughout the life of a person new fibers are constantly forming. As the formation of new fibers takes place, the older fibers are compressed and pushed in toward the center. This results in an increasing density of the lens from the surface to the center. Since the inner fibers are the older, they are more sclerosed and less translucent than the more recently formed peripheral fibers. There is no sharp boundary between the various portions of the lens but, in general, two main parts can be recognized, i.e., a dense center or nucleus, and the surrounding cortex (Fig. 2.5). [27)]

—The Structure of the Lens as shown in the Optical Beam of the Slit-lamp.

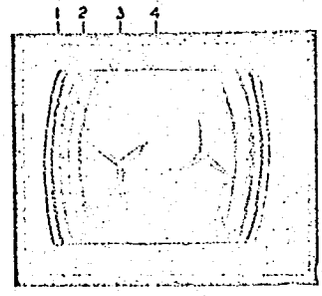

—The lens of a 3-year-old infant.

1. Anterior capsule.
2. Infantile nucleus.
3. Fœtal nucleus.
4. Embryonic nucleus.

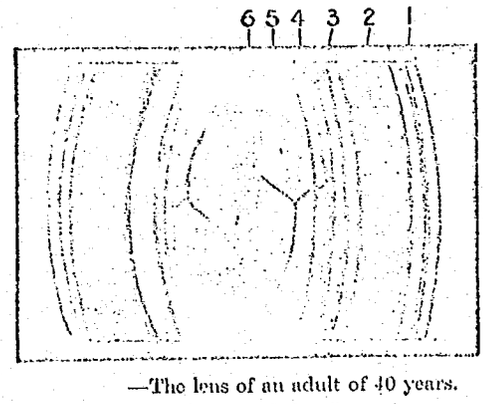

—The lens of an adult of 40 years.

1. Anterior capsule.
2. Cortex.
3. Adult nucleus.
4. Infantile nucleus.
5. Fœtal nucleus.
6. Embryonic nucleus.

The various dimensions of the lens vary considerably between different persons and with age. Table 2.1 summarizes some average values quoted by Duke-Elder.[18]

	Child	Adult
Axis	3.5-4 mm	4-4.2 mm
Equatorial Diameter	4.5-9 mm	9 mm
Radius of Curvature Anterior Surface	5 mm	10 mm
Radius of Curvature Posterior Surface	4 mm	6 mm
Weight	----	200 mg
Volume	----	200 mm^3

TABLE 2.1-- Some average values of various lens dimensions (unaccommodated eye).

b. The Zonule. The zonule fibers (suspensory ligament of the lens) stretch from a broad origin at the ciliary body to the periphery of the lens. It is essentially a series of fibers that hold the lens in position and that play an important role in the mechanism of accommodation, since the zonule forms one of the main connections between the ciliary muscle and the lens capsule. The fibres are transparent, straight for the most part, stiff in appearance and inextensible. Their caliber, which is very constant for each fiber, varies from 2 to 8μ [50], but can have much higher values in certain instances (up to 40μ). To the side of the lens each fiber

breaks up in a series of extremely fine fibrils, which become continuous with the zonular lamella. A similar process takes care of the attachment at the side of the ciliary body.

c. The Ciliary Muscle. According to Salzmann three groups of muscle fibers can be distinguished which make up the whole of the ciliary muscle--a meridional bundle, a radial portion, and a circular portion (Fig 2.6)

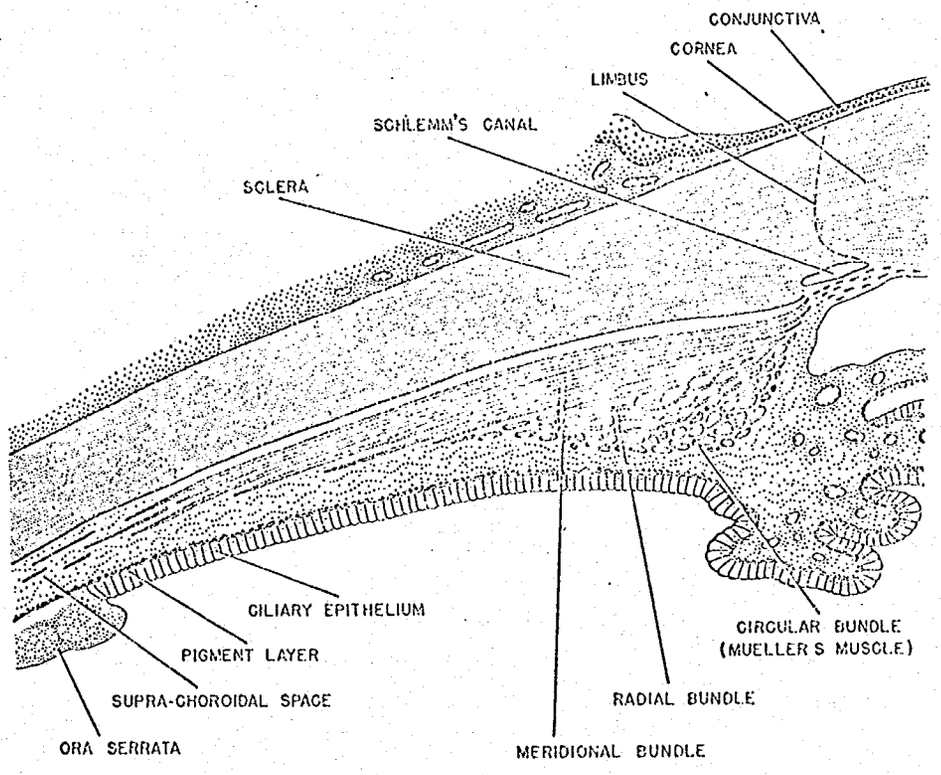

Anteroposterior section through the anterior portion of the eye. (Modified after Wolff.)

Fig. 2.6

The meridional bundle has its origin at the corneoscleral junction just in back of Schlemm's canal. It thins off posteriorly and connects with the fine trabecular which cross the suprachoroidal space. The insertion of this bundle is in the choroid coat near the posterior pole of the eye.

The fibers of the radial portion are very much intermixed with the framework of the connective tissue. This makes it difficult to determine the exact topography of the bundle as a whole, and no definite origin or insertion can be distinguished.[2)]

The circular portion (also called Muller's muscle) consists of fibers that form a circular bundle at the inner, anterior aspect of the ciliary body. They form a sphincter muscle that on constriction narrows the ring formed by the ciliary processes and on which the zonule fibers are attached. The form of the ciliary muscle as a whole depends largely on this circular portion. The circular portion is poorly developed in myopic eyes and well developed in hyperopic eyes. This suggests that this portion plays an important role in accommodation. Contraction of the circular portion of the ciliary muscle alone must result in relaxation of the Zonule (Fig. 2.7).

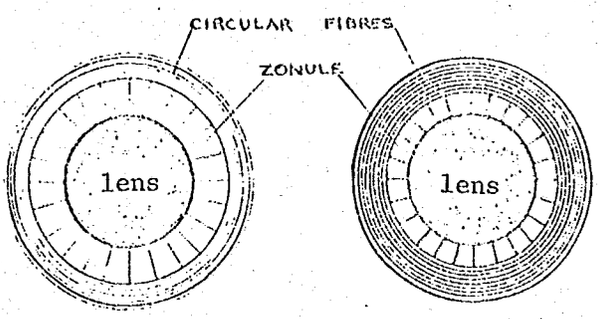

Illustrating the action of the circular fibres in relaxing the tension of the zonule

Fig. 2.7

It is still not known what the exact effect is of contraction of the meridional and radial portions of the ciliary muscle.

d. Mechanisms for Accommodation. Of the various existing theories about the mechanisms of accommodation, only one is supported by sufficient experimental evidence to make a more detailed discussion worthwhile. The relaxation theory was originally formulated by Young and Helmholtz, [31] and recently supported by Fincham. [21] It assumes that in the unaccommodated eye at rest, the lens is compressed in its capsule by a pulling force of the zonule. In this condition, the lens has its smallest curvature and, consequently, its smallest dioptric power. In the normal eye, objects at infinity will be imaged at the retina, in other words, the eye is accommodating at infinity. The zonule is not supposed to have elastic properties but is kept constantly stretched by

its attachments to the ciliary body. In Helmholtz's original theory the elasticity of the choroid was supposed to balance the tension of the zonule. In the process of accommodation, the ciliary muscle contracts and the choroid is pulled forward, releasing the tension of the zonule. Also the ring formed by the circular portion of the ciliary muscle is narrowed, releasing the tension of the zonule even more. When the lens capsule is freed from the pulling force of the zonule, as all elastic bodies it tries to take a more spherical shape, thus increasing the curvature and dioptric power of the lens. There are strong objections against the role of the choroid in sustaining the elastic traction of the lens capsule. It does not seem logical to expect the choroid, being a richly vascular network, to act as a counterweight for such a continually acting force. Therefore, Henderson [3] suggested that the traction of the zonule was achieved mainly by the radial and longitudinal (meridional) portions of the ciliary muscle. He pointed out that the non-rigid structure of the zonule and the ciliary processes follows in its course from the choroid to the lens a curve rather than a straight line. This curvature cannot exist without support, and the support must take an active part in transmitting the strain. Henderson gave anatomical evidence that the ciliary muscle supported the arch formed by the zonule and the ciliary processes. He ascribed different functions to each part of the ciliary muscle.

The longitudinal fibers act as support to the distal extremity of the zonule; the radial fibers support the zonular arch and act as a tensor zonuli; the circular fibers act as a sphincter in the generally accepted manner. Henderson was convinced that the zonule is constantly stretched by means of the longitudinal and radial fibers and that the pull on the zonule by the elasticity of the lens capsule is counterbalanced by the tone of these fibers. This seems also a much more logical function for a muscle instead as for a vascular structure such as the choroid.

The following two main functions of the ciliary muscle were thought to be mediated by different muscle bundles and innervated by different nerve supplies. The radial and longitudinal fibers maintain a constant postural activity to counterbalance the pull of the zonule. The sphincter, or circular muscle, overcomes the tension on the zonule and permits it to become slack. These ideas are in agreement with the evidence that both parasympathetic and sympathetic innervation are concerned in accommodation. Accommodation is accomplished by inhibition of the postural activity of the longitudinal fibers and by active contraction of the circular fibers (sphincter). Henderson regarded the sympathetic nerve as excitatory and the third cranial nerve as inhibitory.

Another interesting experimental finding is strong evidence for the relaxation theory. Namely, the fact that during the accommodation the lens sinks in the direction of gravity. Fincham [21] found the distance from the anterior surface of the lens to the cornea in the accommodated state to be 0.2 mm. less when the head was held forward parallel to the floor than when the head was held erect, showing the effect of gravity on the position of the lens during accommodation. No change in this distance was observable with a change in position of the head when the eye was not fully accommodated.

SECTION 3

3. THE HUMAN EYE AS AN OPTICAL SYSTEM

Before a ray of light hits the retina, it has to go through a number of media (Fig. 2.1). The optical densities of these media are different, the indices of refraction are different, and the curvature of the borderline between two successive media changes along the light path. It can be assumed that the transmission-coefficient of the various media for light in the visible part of the spectrum (400-800 mμ) is independent of the wavelength. In order to calculate the characteristics of the retinal image, it would be very convenient if the laws of geometrical optics could be applied. However, this is not simply possible because in the lens substance the index of refraction changes continuously with position. This means that the lens represents a nonhomogeneous medium, and one of the basic assumptions of geometrical optics, i.e., rectilinear propagation, is not satisfied. To get around this difficulty various investigators have constructed schematic eyes in which the lens was composed of several layers of constant index of refraction. The number of layers should be small to avoid long and complicated calculations. On the other hand, care must be taken to approximate the real role of the lens in the image formation process as closely as possible. In the following discussion we will use the schematic eye of Gullstrand.[28] Gullstrand's data are closelto reality and generally accepted in the major portion of ophtalmic literature.

a. The Schematic Eye. Some of the data from Gullstrand's schematic eye (unaccommodated) are summarized in Table 3.1. The schematic lens consists of a core lens of refractive index 1.406 surrounded by a cortex of refractive index 1.386. This situation is also found in the real lens of an adult person. The cortex consists of young fibers (lower refractive index) and the core consists of older, more compressed fibers (higher refractive index). Experimentally, the index of refraction at the center of the core lens is found to be equal to 1.406, while the index of refraction at the vertices of the crystalline lens is found to be equal to 1.386.

Medium	Refractive Index	Surface	Radii of Curvature	Axial Separation
Air	1.000	Ant. Cornea	7.7 mm	
Cornea	1.376			0.5 mm
		Post. Cornea	6.8 mm	
Aqueous humor	1.336			3.1 mm
		Ant. Lens (Cortex)	10.0 mm	
Lens (Cortex)	1.386			0.55 mm
		Ant. Lens (core)	7.91 mm	
Lens (Core)	1.406			2.42 mm
		Post. Lens (Core)	-5.76 mm	
				0.63 mm
		Post. Lens (Cortex)	-6.0 mm	
Vitreous humor	1.336			

TABLE 3.1

In the schematic eye, these values are chosen for the constant indices of refraction of the core lens and the cortex. The radii of curvature and the positions of the anterior and posterior surfaces of the core lens do not correspond to reality but are chosen to make the optical properties of the schematic

lens as close to those of the crystalline lens. However, the radii of curvature and the positions of the anterior and posterior surfaces of the cortex have the same values as found in the average adult person.

Another approximation in the schematic eye is that all the surfaces are supposed to be spherical. In reality, this holds only in the neighbourhood of the vertices, but is certainly not true for any of the surfaces as a whole. However, for paraxial rays this approximation is quite acceptable.

From the foregoing it is obvious that in characterizing the human optical system it is impossible to use a thin lens approximation. Instead, a characterization using the six cardinal points must be employed. The "thick lens" formula is

$$\frac{n'}{l'} - \frac{n}{l} = \frac{n'}{f'} = -\frac{n}{f} \qquad \text{Eq. (3.1)}$$

In Eq. (3.1) l' is the image distance measured with respect to the second principle plane (H_2) and l is the object distance measured with respect to the first principle plane (H_1). Similarly, f' is the distance of the second principle focus from the second principle plane, and f is the distance of the first principle focus from the first principle plane. n and n' are the refractive indices of object and image space respectively. Distances measured in the same direction as the light is travelling are regarded positive. The two principle planes are conjugate planes of unit transverse magnification. In the construction of the image, one often uses the concept of nodal planes. These are also conjugate

planes and their intersections with the optical axis are the nodal points. Any ray directed towards the first nodal point (N_1) leaves the system as coming from the second nodal point (N_2), and parallel with its original direction. The distance between the two principle planes is always equal to the distance between the two nodal planes. Also the distance from the first principle focus to the first principle plane equals the distance from the second principle focus to the second nodal plane.

We will now give a scheme to calculate the cardinal points of a system of co-axial surfaces separated by regions of different indices of refraction (Fig. 3.1).

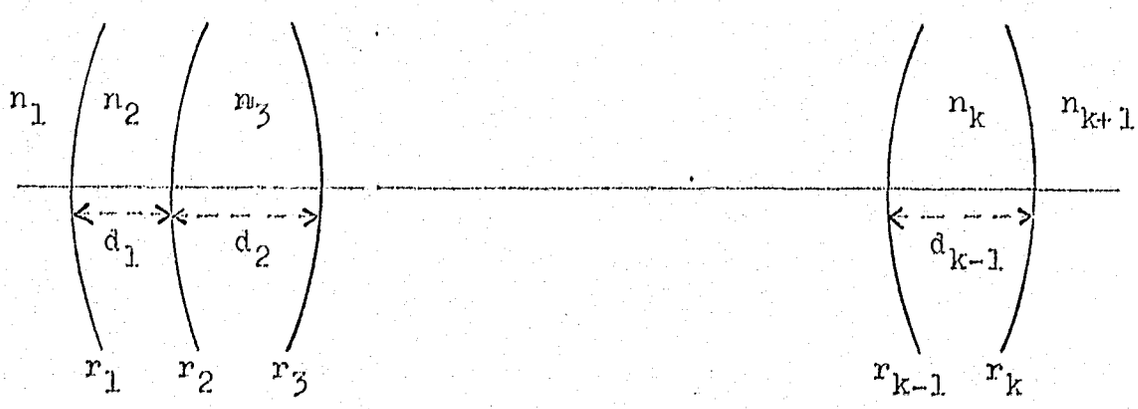

Fig. 3.1

Explanation of symbols:

r_p : radius of curvature of the pth surface (meters)

n_p : index of refraction of the medium in front of the pth surface

d_p : axial separation between the pth and the $(p+1)^{th}$ surface (meters)

$F_p = \frac{n_{p+1} - n_p}{r_p}$: surface power of the pth surface (diopters)

L_p : object distance for the pth surface (diopters)

L'_p : image distance for the pth surface (diopters)

(L_p and L'_p are measured with respect to the vertex of pth surface)

In Fig. 3.1 the light is supposed to travel from left to right. The next step is to solve the following set of equations.

$$L_1 = 0; \quad L'_1 = L_1 + F_1 = F_1$$

$$L_2 = \frac{1}{\frac{1}{L'_1} - \frac{d_1}{n_2}} \; ; \; L'_2 = L_2 + F_2$$

$$L_3 = \frac{1}{\frac{1}{L'_2} - \frac{d_2}{n_3}} \; ; \; L'_3 = L_3 + F_3 \qquad \text{(Eq. 3.2)}$$

$$\cdots\cdots\cdots\cdots\cdots\cdots\cdots\cdots\cdots\cdots$$

$$L_k = \frac{1}{\frac{1}{L'_{k-1}} - \frac{d_{k-1}}{n_k}} \; ; \; L'_k = L_k + F_k$$

It can be shown that the equivalent focal length of the optical system in Fig. 3.1 is given by Eq. 3.3

$$F_{eq} = L'_1 \left(\frac{L'_2}{L_2}\right) \left(\frac{L'_3}{L_3}\right) \cdots\cdots \left(\frac{L'_k}{L_k}\right) \qquad \text{(Eq. 3.3)}$$

F_{eq} in Eq. 3.3 provides the distance f' between the second principle focus and the second principle plane, namely $f' = \frac{n_k + 1}{F_{eq}}$. L'_k in Eq. (3.2) provides the distance v between the second principle focus and the vertex of the last refracting surface, namely $v = \frac{n_{k+1}}{L'_k}$. From the foregoing it is clear that Eq. (3.2) and Eq. (3.3) determine together the position of the second principle focus, the position of the second principle plane, and the position of the second nodal plane, all with respect to the optical system. By letting the light travel from right to left in the optical system of Fig. (3.1), we find analogous equations to determine the first principle focus, the first principle plane, and the first nodal plane.

In the case of the human eye, values of n, r and d can be found from Table 3.2, and the calculation of the cardinal points is a straighforward but laborious job. Calculated values from Gullstrand are given in Table 3.2 for the unaccommodated eye.

Cardinal Point	Position with respect to anterior surface of cornea
1st principle point	1.348 mm
2nd principle point	1.602 mm
1st focal point	-15.707 mm
2nd focal point	24.387 mm
1st nodal point	7.078 mm
2nd nodal point	7.332 mm

Table 3.2

b. The Simplified Eye. It is possible to reduce the model of the crystalline lens, as used in the schematic eye, even more. In Gullstrand's simplified eye the crystalline lens is represented as one single thick lens. The positions and radii of curvature of the anterior and posterior surfaces of this thick lens are equal to the corresponding values for the crystalline lens. However, the constant index of refraction must be chosen equal to 1.413, to make the optical properties of the single thick lens as close as possible to those of the crystalline lens.

Gullstrand has shown that this simplification describes the optical image formation of the real eye still quite accurately. The obvious advantage is the reduction of the number of refracting surfaces, which makes the calculation of the cardinal points much simpler. Another reduction in the simplified eye concerns the cornea. In the schematic eye the cornea is represented by an anterior and posterior surface (radii of curvature 7.7 mm and 6.8 mm, respectively) separated by a medium of refractive index 1.376 (axial separation 0.5mm). The equivalent power of the cornea can be calculated easily with Eq. (3.2) and Eq. (3.3), using the following values in Fig. 3.1:

$n_1 = 1$ $\quad r_1 = 7.7$ mm $\quad F_1 = \frac{0.376}{0.0077} = 48.83$ D

$n_2 = 1.376$ $\quad r_2 = 6.8$ mm $\quad F_2 = \frac{0.040}{0.0068} = -5.88$ D

$n_3 = 1.336$ $\quad d_1 = 0.5$ mm

Substitution of these values in Eq. (3.2) gives

$$L_1 = 0 \qquad L'_1 = 48.83$$

$$L_2 = \frac{1}{\frac{1}{48.83} - \frac{0.0005}{1.376}} = 49.75 \qquad L'_2 = 49.75 - 5.88 = 43.87$$

$$F_{eq} = 48.83 \frac{(43.87)}{(49.75)} = 43.05 \text{ D}$$

In the simplified eye the cornea is replaced by a single surface with radius of curvature equal to 7.8 mm at the position of the anterior surface of the cornea. This single surface separates the media air and aqueous humor (index of refraction 1.000 and 1.336, respectively). The equivalent power of this surface is simple $F_{eq} = \frac{0.336}{0.0078} = 43.08$ D, which is very close to that of the schematic cornea.

We will use Gullstrand's simplified eye as a basis for calculation of the characteristics of the retinal image. The basic data are shown in Fig. 3.2. For the unaccommodated simplified eye we have

$n_1 = 1$ $\quad d_1 = 3.6$ $\quad r_1 = 7.8$ mm

$n_2 = 1.336$ $\quad d_2 = 3.6$ $\quad r_2 = 10$ mm

$n_3 = 1.413$ $\quad d_3 = 16.97$ $\quad r_3 = -6$ mm

$n_4 = 1.336$

Using these data in Eq.(3.2)and Eq.(3.3) it is easy to calculate the positions of the principle points. The results are summarized in Table 3.3 for the unaccommodated eye.

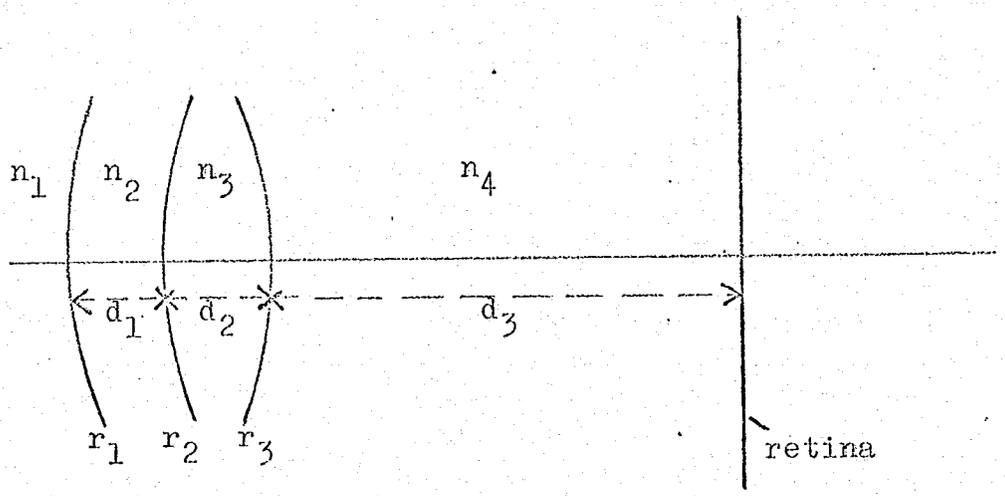

Fig. 3.2

Cardinal Point	Position with respect to anterior surface of cornea	
	Unaccommodated	Accommodated 8.62 D
1st principle point	1.47 mm	1.70
2nd principle point	1.75 mm	2.03
1st focal point	-15.31 mm	-12.96
2nd focal point	24.17 mm	21.61
1st nodal point	7.11 mm	6.62
2nd nodal point	7.39 mm	6.95

Table 3.3

c. Accommodation In the process of accommodation three parameters are changing significantly, increasing the dioptric power of the eye as a whole. First, the radii of curvature of the anterior surface and the posterior surface of the lens both decrease. Secondly, the anterior surface of the lens moves forward. In the case where the eye is accommodated 8.62 D, i.e., focused for an object 11.6 cm in front of the first principal plane, we have the following parameters:

Radius of curvature of the posterior lens surface = +5.00 mm

Radius of curvature of the anterior lens surface = -5.00 mm

Axial thickness of lens = 4.00 mm

Axial thickness of anterior chamber = 3.2 mm

All the other parameters remain more or less unchanged. Again the cardinal points of the system can be calculated and the results are shown in Table 3.3 for the simplified eye.

d. Entrance and Exit pupils. The entrance pupil of the human eye is the image of the actual pupil formed by rays which have been refracted by the cornea. The plane of the pupil cuts through the axis of the eye at the front vertex of the lens, i.e., 3.60 mm from the cornea in the unaccommodated eye and 3.20 mm from the cornea in an 8.62 D accommodated eye.

Unaccommodated eye

Equation (3.1) is used to calculate the position of the entrance pupil:

$$L' = F + L$$

In this case

$$L = \frac{n}{l} = \frac{1.336}{3.6 \times 10^{-3}} = -371 \text{ diopters}$$

F= 43 diopters (surface power of cornea)

Substitution of these values in Eq. (3.1) yields

$$L' = -371 + 43 = -328 \text{ diopters}$$

Thus the position of the entrance pupil is

$$l' = \frac{n'}{L'} \times 10^3 = \frac{1}{-328} \times 10^3 = -3.05 \text{ mm (measured with respect to the cornea)}$$

The magnification is given by

$$m = \frac{L}{L'} = \frac{-371}{-328} = +1.13$$

Accommodated eye. In this case $L = \frac{-1.336}{3.2 \times 10^{-3}} = -417$ diopters. Consequently we find $L' = -417 + 43 = -374$ diopters.

The position of the entrance pupil is

$$l' = \frac{10^3}{-374} = -2.67 \text{ mm (measured with respect to the cornea)}$$

The magnification is

$$m = \frac{-417}{-374} = +1.12$$

The exit pupil of the human eye is the image of the actual pupil formed by refraction through the crystalline lens. Again the center of the actual pupil is taken as coincident with the anterior vertex of the lens, i.e., 3.60 mm from the posterior surface of the lens in the unaccommodated eye and 4.00 mm from the posterior surface of the lens in a 8.62 D accommodated eye.

Using again Eq. (3.1) we find for the unaccommodated eye.

$l' = -3.52$ mm (with respect to the posterior surface of the lens)

$$m = \frac{L}{L'} = +1.03$$

For a 8.62 D accommodated eye, these values are

$l' = 3.94$ mm and $m = +1.04$

The results are summarized in Table 3.4

	Unaccommodated	8.62D Accommodated
Position of actual pupil behind the vertex of the cornea	3.60 mm	3.20 mm
Position of entrance pupil behind the vertex of the cornea	3.05 mm	2.67 mm
Position of exit pupil behind the vertex of the cornea	3.68 mm	3.26 mm
Magnification entrance pupil	1.13	1.12
Magnification exit pupil	1.03	1.04

Table 3.4

SECTION 4

4. IMAGE CHARACTERISTICS

a. Magnification. The calculation of the position and the size of the image formed on the retina is a straightforward procedure as soon as the cardinal points of the system are known. A difficulty is that the position of the cardinal points depends on the accommodative state of the eye in a way which is difficult to predict because of a lack of enough data. Since the most dependable data are given by Gullstrand [28], for an unaccommodated eye and a 8.62 D accommodated eye, we will make some calculations for these two extreme situations. For all practical purposes the actual results will fall in the range between these two limits.

First, let us consider the unaccommodated eye looking at an infinitely distant object, situated on the optical axis and subtending an angle α. This means that all the rays from the upper extremity of the object make the same angle α with the reference axis. By definition we know that the ray directed towards the first nodal point leaves the optical system as coming from the second nodal point and parallel to the incoming ray. Furthermore, the image of an object at infinity will be at the retina, which is about 16.8 mm from the second nodal point. This means that the height h of the image is equal to

$$h \text{ (in mm)} = -16.8 \operatorname{tg} \alpha \qquad \text{Eq. (4.1)}$$

The (-) sign in Eq.(4.1) indicates that we have a reversed image.

In case the eye is accommodated XD, an object $\frac{1}{X}$ meter in front of the first principle plane will be focussed on the retina. We assume that the positions of the cardinal points remain more or less constant with respect to the retina during the process of accommodation. In that case we have $L_1 = -XD$; $F = (59.60 + X)$ D and $L'1 = 59.60D$.

Thus the transverse magnification for an object $\frac{1}{X^m}$ in front of the first principle plane is

$$M = -\frac{X}{59.6} \qquad \text{Eq. (4.2)}$$

For example, if the object-height is 100 mm and the object is located at a distance of 1 meter in front of the first principle plane, then the image-height will be $-\frac{1}{59.6} \times 100 = -1.68$ mm if the eye is accommodated 1 diopter.

b. Blur. Although the blur can have many causes, in this particular section we will only discuss the blur due to an out-of-focus image on the retina. First, let us consider the blur caused by an object-point located on the optical axis. If the image is out of focus it becomes a blur circle of the same shape as the exit pupil, which we assume to be perfectly round. The following quantities are defined:

object distance:	-X diopters
distance for which eye is accommodated:	Y diopters
diameter exit pupil:	P mm
diameter blur circle:	B mm

Under the assumption that the exit pupil is located 3.47 mm behind the vertex of the cornea and that the location of the exit pupil as well as the location of the principle planes do not change during accommodation, Eq (4.3) can be

derived from simple geometric considerations

$$B = 0{,}0\,18\ P\ /\ y \pm x/\ \text{mm} \qquad \text{Eq. (4.3)}$$

In the process of deriving Eq. (4.3) some additional numerical approximations have been made. We note from Eq. (4.3) that the size of the blur circle depends on the absolute value of the difference between object distance X and accommodation Y (both in diopters). For example, with a fixed accommodative state Y, the blur circles that belong to the positions (Y-X) diopters and (Y+X) diopters of the object-point, will have the same size. Furthermore, with incoherent light and in the absence of any aberration, the light is uniformly distributed over the blur circle. The illuminance E at any point of the blur circle is equal to $\frac{F}{\pi r^2}$ where F is the total amount of light in the image and r is the radius of the blur circle. Under these conditions, in a first order approximation the blur will only contain even-error information for the accommodative control system. Experimental results indicate that the human accommodative control system in which the size of the blur is the only error criterion, behaves indeed as an even-error control system.[52,53,55] However, in normal life there are so many additional clues (size, brightness, movement) which, together perhaps with higher order aberrations, provide enough directional information to guarantee odd-error control.

The value P of the exit-pupil diameter can be determined by measuring the entrance-pupil diameter. This is the pupil diameter which we see by looking at a person's actual pupil and which is measured by all common-type pupillometers. The exit-pupil diameter is approximately a factor 0.92 times the entrance-pupil diameter. (See section 3.d).

An interesting phenomenon can be observed when light of a continuous laser is scattered at a surface such as, for example, the laboratory wall. The scattered laser light shows a peculiar granularity, the apparent size of which increases with decreasing apertures of the optical system. Rigden and Gordon [46] show that the optical system acts as a band-pass filter for the noise input that arises from the random Fourier components of the scattering surface. The granularity is explained as two-dimensional beats in the output of a band-limiting filter fed by noise, at a frequency approximating the band-pass.

If the observer moves, and the plane of focus of the observer does not correspond to the scattering surface, the granular pattern shows a motion as a result of parallax. The relative direction of motion reverses as the plane of focus is moved from behind to in front of the scattering plane. This can be explained as follows. In contrast with the homogeneous blur caused by incoherent light, we have now a "structured" blur that arises from the interference of completely

coherent diffraction patterns. The light rays composing the blur, will reverse when the image plane passes through the conjucate plane (Fig. 4.1)

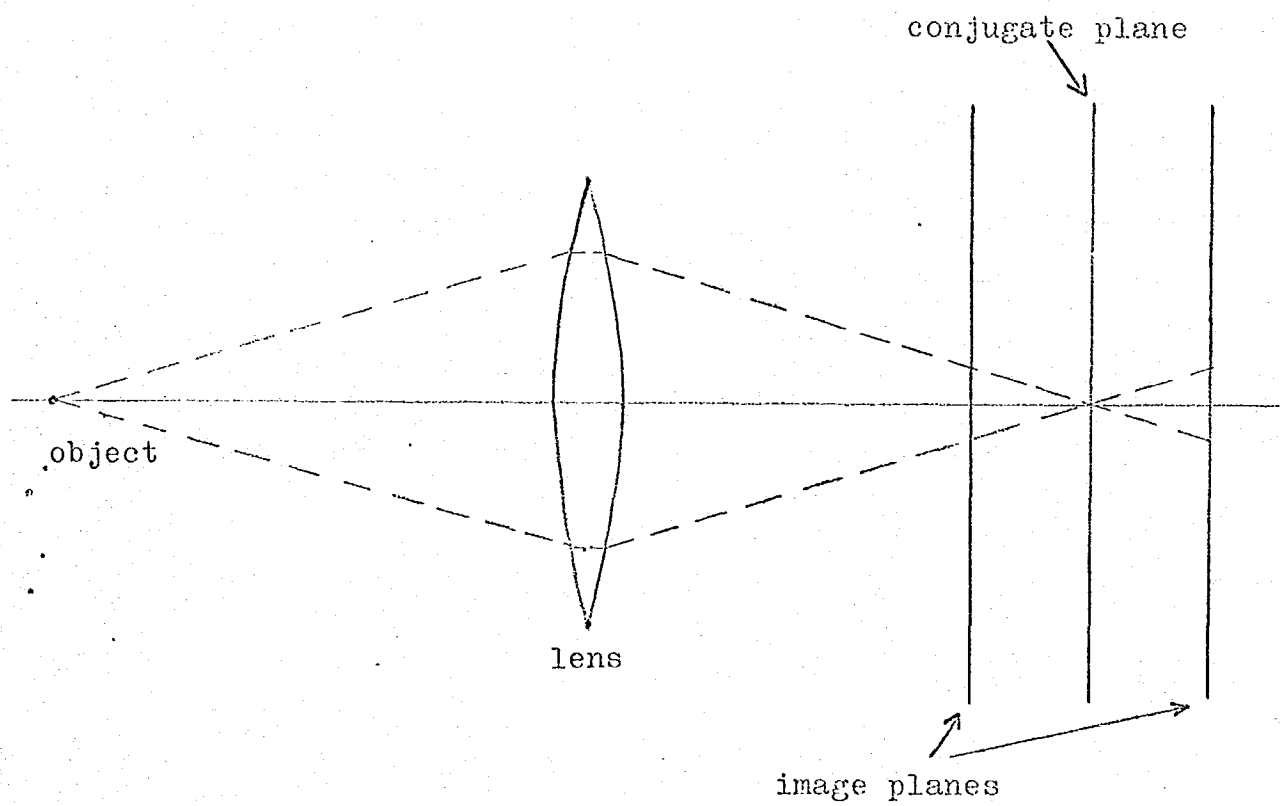

Fig. 4.1

If the blur is homogeneous, we can never detect from the change in blur in which direction the image plane is moving (even-error). If the blur is structured, however, we can detect the reversal of the pattern (odd-error). In an analogous way, we can detect a reversal of relative motion, in case the object is moving slowly and perpendicular with respect to the optical axis. This principle is used in a subjective optometer, in which the subject indicates in which direction a scattered

laser pattern on a slowly rotating drum is moving. [35]

If a point source of light is imaged onto the retina, the image will never be a point but a light distribution centered on the theoretical image of the point (the chief ray image). This light distribution is caused and determined by the aberrations, the scattering and the transmittance of the optical system (the eye) in a way which is difficult to predict. The total amount of light F contained in the chief ray image is given by the following equation. [24]

$$F = \frac{I \cos \theta}{r^2} \pi a^2 t \qquad \text{Eq. (4.4)}$$

In Eq. (4.4):

I = candle power of light source

r = distance from light source to entrance pupil

θ = angle of incidence (angle between the line which connects the light source with the center of the pupil and the normal to the plane of the pupil).

a = diameter of entrance pupil

t = transmittance of the media of the eye

F is expressed in lumens. The light distribution around the chief ray image is rotational symmetric, thus the illumination at any point depends on the distance from the chief ray image only. The point image distribution function is defined as a function P (r) of r with which F has to be multiplied in order to obtain the illuminance E at a point at distance r from the chief ray image.

$$E(r) = P(r)\ F$$

A hypothetical point image distribution function is shown in Fig. 4.2.

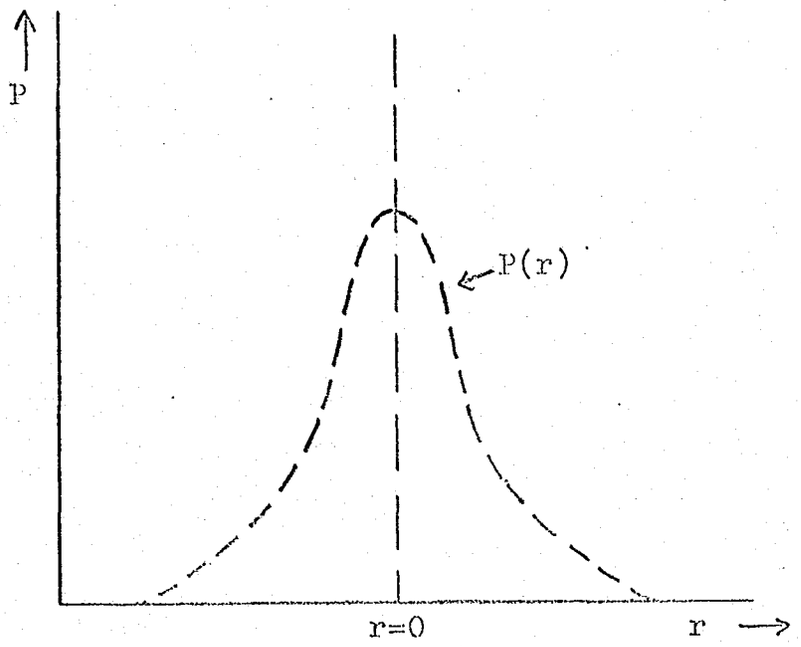

Fig. 4.2

By definition we have

$$2\pi \int_0^\infty r P(r) F dr = F \quad \text{or} \quad \int_0^\infty r P(r) dr = \frac{1}{2\pi} \qquad \text{Eq. (4.5)}$$

As soon as the point spread function is known, it is possible to calculate quite easily the spread function for other geometrical configurations. We will give the formulas for an infinite line and an infinite light-dark border.

Line. Suppose the light flux in the chief-ray image of the line is D lumens per unit length. Then the illuminance in a point P at a distance a from the line is given by

$$E(a) = 2D \int_{|a|}^{\infty} \frac{P(r)\, r}{\sqrt{r^2 - a^2}}\, dr \qquad \text{Eq. (4.6)}$$

Border. Suppose the light flux in the chief ray image of the bright half of the plane is D lumens per unit area. Then the illuminance in a point P_1 in the dark half of the plane at a distance -a from the chief-ray border is given by

$$E(-a) = 2E \int_{-a}^{-\infty} P(r)\, r \cos^{-1}\left(\frac{a}{r}\right) dr \qquad \text{Eq. (4.7)}$$

The illuminance in a point P_2 in the bright half of the plane at a distance a from the chief-ray border is given by

$$E(a) = 2E \int_{0}^{a} P(r)\, r\, \pi\, dr + 2E \int_{a}^{\infty} P(r) \cos^{-1}\left(\frac{a}{r}\right) dr \qquad \text{Eq. (4.8)}$$

Now in the case of homogeneous blur, the point image distribution function has a rectangular shape as shown in Fig. 4.3.

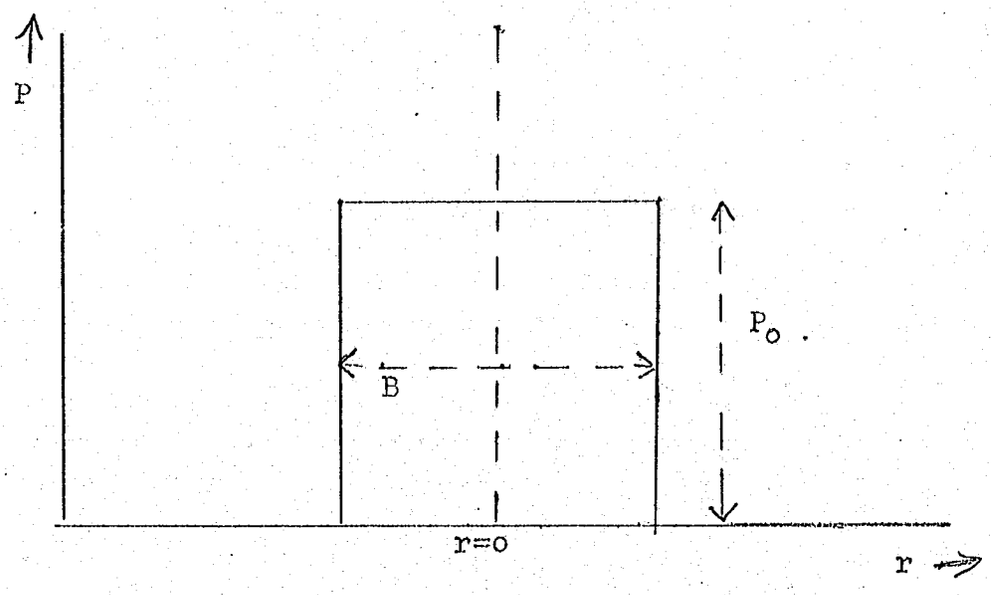

Fig. 4.3

The width B of this rectangular distribution is given by Eq. (4.3):

$$B = 0.018\ P/y-x/\ \text{mm}$$

Using Eq. (4.5) and Eq. (4.6) we find for the line image distribution function:

$$E(a) = \frac{8D}{\pi B^2}\sqrt{\frac{B^2}{4} - a^2} \quad \text{for } -\frac{B}{2} < a < +\frac{B}{2} \qquad \text{Eq. (4.9)}$$

$$E(a) = 0 \qquad \text{for } a < -\frac{B}{2} \text{ or } a > +\frac{B}{2}$$

From Eq. (4.9) we can calculate the width of the line spread function. For example, at half its maximum value:

$$W(1/2) = 0.86\ B$$

Substitution for B the expression given in Eq. (4.3):

$$W(1/2) = 0.0155\ P/y-x/\text{mm}$$

For a 5 mm pupil, this corresponds to

$$W(1/2) = 0.0675\ /y-x/\text{mm}$$

From experimental data by Krauskopf [37] of the linespread function for a 5 mm pupil we determine

$$W(1/2) = 4 \text{ min. of arc} \approx 0.02 \text{ mm}$$

Combining these results gives

$$0.0675\ /y-x/ = 0.02$$

$$/y-x/ \approx 0.3 \text{ diopters}$$

This means that the spread function of the human eye corresponds to defocussing an ideal eye approximately 0.3 diopters.

5. FOURIER ANALYSIS OF IMAGE FORMATION.

In this section we propose an alternate technique of calculating the retinal image for any object. This technique makes very few approximations about the optical system and consequently results in a very realistic model. The price paid for such exactness is the necessity of computer solutions for the retinal distributions. A simple hand calculable example is included.

a. Spatial Transforms. The error detector of the system is the retina which is thought to detect blur in the object to be seen. However, as seen in the previous sections, even a subjectively focused object is blurred due to a dioptric dead-band of 0.3 diopters.

The most straightforward way of determining the actual image on the retina and still account for all of the optical parameters of the eye is to formulate the optical system in terms of block diagrams using Fourier transform techniques. This method then allows one to calculate the image on the retina of any object. The block diagram consists of an interconnection of only two basic elements--a multiplier and a block characterized by an impulse response. These two elements are derived by considering the general form of electromagnetic propagation of energy. The electric field of such a wave will have the form:

$$\bar{E}(x,y,z,t) = \bar{E}(x,y,z)\,e^{j\omega t}$$

The vector $\bar{E}(x,y,z)$ is composed of components

$$E_i = E_i'(x,y,z)\,e^{j\Theta(x,y,z)} \qquad i=1,2,3$$

where $\Theta(x,y,z)$ represents the spatial contribution to the

the total phase of the component field. Since light intensity is the variable usually measured and is proportional to the square of the electric field, a light wave can also be represented by a wave (traveling in the direction) of the form

$$A(x,y) = |A(x,y)| e^{j(\varphi(x,y)+\omega t)}$$

where φ is in units of radians. This equation represents the intensity for a given z. Thus, a modulating medium (a lens, film, etc.), serves only to modify the magnitude of A(x,y) and/or its phase $\varphi(x,y)$ if the modulating medium is time invariant. Hence, the modulating medium is representable by

$$f(x,y) = |f(x,y)| \, e^{j\varphi'(x,y)}$$

where f and φ' depend on the particular media parameters and geometry. For a simple lossless spherical thin lens, it is easy to show that

$$f(x,y) = e^{-j\frac{k}{2F}(x^2+y^2)}$$

where $k = \frac{2\pi}{\lambda}$, λ is wavelength and F is the focal length of the lens. In the case of a lens, if the input light distribution is of the form

$$g(x,y) = |g(x,y)| e^{j(\psi(x,y)+\omega t)}$$

then the transmitted light will be

$$g'(x,y) = e^{j(\psi(x,y)-\frac{k}{2F}(x^2+y^2)+\omega t)}$$

From this equation, it can be seen that the multiplicative element will in general only effect the phase of the incident light.

The other element of the block diagram representation scheme takes into account any media that has thickness along the axis of wave propagation-- the direction in this case. It can be shown that if h (x,y) is a light distribution in the x,y plane, then the propagated light in the u,v plane a distance D away is

$$g(u,v) = \frac{C}{D}\int_{-\infty}^{\infty} h(x,y)\exp\left[\frac{jk}{2D}\{(x-u)^2+(y-v)^2\}\right]dx\,dy$$

where C is a constant. This has the form of an element with an impulse response of $\frac{1}{D}\exp\left[\frac{jk}{2D}(x^2+y^2)\right]$.

As an example, a thin lens with focal length F a distance D_1 from the object plane and D_2 from the image plane would have a block diagram as shown in Figure 5.1.

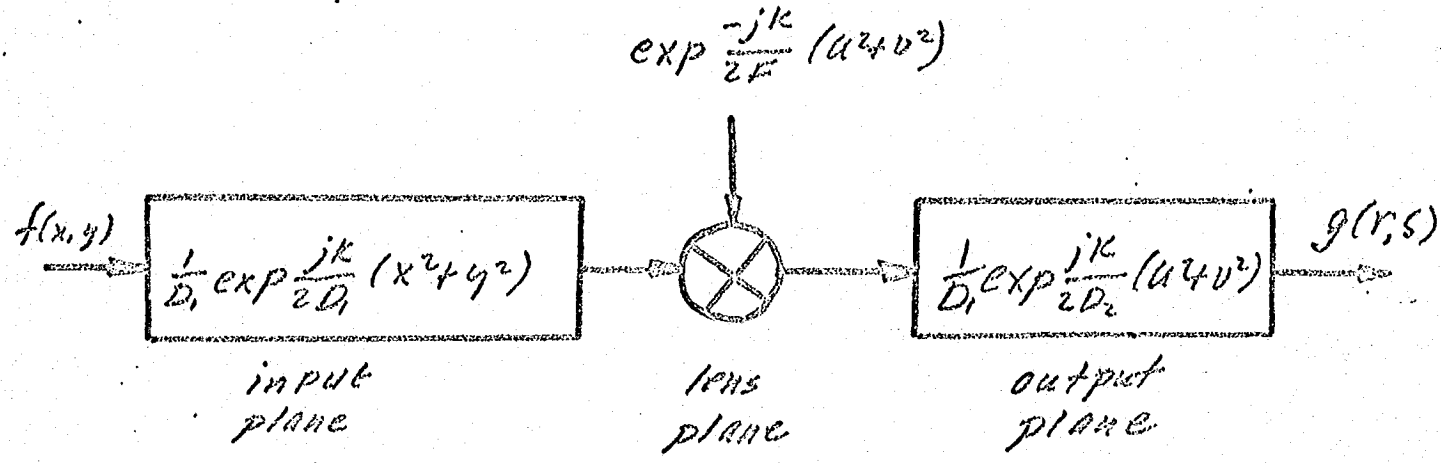

Figure 5.1

The output plane distribution would be given by

$$g(r,s) = \frac{C}{D_1 D_2} \iint_{-\infty}^{\infty} \left[\exp \frac{-jk}{2\pi} |u,v|^2 \iint_{-\infty}^{\infty} f \exp \frac{jk}{2D_1} |x,y-u,v|^2 \, dx\,dy \exp \frac{jk}{2D_2} \right] du\,dv \qquad (5.1)$$

When the refracting media is not a spherical lens then the multiplying element will have the general form

$$\exp\left[-j \frac{2\pi}{\lambda} \alpha(x,y)(n_2 - n_1)\right]$$

where $\alpha(x,y)$ is the thickness function of the refractor and n_2, n_1 represent the indices of refraction of the refractor and the media in which it is placed respectively.

An obvious over-simplification in equation (5.1) is the assumption of an infinite aperture lens as evidenced by the infinite limits on all integrals. Finite aperture lenses complicate the calculation of the output distribution but must be considered in the practical cases.

b. <u>An Application to the Human Eye.</u>

Consider an eye focused on an object with an intensity distribution f (x,y) a distance D_1 from the cornea and let it be proposed to determine the retinal image of f(x,y). The distances and refracting surfaces in this system are listed in Table 5.1.

Table 5.1

Refracting surface or distance function	Thickness function, or distance D
Object distance	D_o
Cornea	$\alpha_c(x,y)$
Anterior chamber	D_a
Anterior lens surface	α (x,y)
Lens thickness	D_l
Posterior lens surface	$\alpha_p(x,y)$
Posterior chamber	D_p

Let N_i be the indices of refraction of the various media of the eye with $N_0 = 1$ being the index of free space. Thus, N_a, N_e, and N_p are the indices of the anterior chamber, lens and posterior chamber, respectively. For simplicity of notation define

$$\psi_i = \frac{\exp\left(j \frac{k}{2D_i}(x^2+y^2)\right)}{D_i}$$

and

$$\phi_{s,t}(x,y,n_s,n_t) = \exp\left(j\frac{2\pi}{\lambda} a_s(x,y)(n_s - n_t)\right)$$

while $\psi_i * (\cdot)$ will represent the convolution operation of ψ_i and the input function.

With these definitions the block diagram of the human eye takes the form illustrated in Figure (5.2).

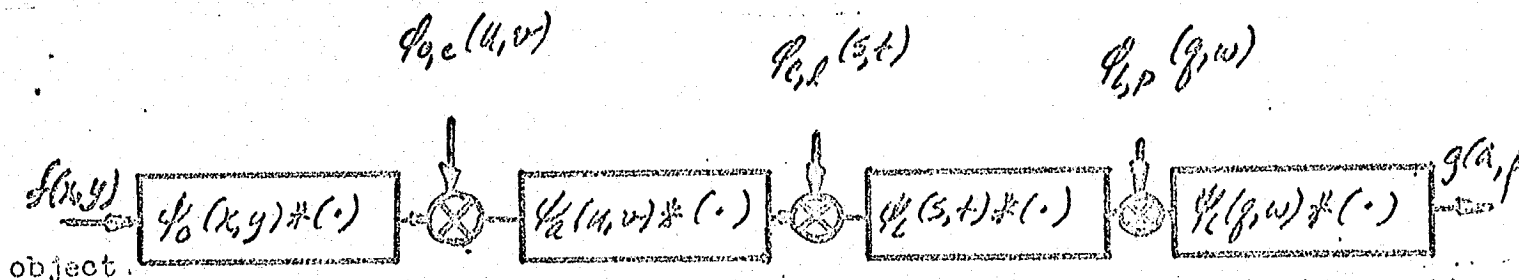

Figure 5.2

In this figure f(x,y) represents the object distribution whose retinal image (distribution $g(\alpha,\beta)$) must be determined. The calculations for determining are somewhat more complex than those for simple optical systems because the iris introduces a finite aperture after the anterior chamber distance operator. This requires the

integral associated with the operation be evaluated over finite limits. However, the evaluation of the multiple integrals is of sufficient complexity without the finite aperture condition to warrant a computer solution so that the aperture problem is more apparent than real.

The finite aperture condition introduces the dead-band of approximately 0.3 diopters that is noted in the previous sections. As far as the optical block diagram is concerned, without a finite aperture there is no dead-band. This is illustrated by the simple system depicted in Figure (5.3).

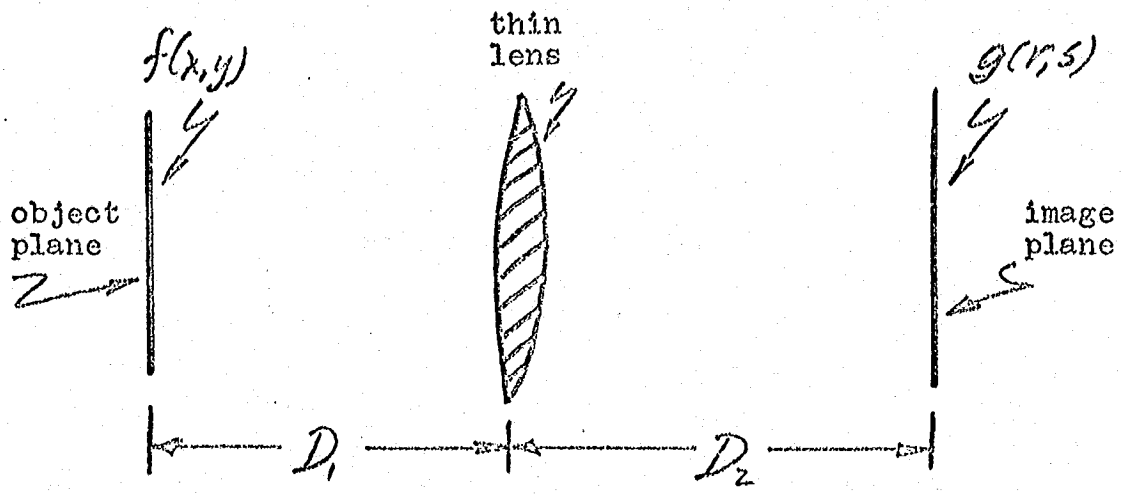

OPTICAL SYSTEM

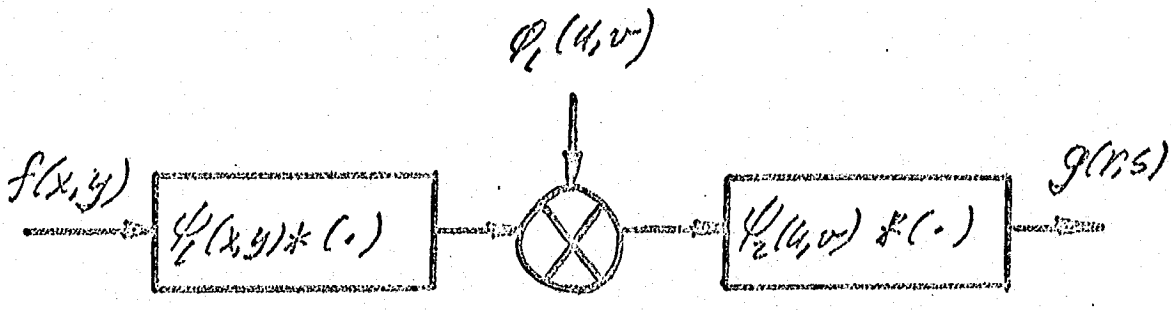

BLOCK DIAGRAM

FIGURE 5.3

where

$$\psi_1(x,y) = \frac{1}{D_1} \exp\left[-j\frac{k}{2D_1}(x^2+y^2)\right]$$

$$\psi_2(u,v) = \frac{1}{D_2} \exp\left[-j\frac{k}{2D_2}(u^2+v^2)\right]$$

and

$$\phi_1(u,v) = \exp\left[j\frac{k}{2F}(u^2+v^2)\right]$$

with F being the lens focal length.

The output is given by

$$g(r,s) = \left\{\left[\psi_1(x,y) * f\right]\phi_1\right\} * \psi_2.$$

Let $f(x,y) = \delta(x,y)$ i.e. a point of light and let $\frac{1}{D_1} + \frac{1}{D_2} = \frac{1}{F}$ i.e. the point is to be focused on the image plane. For these conditions

$$g(r,s) = \frac{1}{D_1 D_2} \exp\left[\frac{jkD_2^2}{2D_1}(r^2+s^2)\right]\delta\left(-\frac{D_2}{D_1}r, -\frac{D_2}{D_1}s\right).$$

From the last expression, it is seen that the image of an impulse (except for the multiplying phase factor which is undetectable) is merely a scaled impulse. Such a result is expected for infinite apertures since the theory just echoes geometrical optics in the infinite aperture case.

Now take the same system but introduce a finite circular aperture immediately in front of the lens and again assume $f(x,y) = \delta(x,y)$. From the block diagram of Figure 5.1 the signal entering the multiplier is merely $\psi_1(0,0) = \frac{1}{D_1}$ and the signal leaving the multiplier is just $D_1^{-1}\phi_1(u,v)$.

Thus the output signal (the image plane distribution) is

$$g = \psi_2 * D_1^{-1} \varphi_i(u,v).$$

where the "convolution" here is over finite limits and is given by

$$g = \frac{1}{D_1 D_2} \iint_{ap.} \exp\left[-j\frac{k}{2D_2}|u,v|^2\right] \exp\left[j\frac{k}{2F}|u,v-r,s|^2\right] du\,dv.$$

Let the radius of the aperture be R and use the transformation $u=\rho\cos\theta$, $v=\rho\sin\theta$ to take advantage of the cylindrical symmetry inherent in the problem geometry. This reduces the above to

$$g(r) = (D_1 D_2)^{-1} \int_0^{2\pi} \exp\left[-\frac{jk\rho^2}{2D_2}\right] \exp\left[j\frac{k}{2F}(\rho^2+2r^2-2\rho r(\cos\theta\cos\sin\theta)\right] \rho\,d\rho\,d\theta.$$

Itis easily demonstrated that this integral yields the following series for g(r),

$$g(r) = \frac{\sqrt{\pi}R^2}{D_1 D_2} e^{j\frac{kr^2}{2D_2}} \sum_{k=0}^{\infty}{}' (-1)^k \frac{\Gamma(k+1/2)}{k\,\Gamma(k)(k+1)(2k)!} \left(\frac{2\pi}{\lambda D_2} Rr\right)^{2k}.$$

Whereas with an infinite aperture, the block diagram merely gave a distribution reiterating the trivial result one would obtain using first order geometrical optics, consideration of the finite aperture yields an image distribution that is finite over a non-zero measurable set of points in the image plane. Even without the complexities introduced by the actual human optical system, it is obvious that even for this idealized system a "focused" object actually depends on the spatial sensitivity and resolution of detectors in the image plane. This so-called "spread function" for an impulse into the block diagram of figure 5.1 will obviously be more complex but for two reasons:

1) The system consists of more elements and the functions representing these elements are not as elementary as those of the one lens system.

2) The elements of the eye are not representable by static functions as those of the simple optical system.

The second reason is by far the more important because it implies that the parameters of the eye system (distances, radii of curvature, etc.) are time varying. These time variations are indeed slow relative to the excitation frequency (typically fifteen orders of magnitude slower) but the consequences of these time variations are that the distribution is now time varying. As can be seen from the distribution derived for the simple lens system, the parameters R, D_1 and D_2 determine the scaling of the distribution (the exponential is undetectable) while the ratio R/D_2 determines the functional form of the distribution. In the last regard, it is interesting to note that the distribution could not distinguish between a slowly varying aperture and a change in wavelength if D_1 were such as to cancel the radial effect in the scaling factor. The importance of the time variations in R is of experimental interest because of the oft reported "pupil noise" accompanying measurements of pupil area. One could conjecture that this noise is intentional so as to bring in retinal velocity receptors in order to focus on an otherwise stationary object.

In any case, the block diagram type analysis brings to light the dominant role the eye parameters play in the retinal light distribution of a focussed object and will hopefully reveal the actual error signal transmitted by the retinal fibres to the central nervous system controller. Computer analyses of the eye-block diagram (Fig. 5.2) are presently being undertaken using documented average eye parameters from the medical literature.

SECTION 6

6. CONTROL ASPECTS OF THE ACCOMMODATIVE SYSTEM.

In this section the accommodative system is considered as an automatic control system. A plant mathematical model is proposed to illustrate a quantitative approach applicable to a known physiological system. The model is necessarily incomplete due to a lack of pertinent elastic parameters.

a. System Definition. For monocular vision the accommodation system can be considered as a control system whose controlled object or plant is the lens. The controlled variable is the dioptic strength of the lens and the controller is the central nervous system with its appropriate transducers. Figure 6.1 illustrates a functional block diagram of the system.

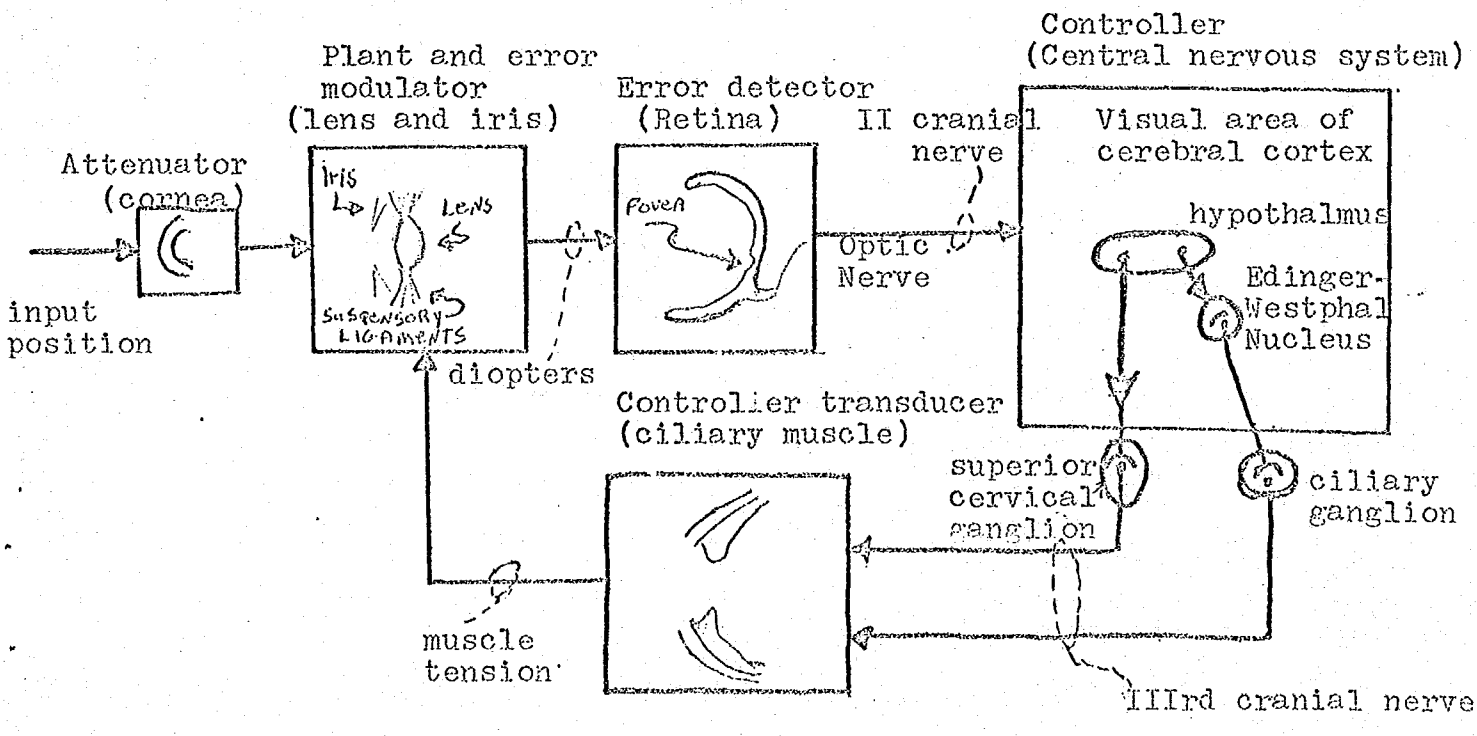

Figure 6.1

It appears that the only error detector for the system is the retina since the ciliary body has no known proprioceptors, i.e. sense organs stimulated by movement or relative position. This does not mean however that ciliary muscle can be innervated only when the retina detects an error in the object image. The C.N.S. can produce other inputs capable of accomplishing accommodation. The command for such inputs are considered in Section 7.

b. System Function. The flow of signals through the accommodation system begins with the input position of the object to be focused on the foveal area of the retina. The light rays are initially refracted by the cornea (approximately 43 diopters) and then by the lens. The lens has a spatially variable index of refraction (1.386 cortex; 1.406 core) which in fact determines its high dioptic strength since the aqueous humor bathing its anterior surface has a refractive index of 1.336. A calculation of its dioptic strength with its anterior surface at maximum accommodation (minimum radius of curvature) using the cortex and aqueous humor indices does not yield the diopters observed experimentally. The equivalent power of the lens ranges from 20.78 diopters unaccommodated to 30.13 diopters fully accommodated.

After refraction by the lens the rays fall on the retina. If the image is blurred an error signal is developed by the retina and transmitted to the C.N.S. by the optic nerve. Some doubt exists as to whether or not the sign of the blur can be detected in monocular vision if the only error signal is the

blur itself. If the retinal error signal does contain the information that the image is falling in front of the retina or behind it, then this retinal error signal is sufficient for the C.N.S. to send the proper impulses to the ciliary muscle. The retinal error detector is treated in more detail in Section 8.

The circular ciliary muscle is relaxed when the eye is unaccommodated and contracts when accommodation is called for by the C.N.S. signals. This contraction reduces the tension on the suspensory ligaments allowing the elastic capsule of the lens to shape the lens into a more convex body. The posterior side of the lens moves little if at all in accommodation with most of the dioptic strength coming from the decreased radius of curvature and forward motion of the anterior side of the lens. By varying the ligament tension the whole range of 10 diopters accommodation can be achieved.

c. System Dynamics.

A. Present Models.

The dynamics of the human visual accommodation system have been studied intensively in the past and will be a continued subject of research for the future. The past studies have been exclusively "black box" identification schemes aimed at arriving at a mathematical model to fit the response data. A basic difficulty has been the lack of a high quality optometer to directly measure the lens dioptic power. A second and perhaps more important criticism is the lack of any physiological basis for the parameters of the models derived by the "black box" techniques.

The most current model of the accommodation system is that of Stark, et al.[51] Figure 6.2 indicates this model's block diagram.

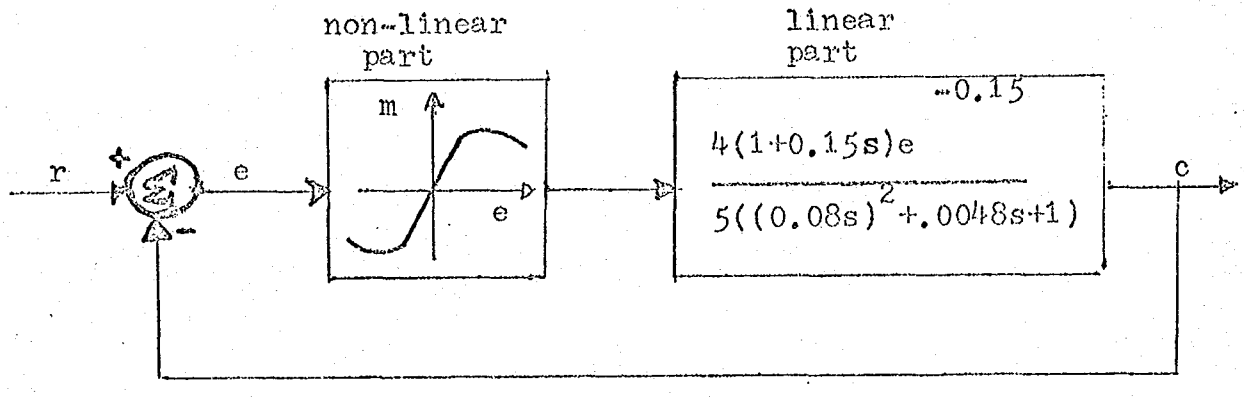

Figure 6.2

Some of the discrepancies between the model response and the system response are:

1. The model dead time is 100 ms while experimental dead time is 360 ms.

2. The phase of the model approaches 90° lag for increasing frequency while the experimental phase data approaches zero degrees.

3. No even-error signal processor is present in the model while experiments have indicated monocular vision requires such a device.

Another servoanalytic treatment of the accommodation system was made by Carter using a Badal infra-red optometer.[6]

The resulting closed loop transfer function obtained was

$$G(j\omega) = (0.6\, e^{-j\,0.3\omega})(1 - 0.4\cos.3\omega + j(0.2\gamma\omega + 0.4\sin.3\omega))^{-1}$$

Such a transfer function describes an unstable system even though it was derived from curve fitting the Nyquist plot of the experimental data. The end conclusion of the author is that the model was useful as a point of speculation concerning possible means of obtaining a stable transfer function to fit the empirical data.

Campbell and Westheimer do not put forth a transfer function per se but do plot a Nyquist diagram of their data. [9] This plot is very close to Carter's in all of its essential features.

These models represent the "black box" identification schemes and as such their parameters lack physiological significance. This is typical of input-output data curve fitting.

d. A Partial Distributed Parameter Model. An alternative identification scheme is to treat isolated elements of the block diagram of Figure 6.1 from a physics and physiological viewpoint. This leads to a theoretical mathematical model which later must be subject to actual experiment for verification. The advantages of such an attack is the knowledge of the physiological significance of the system parameters and an apriori knowledge of what type of input signals to use to identify those parameters.

As an example the plant of Figure 6.1 is chosen. Obviously, the corneal effect is easily computable so that the system under consideration is shown in Figure 6.3 where the iris effect is temporarily neglected.

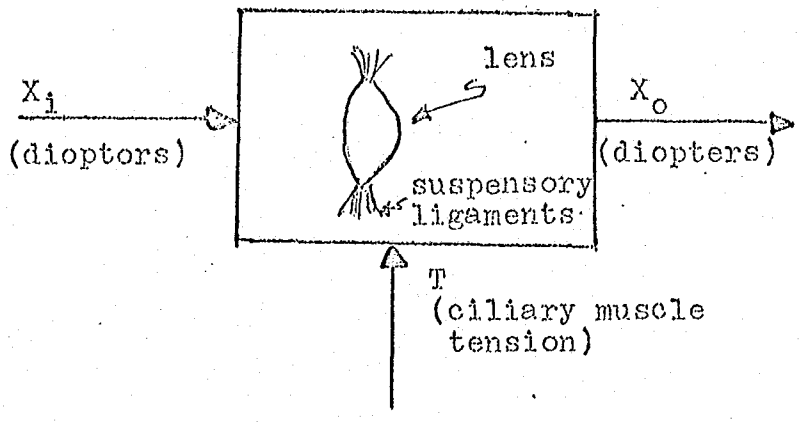

FIGURE 6.3

As explained in previous sections the lens is composed of an elastic capsule enclosing a highly viscous, plastic-like core. The lens capsule varies in thickness from 2.3 to 23 microns, the thinnest locale being at the posterior pole. The unaccommodated lens is approximately 3.6 mm thick (pole to pole) and 8.3 mm diagonally. It can be assumed that the capsule acts as a thin elastic membrane shaping the lens substance since the membrane thickness-to-diameter-ratio is, in the worst case,

$$\frac{22(10^{-6})}{83(10^{-3})} = 0.265\ (10^{-3})$$

i.e. the membrane is about 3780 times wider than it is thin. Additional simplifications can be made upon physiological evidence. In accommodation the posterior capsule moves

little if at all because of the support of the gel-like vitreous humor. This means that the significant dynamics of the lens occurs only to the anterior capsule. This is evidenced by the fact that the fully accommodated lens moves its anterior pole about 0.44 mm from the unaccommodated state while the posterior pole moves 0.02 mm. This represents a percentage change (anteriorly) of

$$\frac{44}{3.79} = 11.6\%$$

and only

$$\frac{11.6}{22} = 0.527\%$$

posteriorly.

The anterior capsule dynamics induce dynamics to the lens plastic-like core or substance by its shaping ability. It seems then that a plausible model takes the form of a thin, elastic membrane acted upon by forces from two directions. Anteriorly the viscous damping of the aqueous humor and posteriorly from the viscous and static force of the plastic lens substance. It is assumed that the membrane tension T is uniform throughout the anterior area of the capsule. Since the membrane is thin the units of T are newtons per meter. A section of the lens capsule, dA, is isolated in Figure 6.4 in order to derive the dynamic equations governing its motion.

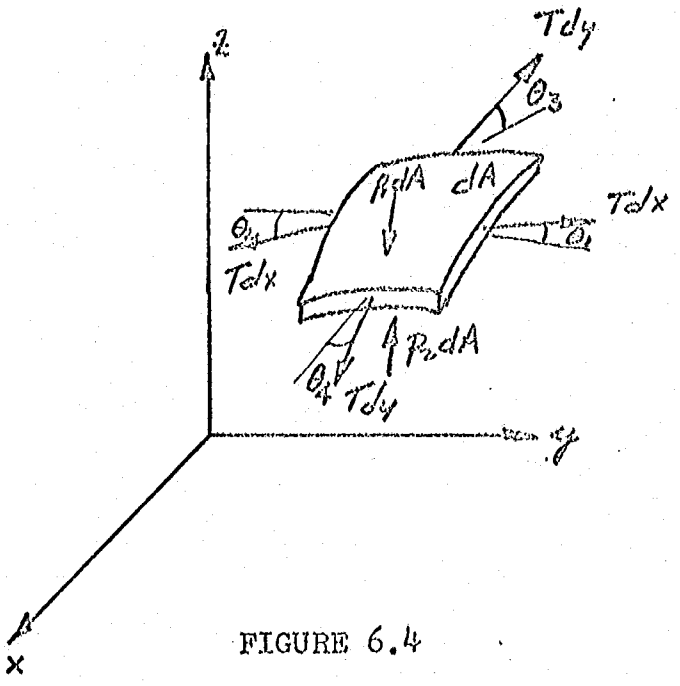

FIGURE 6.4

The forces TdX and Tdy make angles θ_1, θ_2, θ_3, and θ_4 with the x-y plane. The other forces are P_1dA and P_2dA representing respectively the viscous influence of the aqueous humor and the viscous and static influence of the lens interior substance. To derive the equations of motion of a point $z(x,y)$ on the lens capsule we note that

$$\Sigma F_z = m a_z = \rho_A \, dA \, \frac{\partial^2 z}{\partial t^2} \qquad \text{Eq. (6.1)}$$

where ρ_A is the mass density of the lens capsule in kilograms per square meter. From Figure 6.4

$$\Sigma F_z = T[(\sin\theta_1 - \sin\theta_2)dx + (\sin\theta_3 - \sin\theta_4)dy] - (P_1\cos\theta_2 + P_2\cos\theta_1)dA \qquad \text{Eq. (6.2)}$$
$$= \rho_A \, dA \, \partial^2 z/\partial t^2.$$

But if $\theta_1, \ldots, \theta_4$ are small, it is approximately true that*

* These approximations are within 10% if $|\theta_i| \leq 25.8°$
In the case of the lens capsule, $\theta_{i,max} = 25.4°$.

$$\sin\theta_1 = \tan\theta_1 = \left(\frac{\partial z}{\partial y}\right)_1$$
$$\sin\theta_2 = \tan\theta_2 = \left(\frac{\partial z}{\partial y}\right)_2$$
$$\sin\theta_3 = \tan\theta_3 = \left(\frac{\partial z}{\partial x}\right)_3$$
$$\sin\theta_4 = \tan\theta_4 = \left(\frac{\partial z}{\partial x}\right)_4. \qquad \text{Eq. (6.3)}$$

Using Taylor series expansions

$$\left(\frac{\partial z}{\partial y}\right)_1 = \left(\frac{\partial z}{\partial y}\right)_2 + \left(\frac{\partial^2 z}{\partial y^2}\right)_2 dy + O(dy^2)$$

and

$$\left(\frac{\partial z}{\partial x}\right)_3 = \left(\frac{\partial z}{\partial x}\right)_4 + \left(\frac{\partial^2 z}{\partial x^2}\right)_4 dy + O(dx^2).$$

in Eq. (6.2) and Eq.(6.3) gives

$$T dx dy \frac{\partial^2 z}{\partial y^2} + T dx dy \frac{\partial^2 z}{\partial x^2} = -(p_1 + p_2) dA = \rho_A dA \frac{\partial^2 z}{\partial t^2}. \qquad \text{Eq. (6.4)}$$

Equation (6.4) further simplifies to

$$\nabla^2 z = \frac{\rho_A}{T} \frac{\partial^2 z}{\partial t^2} + \frac{1}{T}(p_1 + p_2) \qquad \text{Eq. (6.5)}$$

where

$$\nabla^2 = \frac{\partial^2}{\partial x^2} + \frac{\partial^2}{\partial y^2}.$$

Recall that P_1 represents a pure viscous force dependent only on $\partial z/\partial t$ because of the relatively low viscosity of the aqueous humor. On the other hand P_2 represents static and dynamic forces attributable to the very viscous and incompressible, plastic lens substance. It is easy to show that P_2 must satisfy the equation

$$\frac{\partial p_2}{\partial z} = -\rho_w \frac{\partial^2 z}{\partial t^2} \qquad \text{Eq. (6.6)}$$

Where ρ_v is the mass density of the lens substance in Kg per cubic meter. Thus Eq. (6.5) and Eq.(6.6) combine to give the equations of motion of the lens capsule in the Z direction. These equations, repeated as Eq.(6.7) below,

$$\nabla^2 z = \frac{\rho_A}{T}\frac{\partial^2 z}{\partial t^2} + \frac{1}{T}(p_1 + p_2)$$

$$\frac{dp_2}{dz} = -\rho_v \frac{\partial^2 z}{\partial t^2} \qquad \text{Eq. (6.7)}$$

indicate that the forcing function of these equations is the capsule tension T. This tension with the given boundary and initial conditions determines Z as a function of x, y and t. Knowing Z allows one to calculate the dioptic strength of the lens and thus completes the input/output determination of X_i and X_o of Figure 6.3. Solutions of Eq. (6.7) are presently being sought by means of hybrid simulations. A major problem has been getting realistic values of the parameters since most of them have never been measured. Thus a small program has been undertaken to perform physiological experiments that will measure the pertinent parameters. A subsequent section considers conclusions that may be derived from equation (6.7) in their unsolved form.

e. The Accommodative System as a Time Optimal Controller

Equations (6.7) of the previous section are of interest in their unsolved form since they can be studied in the light of optimal control theory without knowledge of an explicit solution. They allow one to determine the optimal control function for the system for a variety of performance

criteria; in particular, for a minimum time criterion, that is, a time optimal control regime. This criterion allows one to formulate a theoretical explanation of the oft reported lens oscillations that occur in steady state viewing.

If we let $\Delta x = \Delta y = h$ on a finite difference grid formulated to solve Eq. (6.7) it is easy to show that the finite difference equations resulting from (6.7) are

$$-4 z_{ij} + \sum_{-1,0,1}^{p,\ell}{}' z_{i+p,j+\ell} = \frac{h^2 \rho}{T} \ddot{z}_{ij} + \frac{h^2}{T}(p_1 + p_2) \qquad \text{Eq. (6.8)}$$

$$i = 1, 2, \ldots n$$
$$j = 1, 2, \ldots n$$

where i and j are the x and y indices respectively, n^2 the number of grid points, and t the time.

Equations (6.8) clearly indicate that the resulting ordinary differential equations have T (t), the spatially uniform membrane tension per unit length, as their forcing function. It is physiologically obvious that T (t) must have an upper and lower bound as shown in an arbitrary time plot in Figure 6.5.

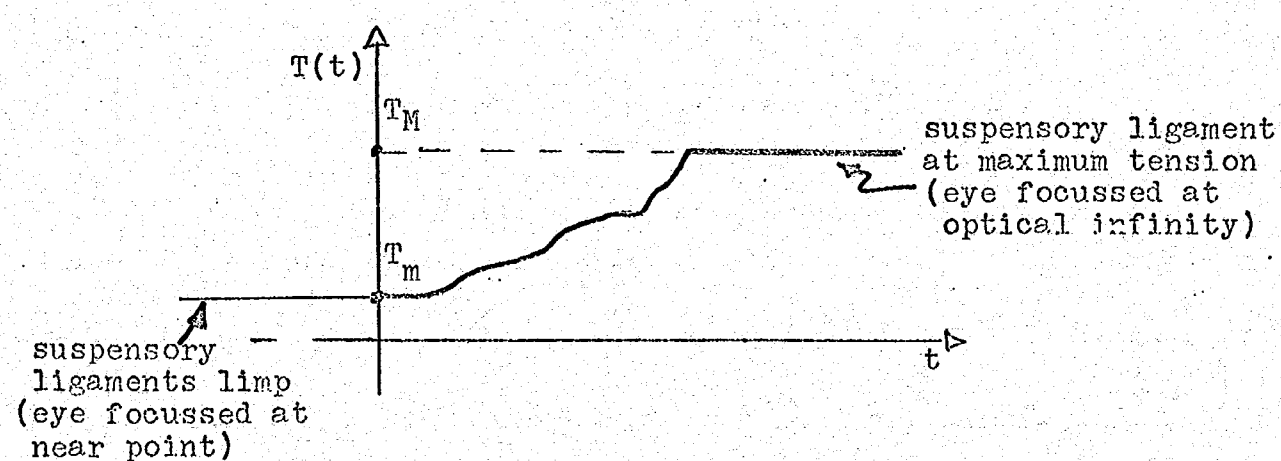

Figure 6.5

From Eq. (6.8) we note that the equations are n^2 in number and second order. This implies a state space vector of $2n^2$ components. If Eq. (6.8) is solved for $\ddot{z}_{ij}$ the result is Eq. (6.9).

$$\ddot{z}_{ij} = \frac{T}{k^2 \rho_A}\left(-4 z_{ij} + \sum_{p,l=-1,0,1}^{} z_{i+p,j+l}\right) + \frac{1}{\rho_A}(p_1 + p_2) \qquad \text{Eq. (6.9)}$$

Let

$$z_{ij} = x_k \qquad z_{i-1,j} = x_{k+3}$$

$$\dot{z}_{ij} = x_{k+1} \qquad z_{i,j+1} = x_{k+4}$$

$$z_{i+1,j} = x_{k+2} \qquad z_{i,j-1} = x_{k+5}$$

$$k = 1, 4, \ldots, n^2$$

This gives the transformed equations the form

$$\dot{x}_k = x_{k+1}$$

$$\dot{x}_{k+1} = \frac{T}{k^2 \rho_A}\left(\sum_{s=1}^{5} x_{k+s} - 4x_k\right) - \frac{p_1 + p_2}{\rho_A} \qquad \text{Eq. (6.10)}$$

To Eq. (6.10) we can apply the Maximum Principle to ascertain the form of T(t) to maximize or minimize some criterion of performance. An obvious one is the time optional criterion where it is required to move the lens from one position Z, to another under the constraint that T(t), the input, must satisfy the inequality

$$T_m \leq T \leq T_M$$

From Eq. (6.10) if ξ is the costate vector then the Hamiltonian for the system is

$$\mathcal{H} = 1 + \xi^T \dot{x} \qquad \text{Eq. (6.11)}$$

Where (T) denotes transpose and the bar denotes a $2n^2$ vector. Equation (6.11) is merely a sum of terms of the form

$$\xi_k x_{k+1} + \xi_{k+1}\left[\frac{T}{\rho_1 \ell^2}\left(\sum_{s=1}^{s'} x_{k+s} - 4x_k\right) - \frac{\rho_1+\rho_2}{\rho_A}\right]$$

and thus $\mathcal{H}$ is a linear function of T(t) for fixed values of ξ and $\underline{x}$. This implies that the time optional control for the system is "bang-bang" i.e. T(t) always resides at either its maximum T_n or minimum T_m, tension per unit length if the plant is to minimize the time to focus. It should be pointed out that a "bang-bang" type control function can also exist for other performance criteria than time.

As of yet the above theory does not explain the oft observed 2 cps accommodative oscillations that occur during steady state viewing or gaze. It is important to note that 2 cps is about the maximum frequency the accommodative plant can respond so that experimental evidence indicates a steady state oscillation at about the maximum frequency response of the system.

Consider now that the system has focused on a target; the control function T (t) must be such that this value of accommodation is maintained in the presence of disturbances. The disturbances tend to change the steady accommodative value and the control responds in such a magnitude as to restore the desired value of accommodation.

It is reasonable to assume that if the control is time optimal then the plant will respond as rapidly as possible to any disturbances and thus will operate at its maximum frequency limit. This limit has been experimentally determined as 2 cps. Thus, an assumption of time optimality yields a reasonable explanation of experimentally determined behavior.

The above analysis is typical of the methods available from control theory as applicable to any system describable by ordinary or partial differential equations. The advantage accruing from such analysis is considerable knowledge about system behaviour without explicit knowledge of solution behavior. Another typical example of a related analysis is Lyapunov stability theory where the stability of the system is determinable without knowing a system trajectory. Due to the complexity of biological systems, such methods are of utmost utility. It should be remembered however that most of the previous analysis is based on conjecture and as such must be verified to be of ultimate value. To this end the experimental equipment must be made available in order to allow rigorous experiments to be performed on the physiological system so that the latest techniques of systems theory can be applied to the resultant model.

SECTION 7

7. UTILIZATION OF IMAGE ERRORS FOR ACCOMMODATIVE CONTROL

We will outline briefly what the main variables are that contribute to the spread function of the retinal image of a point source. Also we will investigate which variables may contain odd-error information for the accommodative control system. No attempt will be made to go into detailed calculations, but rather some estimates of orders of magnitude will be made and results from the literature will be mentioned. One should keep in mind that all quantitative results are usually derived under rather crude assumptions and only represent an approximation of reality.

An ideal optical system, where the object-image relationships are completely governed by the laws of geometrical optics for paraxial rays (rays making small angles with the optical axis) does not exist. The human eye is a good example since the refractive surfaces are not spherical, the index of refraction is not constant in each separate medium, and it shows all the other defects of optical systems in general, such as spherical aberration, chromatic aberration, astigmatism, light scattering, etc. Also the physical wave properties of light that give rise to diffraction effects have to be taken into account. The effect of all these factors is that the optical image of a point source is not a point but a light distribution centered around the point image. This light distribution, contrary to the pure geometrical blur, will in general change asymmetrically if the image goes out of focus in different directions. Hence, we have a possible source here that governs the odd error for the operation of the accommodative control system.

"REPRODUCIBILITY OF THE ORIGINAL PAGE IS POOR."

a. Spherical Aberration. This type of aberration refers to the fact that peripheral light rays are deviated more strongly than central rays close to the optical axis. The phenomenon is not restricted to spherical surfaces but occurs, in general, for every curved surface that separates two media of different index refraction. Figure 7.1 illustrates the effect for incoming rays parallel to the optical axis. M is the image formed by the most peripheral rays and F is the image formed by the most central rays. H is the second principle point and n is the index of refraction of the image space. The amount of spherical aberration is usually expressed

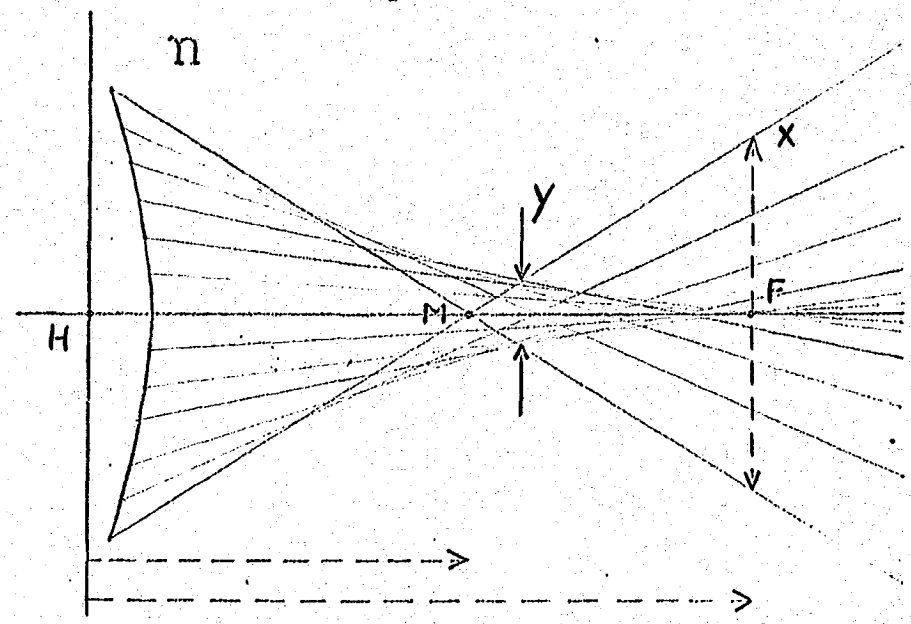

Fig. 7.1

in diopters as the quantity $(\frac{n}{HM} - \frac{n}{HF})$. The distances HM and HF are expressed in meters. It is obvious that the amount of spherical aberration will depend on the diameter of the entrance pupil, the shape of the refracting surfaces, the location of the object point-source, and the refractive indices of the various media. Ivanoff [33] measured the values of spherical aberration for ten subjects and for several levels of accommodation. His mean values are shown in

"REPRODUCIBILITY OF THE ORIGINAL PAGE IS POOR."

Fig. 7.2. As can be seen, the variation in aberration is strongest in the neighborhood of the axis up to 0.5 mm eccentricity. The theoretical curve (shown as a dotted line) was calculated by Ivanoff for the unaccommodated schematic eye. This curve is considerably different from the measured one, probably because of the flattening of the

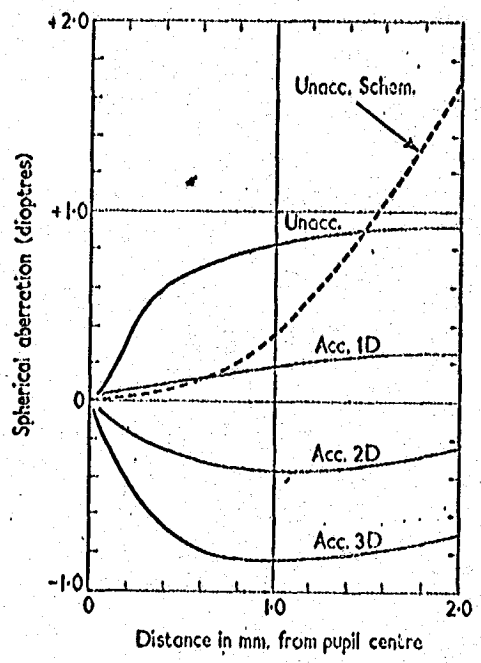

Spherical aberration of the eye, plotted in dioptres against height of incidence in mm. from the pupil centre. The unbroken curves, each marked with the stimulus to accommodation, show Ivanoff's mean results for 10 subjects. The dotted line shows the theoretical spherical aberration, computed by ray-tracing methods, of the unaccommodated schematic eye.

Fig. 7.2

ocular refracting surfaces in the periphery and because of the refractive index gradient in the crystalline lens.

In order to obtain a very rough order of magnitude for the contribution of spherical aberration to the spread function in the unaccommodated eye, we assume the following numerical values in Fig. 7.1

Exit pupil = 4 mm HF = 22.5 mm n = 1.336.

For a 2 mm eccentricity and relaxed accommodation the amount of spherical aberration is 0.9 diopters. This means that the distance HM can be found from the equation: $\frac{1336}{HM} - \frac{1336}{22.5} = 0.9$. And HM = 22.17 mm.

Furthermore, the "spread" x in the paraxial focal plane can be found from the equation: $\frac{x}{4} = \frac{22.5 - 22.17}{22.17}$ or $x \approx 0.06$ mm = 60 μ. The smallest "spread" y corresponds to the diameter of the circle of least confusion, and for this plane the spread function is usually determined experimentally.

It is difficult to calculate y exactly, but the order of magnitude is given by $y = \frac{x}{5}$. This results in a value for $y \approx 12 \mu$. Often the retinal distance is expressed in degrees or minutes of arc, measured with respect to the second nodal point. The relationship is y (measured in mm) $\approx \frac{1}{200} \varphi$ (measured in minutes of arc). In other words the "spread" would amount to approximately $12 \times 10^{-3} \times 200 = 2.4$ minutes of arc.

Figure 7.3 shows the experimental spread functions as determined by Krauskopf [37] for the unaccommodated eye and various pupil diameters. Comparing his results for the 4 mm pupil with our calculation shows that probably 25% of the spread function is caused by spherical aberration.

"REPRODUCIBILITY OF THE ORIGINAL PAGE IS POOR."

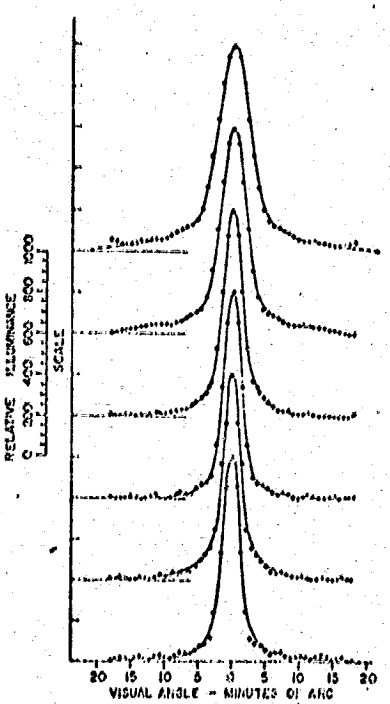

Reconstructed retinal images of bright vertical-line target (1.6′ wide) for various pupil diameters. Ordinates displaced in equal vertical steps. Pupil diameters 3, 4, 5, 6, 7, and 8 mm from bottom to top.

Figure 7.3

Under certain assumptions Fry [24] calculated from Ivanoff's data the light distribution of the retinal image. In these calculations, which are rather complicated, he took the wave properties of light into account. The results are summarized in Fig. 7.4.

"REPRODUCIBILITY OF THE ORIGINAL PAGE IS POOR."

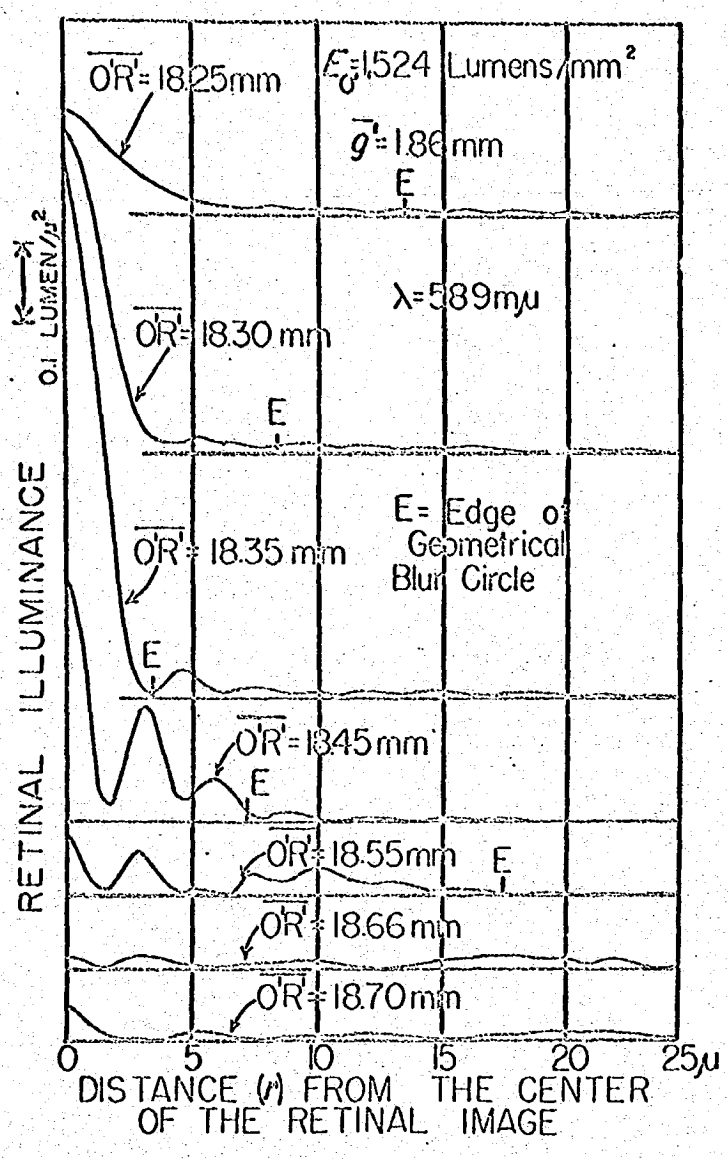

RETINAL IMAGES OF A MONOCHROMATIC POINT IN AN EYE SUBJECT TO SPHERICAL ABERRATION AND THROWN OUT OF FOCUS TO VARIOUS DEGREES.

The eye has been thrown out of focus by changing the distance from O to R. Each curve shows the distribution of illuminance E along the radius of the image.

Fig. 7.4

As can be seen, for the "in focus" condition ($\overline{O'R'}$ = 18.35 mm) and a pupil diameter of 3.7 mm, the blur circle has a diameter of approximately 7μ. This compares satisfactorily with our earlier rough estimation of the order of magnitude of 12μ.

Interesting is the change in light distribution depending on which direction the image is out of focus. It is almost certain that most of the image evaluation for the accommodative system occurs in the fovea. The fovea consists of some 34,000 densely packed cones, which have an average diameter of approximately 1.5μ. Individual cones could very well detect the change in light distribution as shown in Fig. 7.4, and obtain odd error information about the out-of-focus direction. However, up to now there is no experimental evidence for this.

It has been suggested [22] that the use of annular pupils would nullify the contribution of spherical aberration to the blur in the retinal image. This would make experimentation possible to determine the role of spherical aberration in the accommodative error. However, the spherical aberration in the human eye is not radially symmetric with respect to the optical axis, but varies in a non-regular fashion, depending on the subject and the accommodative state of the eye. This makes a quantitative approach to the problem rather impossible.

b. Chromatic Aberration. Chromatic aberration is caused by the fact that the index of refraction is not constant but depends on the wavelength. The result is that when the eye is in focus for yellow light, the foci for blue and red light are in front of and behind the retina, respectively. This is shown schematically in Fig. 7.5. The spread function

"REPRODUCIBILITY OF THE ORIGINAL PAGE IS POOR."

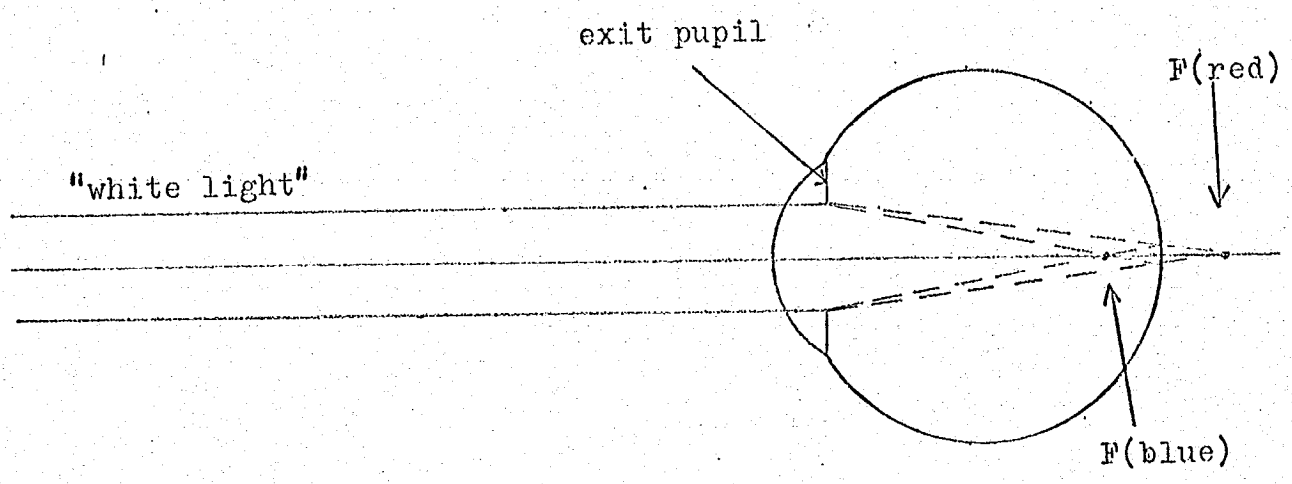

Fig. 7.5.

due to chromatic aberration depends on the spectral composition of the incident light beam, the diameter of the exit pupil, and the optical properties of the eye. Ivanoff [33] measured also the amount of chromatic aberration of the human eye as a function of the wavelength. His results are shown in Fig. 7.6.

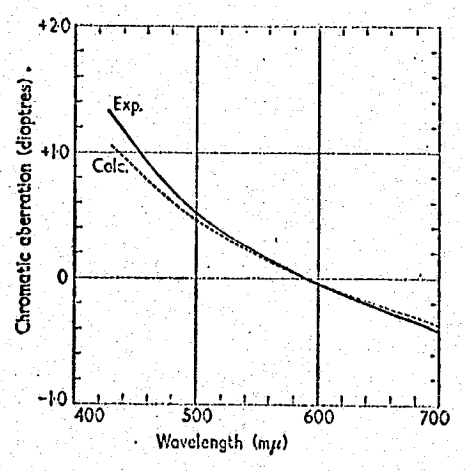

Chromatic aberration of the eye, plotted in dioptres against wavelength. The unbroken curve represents the mean of Ivanoff's results, the dotted curve showing the theoretical values found from calculation on the schematic eye.

Fig. 7.6

There is some ambiguity as to how the amount of chromatic aberration is defined. If we assume that it is equal to the distance in the object space between the two points for which the eye is in focus for different colors (in diopters), the diameter of the blur circle can be calculated simply by using Equation (4.3)

$$B = 0.018\ P|y - x| \text{ mm}$$

B = diameter blur circle

P = pupil diameter

$|y - x|$ = chromatic aberration in diopters

Assuming the eye is focused for a wavelength in the middle of the visible spectrum (e.g. 550 $m\mu$), then, for white light $|y - x|$ will be of the order of 0.5 diopters according to Fig. 7.6.

For a pupil diameter of 4 mm, the diameter of the blur circle will be equal to:

$$B = 0.018 \times 4 \times 0.5 = 0.036 \text{ mm} = 36\mu.$$

The light distribution in the blurred image will, in general, be maximal in the center and decrease rather rapidly toward the periphery, especially if we take into account the effectiveness of light of different wavelengths to stimulate the photoreceptors. This will result in a much smaller "effective" blur circle. Other ways of measuring the chromatic aberration lead to a same order of magnitude for the radius of the blur circle. The chromatic aberration will, of course, contain information regarding the direction in which an object is out of focus under "white" illumination conditions.

When the eye is under-accommodated the blur will contain more blue in the periphery and more red in the center. When the eye is over-accommodated these colors will be just reversed. The use of monochromatic light will nullify this contribution to a possible odd error detector mechanism in the accommodative control system. Fincham [22] performed experiments along these lines, in order to find out how important color is for the achievement of correct accommodative control. His experiments show that in 60% of a large group of subjects the chromatic aberration is possibly an important stimulus to accommodation. In 40 % of his subjects the chromatic aberration did not seem to have any effect, and these subjects could control their accommodation quite well under monochromatic illuminating conditions. This was also found by other investigators. [55] The conclusion is that at least in some subjects another factor must exist to provide odd error information about the blurred image.

c. Astigmatism. This optical aberration is caused by the fact that often the radius of curvature of the refracting surfaces is not constant but varies if measured in different meridians. Usually major and minor meridians can be distinguished, where the radius of curvature changes gradually from one meridian to the other. When the meridian having the greatest radius of curvature is at right angles to the one having the least, the astigmatism is called regular astigmatism; otherwise it is irregular. Astigmatism is generally regular. Its effect on the image formation process is illustrated in Fig. 7.7.

"REPRODUCIBILITY OF THE ORIGINAL PAGE IS POOR."

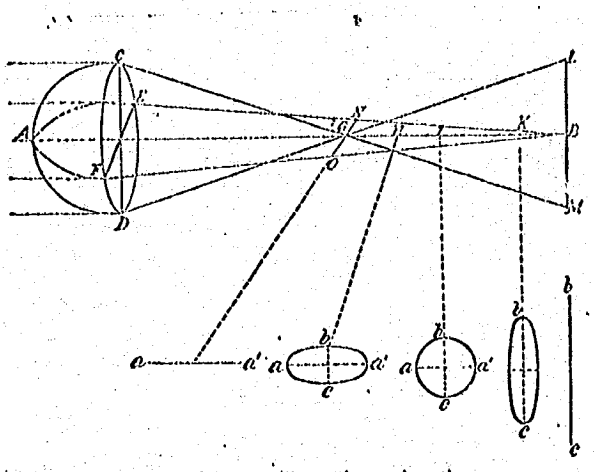

--Diagram illustrating astigmatism.

Fig. 7.7

The main cause for astigmatism is the cornea. The difference in power (in diopters) between the major and minor meridian plane is usually called the amount of astigmatism (diopters). A slight amount of astigmatism (up to 0.25 diopters) is quite normal in every person and is called physiological astigmatism. Higher amounts of astigmatism (generally less than 1.25 diopters) need correction with glasses. In about 90% of the cases the meridian plane of greatest curvature is the vertical plane ("with the rule" or "direct" astigmatism). The opposite condition is called "against the rule" or "inverse" astigmatism.

When the astigmatic optical system has circular apertures (as the human eye) the image of a point source varies considerably, depending on the position of the image plane. In case of regular astigmatism this image varies from a horizontal line corresponding to the power in one principle meridian plane, via a horizontal ellipse, a circle, a vertical

ellipse, to a vertical line in the other principle meridian plane (cf. Fig. 7.7). In case of irregular astigmatism the ellipses and lines are, in general, tilted. If the distance between the plane DECF in Fig. 7.7, and the point B is assumed to be 22 mm and the index of refraction of the image space is 1.336, then the distance GB is approximately 0.35 mm for an astigmatism of 1 diopter, and approximately 0.1 mm for an astigmatism of 0.25 diopter.

Consequently, the dimensions of the lines aa' or bc are approximately 60μ and 20μ for an amount of astigmatism of 1 diopter and 0.25 diopter respectively, and a pupil diameter of 4 mm.

In a normal person ($<$ 0.25 diopter astigmatism), the radius of the circle aba'c will be smaller than 20μ. If we estimate this radius at about 10μ, then the astigmatism can contribute something of the order of 20% to the point spread function.

It is obvious that astigmatism would provide an excellent clue concerning the out-of-focus direction and could serve as an odd error for the accommodative control system. Even slight amounts of astigmatism result in changes in shape of the error-function (retinal blur) that could be detected by single receptors. However, no experimental evidence exists if, and to what extent, astigmatism plays a role as a stimulus for the human accommodative system.

d. Light Scattering. It is estimated that of the amount of light originally incident at the cornea only 50% reaches the retina, due to absorption and scattering in the ocular media in front of the retina. Of this 50%, probably only 20% is effective in stimulating the photoreceptors due to scattering within the retina and absorption by nonphotosensitive retinal substances.

This light scattering will produce a spread function around the geometrical point image at the retina. According to Vos [56] the main sources of stray light are: the cornea, the lens and the fundus, which contribute with equal shares (order of magnitude) to the total amount of stray light. Theoretical predictions about the total amount of stray light are very difficult because of the strong dependence on the angle of incidence of the light and the nature of the scattering particles. However, we can say that, in general, the blur caused by stray light will not contain any odd error information for the accommodative control system.

e. Diffraction. This effect is caused by the presence of a finite aperture in every optical system and can be explained readily by the wave properties of light. The result is that the edge of the "geometrical shadow" is not sharp, but consists of alternating dark and light bands. Contrary to the optical errors discussed before, the importance of which decreases with smaller pupils, the effect of diffraction increases with smaller pupils. The light distribution in the image can be calculated using the formulas derived in Section 5. However, this is very complicated and not straightforward. The light distribution in a point

"REPRODUCIBILITY OF THE ORIGINAL PAGE IS POOR."

image is shown schematically in Fig. 7.8.

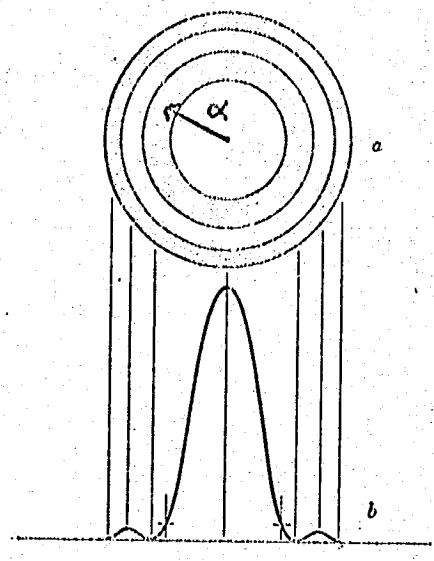

Fig. 7.8

Under certain simplifying assumptions it can be shown that the angular radius α of the first dark ring is approximately equal to: $\alpha = \frac{1.22\,\lambda}{P}$ where λ is the wavelength of the light and P is the diameter of the aperture. The angular distance is measured with respect to the center of the aperture. For the human eye we find approximately: $\alpha \approx \operatorname{tg}\alpha \approx \frac{r}{20}$, where r is the radial distance at the retina from the center of the point image (in mm). This means that for a 4 mm pupil and a wavelength of $\lambda = 555\,m\mu$ the central disc in the diffraction image has a diameter of

$$d = 2r = 40\alpha = \frac{40 \times 1.22 \times 555 \times 10^{-9}}{4} = 6.8\,\mu .$$

Fry [24] calculated diffraction images for various degrees of out-of-focus. As can be seen, in the ideal situation where diffraction is the only source of error, the diffraction pattern changes quite drastically, but it changes symmetrically for equal amounts of under-accommodation or over-accommodation (in diopters), (cf. Fig. 7.9).

"REPRODUCIBILITY OF THE ORIGINAL PAGE IS POOR."

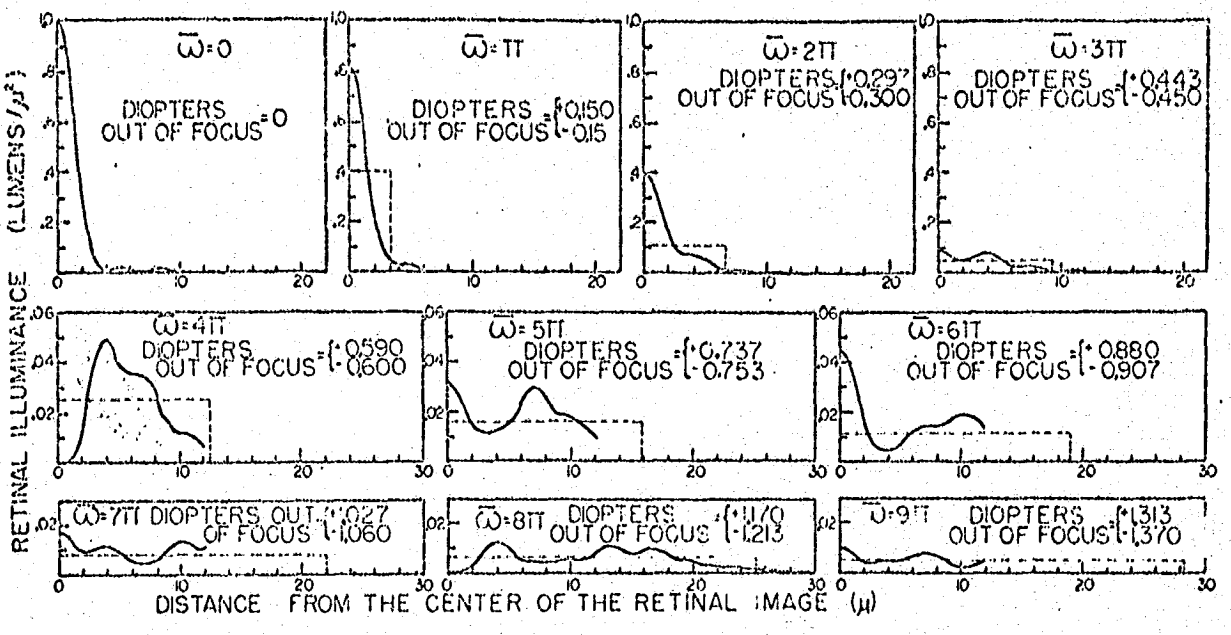

PHYSICAL IMAGES OF A MONOCHROMATIC POINT.

Distributions of illuminance representing retinal images of a monochromatic (589) mμ point source with the eye thrown out of focus to various degrees. The illuminance E_0' at the center of the exit pupil is 3,947 lumens/mm^2. The diameter ($2\bar{g}'$) is 2.624 mm. The distance ($O'\bar{R}'$) from the plane of the exit pupil to the retina is equal to 18.66 mm, and the eye is thrown out of focus by placing lenses in the primary focal plane. Plus and minus values indicate that the eye is overaccommodated or underaccommodated respectively. The various curves are based on calculations made by Lommel and Epstein. The dotted curves represent geometrical images.

Fig. 7.9

Concluding we can say that diffraction gives a sizable contribution to the spread function but does not provide any odd error information.

f. Other Possible Error Mechanisms to Operate the Accommodative Control System.

So far we only mentioned the most important errors in the retinal image formation and we will not consider less important aberrations like coma, curvature of the image, etc.

However, there may be other phenomena that are used for error detecting purposes. Fincham [22] mentions the fact that his subjects who do not utilize chromatic aberration, probably derive information from small movements of the image across the retina. These movements would come from small scanning type fixation movements of the eye of the order of 6 minutes of arc. Fig. 7.10 shows the hypermetropic (under-accommodated) and myopic (over-accommodated) conditions. In both situations the eye has turned to the right from the point of fixation, so that the blurred image falls somewhat to the right of the center of the fovea M. As can be seen from Fig. 7.10, in the hypermetropic situation the light rays closer to M become more normal to the retina, while in the myopic

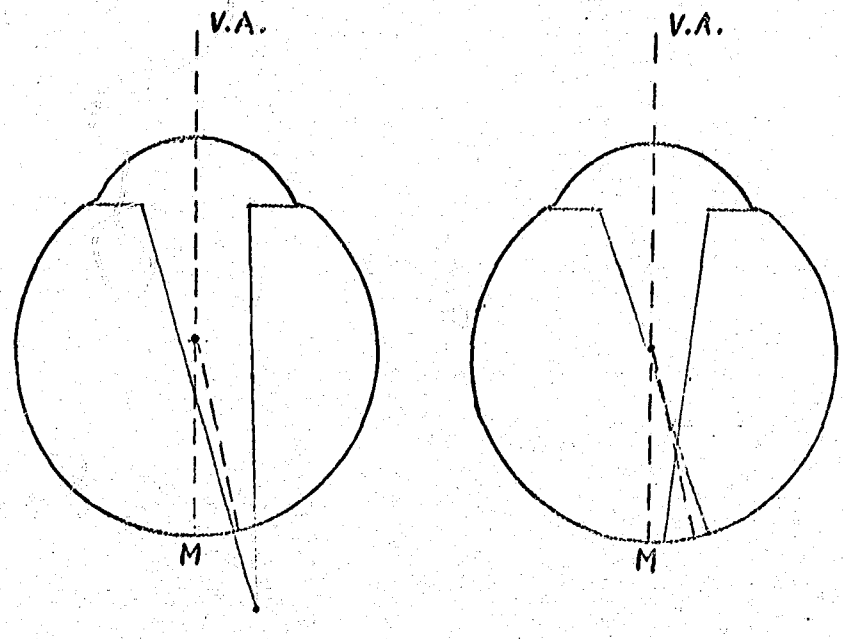

(a) Hypermetropia (b) Myopia

Fig. 7.10

situation the light rays farther away from M become more normal. In its simplest form, the Stiles-Crawford effect is the property of the cone to be more efficient in "trapping" of light that is incident parallel to its axis than of light that is incident at a certain angle. This means that light rays normal to the retina have a higher apparent brightness than light rays making an angle with the retina. In this way the hypermetropic state could be distinguished from the myopic state by making small eye movements. However, the difference in light intensity is quite small for these small eye movements, although Fincham notes that this may still be sufficient, since only the operation of a reflex of the lower centers is involved.

A second possibility for odd error information are the lens oscillations found by Campbell, et.al.[9] The lens power turns out to be fluctuating irregularly with amplitudes ranging between 0 and 0.3 diopters. However, a significant amount of power seems to be present in the frequency range around 2 cps. If for instance, the change in blur diameter was compared with the phase of the lens oscillation that causes the change in blur diameter, the necessary odd error information could be extracted. There is no experimental evidence that the lens oscillations are indeed used for this purpose.[55,53,54] In the model for accommodation proposed by Crane[15] they appear to be no more than normal accommodation correction cycles.

Finally, when an object moves in the space in front of our eyes, there are numerous clues that will tell us if the object is moving farther away or coming closer. For instance,

if it comes closer its size and its brightness usually increase. Also, if we view the object with both eyes, the movements of the retinal images will tell us something about the change in distance of the object to our eyes. This is shown schematically in Fig. 7.11.

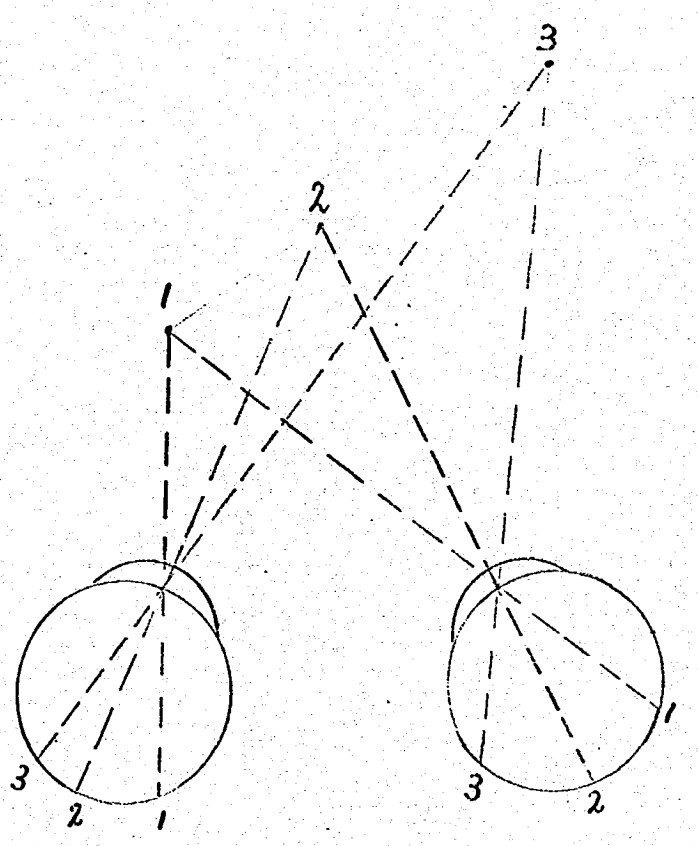

Fig. 7.11

Concluding we can say that still an enormous amount of research has to be done to determine the role of these variables in the control of accommodation. Table 7.1 summarizes the results of this section.

IMAGE ERROR OR VARIABLE	ERROR SIGNAL for ACCOMMODATION	CONTRIBUTION TO MONOCHROMATIC POINTSPREAD FUNCTION
Spherical abberration	possible	25%
Chromatic aberration	possible	--
Astigmatism	possible	20%
Light scattering	no	?
Diffraction	no	15%
Image movement (monocular)	possible	?
Image movement (binocular)	possible	--
Lens oscillations	possible	?

Table 7.1

"REPRODUCIBILITY OF THE ORIGINAL PAGE IS POOR."

SECTION 8

8. MICROSCOPIC ANATOMY OF THE RETINA.

In this section we will briefly summarize the anatomical structure of the retina. The retina is the innermost of three layers that comprise the wall of the eyeball: the retina, the choroid, and the sclera (cf. Fig. 8.1).

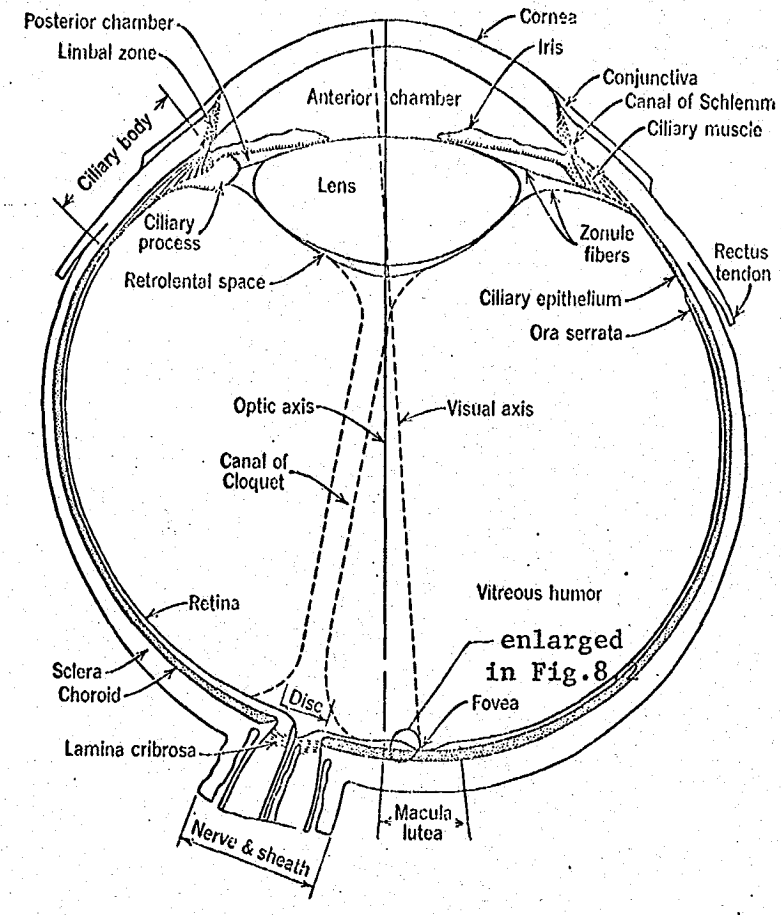

FIG. 8.1 Horizontal section of the right human eye. (From Walls, 1942, as modified from Salzmann, 1912.)

As can be seen, the retina covers about half of the eyeball resulting in a visual field of approximately 180°. However, the visual accuity diminishes rapidly toward the periphery. The region of highest visual accuity is found at the fovea and comprises an area of approximately 1^{0}. This is the region where an object is imaged under fixating conditions.

"REPRODUCIBILITY OF THE ORIGINAL PAGE IS POOR."

Also this is the region where most probably the blur of the image is evaluated in order to get a meaningful error signal for the accommodative control system.

According to Polyak, [44] ten layers can be distinguished in the retina (cf. Fig. 8.2).

HISTOLOGICAL LAYERS OF THE RETINA
AND ITS INTERNEURONAL CONNECTIONS

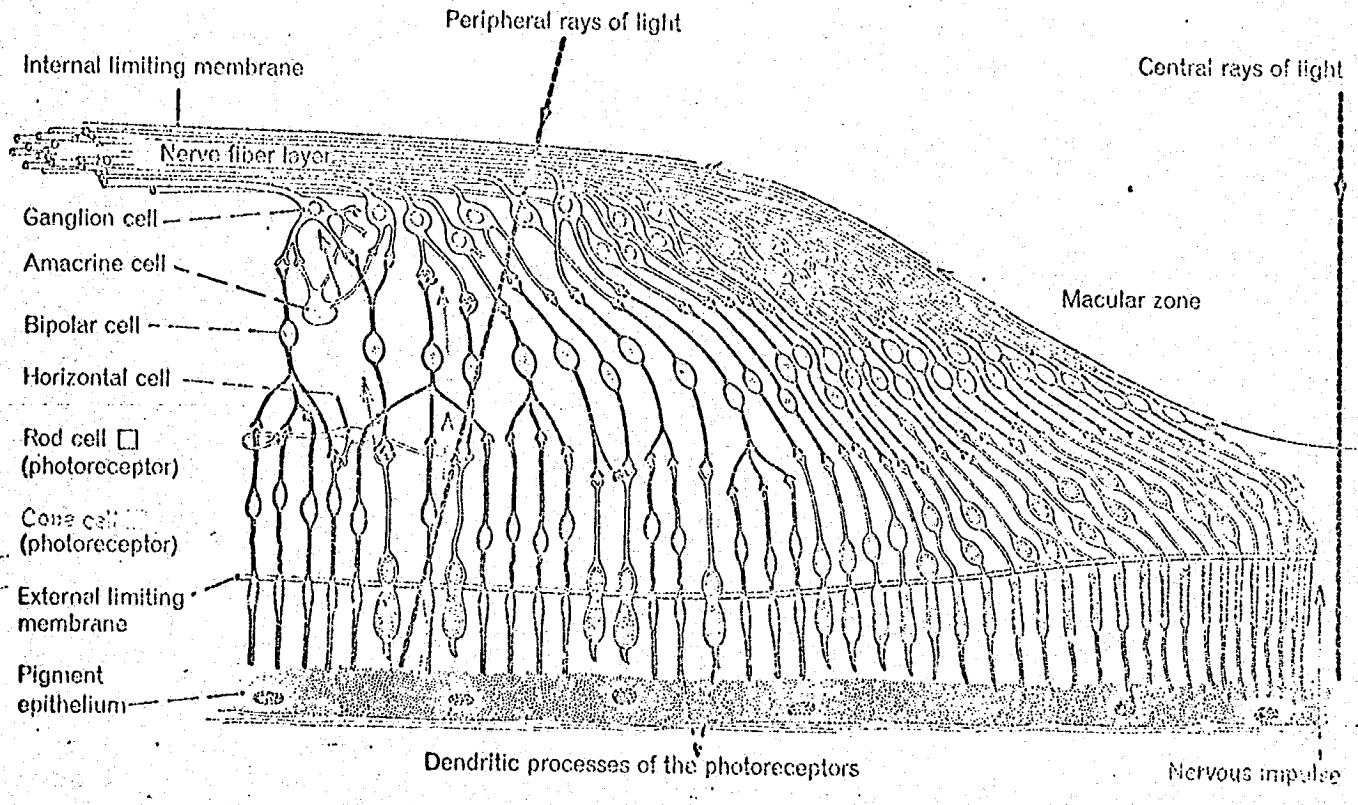

Fig. 8.2

They are:

1. Pigment epithelium - heavily absorbing medium.
2. Rod & cone layer - these are the actual photoreceptors.
3. External limiting membrane.

4. Outer nuclear layer - cell bodies and nuclei of the receptors.
5. Outer plexiform layer - contains fibers from primary receptors and their synapses with dendrites of bipolar and horizontal cells.
6. Inner nuclear layer - contains the bipolar cells.
7. Inner plexiform layer - includes fibers from bipolar cells and their synapses with dendrites of ganglion cells.
8. Ganglion cell layer.
9. Layer of optic nerve fibers.
10. Internal limiting membrane.

There are somewhere between 75-150 million rods distributed over the retinal surface. There are about 6-7 million cones, most densely packed in the fovea centralis. The thickness of the rods varies from the fovea toward the periphery from 1μ to 2.5μ. Their average length is 60μ. The outer segments penetrate in the pigment epithelium, the inner fibers extend into the outer nuclear layer and connect the rods to their cell bodies. From the cell bodies fibers extend into the outer plexiform layer where synaptic contact is made with dendritic filaments of bipolar cells. The cones are found in a wider variety of sizes. The foveal cones are similar in shape to rods. They have a thickness of approximately 1.5μ and may reach a length of about 70μ.

Figure 8.3 shows the distribution of rods and cones along a horizontal meridian of the retina. Before the light reaches the photoreceptors, it has to go through several layers containing nerve cells and nerve fibers. This will certainly

give rise to stray light and absorption (in Section 7 d this was called the fundus contribution). The fovea is a depression in the retina (cf. Fig 8.1 and Fig. 8.2) at the expense of layers 6-9.

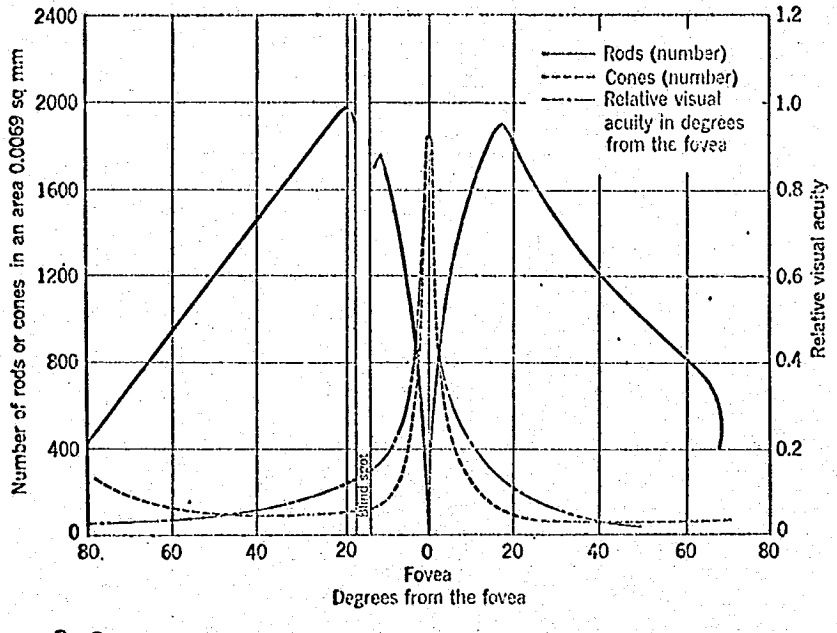

FIG. 8.3 Distribution of rods and cones along a horizontal meridian. Parallel vertical lines represent the blind spot. Visual acuity for a high luminance as a function of retinal location is included for comparison. (From Woodson, 1954; data from Osterberg, 1935, and Wertheim, 1894.)

This means that an important source of image distortion has been diminished, namely the nerve fibers and blood vessels in these particular layers. It makes the foveal region very suitable for sharp vision and detection of the microstructure of the visual image. The foveal region is approximately 1500μ wide. Its central area (central fovea) is 500μ wide, rod free, and contains approximately 34,000 cones.

For the middle and far periphery of the retina it was found that approximately 100 rods converge onto 17 bipolar cells, which, in turn, converge onto 1 ganglion cell. Particularly in the central region of the retina there can be found monosynaptic bipolars and monosynaptic ganglion cells which may provide direct links between single cone receptors and more central regions of the brain.

The rod receptors are supposed to mediate vision under low illuminating conditions (scotopic vision) with no color distinguishing capabilities. The cone receptors mediate vision under normal and high illuminating conditions (photopic vision), and have color distinguishing capabilities.

The axons of the ganglion cells run together in the nerve fiber layers and constitute the beginning of the optic nerve, which leaves the eyeball at the blind spot or optic disc (cf. Fig. 8.1). The region of the blind spot does not contain any photoreceptors as can be seen from Fig. 8.3. On the basis of light microscopy it is estimated that the optic nerve consists of approximately 10^6 fibers. However, this number may be found to be higher if more sophisticated techniques are used. Little is known about the processing of visual information by the various elements in the human retina. The work by Lettvin, McCulloch, Maturana and Pitts [39] on the frog's retina and the work by Hubel and Wiesel [32] on the cat's visual field are important steps in the direction of understanding this complicated process.

Summarizing, we can say that the retinal anatomy is fairly well known. However, the function of the various elements in image evaluation, recognition, and interpretation is still rather obscure and during the past few years, research has just started to learn more about these processes. The exact role of any of the retinal receptors, in providing inputs to the accommodative system, is still unknown.

SECTION 9

9. ACCOMMODATIVE SYSTEM NEUROLOGICAL PATHWAYS

The signal pathways from the retina to higher brain centers and from these centers back to the ciliary muscles that control the shape of the lens, are part of the so-called "near reflex". Figure 9.1 shows schematically the nerve paths and relay stations. This is a highly simplified

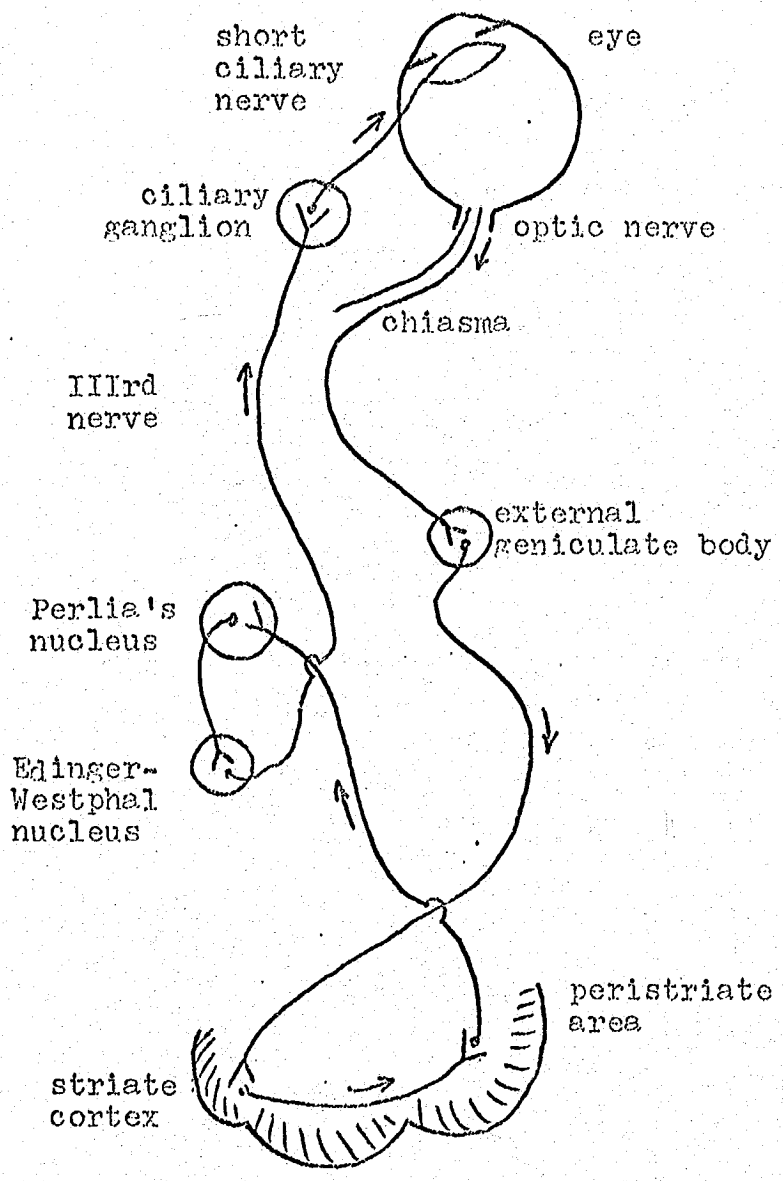

Fig. 9.1

schematic, some of the pathways are not too well established and there may be additional connections that are unknown as yet.

When an object comes near and a person is requested to fixate this object, three main events can be distinguished.

First, the medial or internal rectus muscles are innervated so that both eyes turn in, and the object is imaged on both foveas. This results in the perception of one single fused image.

Second, the pupil contracts. This results, in general, in a reduction of the image errors and increases the depth of focus.

Third, the ciliary muscles are innervated. This increases the power of the eye lens so that the retinal image will be in focus.

The medial recti muscles, the ciliary muscles, and the sphincter muscle of the pupil, are all innervated by branches of the IIIrd (cranial) nerve. There is a high degree of coordination between these actions, but very little is known about the quantitative relationships.

As mentioned before, the accommodation reflex is activated in the retina, probably exclusively in the fovea. The afferent fibers travel up the optic nerve, and pass the optic chiasma (where fibers from the two nasal parts of the retina cross over). Then the fibers travel via the optic tract and are relayed in the external geniculate body. From there a further neuron travels to the striate area of the calcarine cortex (area 17), which is the primary visual area of the cortex. From here the reflex path is relayed to the peristriate area (area 19), which is the secondary visual area of the cortex. The efferent path travels to Perlia's

nucleus via the occipito-mesencephalic tract. After this a connection is made with the Edinger-Westphal nucleus. From this nucleus the efferent path travels down the IIIrd nerve. Fibers for the accommodation reflex relay in the ciliary ganglion from which post-ganglionic fibers innervate the ciliary muscles.

Very little is known about the character of the signals, the properties of the relay stations, and the dynamics of the signal transmission from one part of the system to another. Again we stress the fact that some parts of the signal-flow in Fig. 9.1 are rather speculative and may be subject to changes as more experimental evidence becomes available.

SECTION 10

10. INSTRUMENTATION REVIEW OF DYNAMIC OPTOMETERS

In this section we will give a brief review of the basic principles underlying the operation of dynamic optometers. By a dynamic optometer, we mean an instrument that is capable of measuring instantaneously and objectively the refractive state of the eye. In that way, the dynamics of the accommodative response can be investigated. Also a detailed input-output analysis of the accommodative control system under various modes of operation (open loop, closed loop, even or odd error operation, etc.) can be performed.

a. The Scheiner Method.

Figure 10.1 shows the so-called Scheiner[25] principle, that in one way or another serves as the basis for most of the dynamic optometers which are up to now described in the literature. A light source S is imaged with the lens L on a plane A via two entrance pupils. The entrance pupils are separated by a distance d and located closely to the lens L. If the light source and the plane A are conjugate, we will see a single, sharp image of S on A (see Fig. 10.1). If however, the light source and the plane A' are not conjugate, we will see an unsharp, double image of S on A'.

Two important factors concerning this double image should be taken into account. First, the unsharpness of each separate image is directly proportional to the width of each entrance pupil. Consequently, the smaller the entrance pupil is, the better is the definition of the location of the retinal double images. On the other hand, in that situation the total

"REPRODUCIBILITY OF THE ORIGINAL PAGE IS POOR."

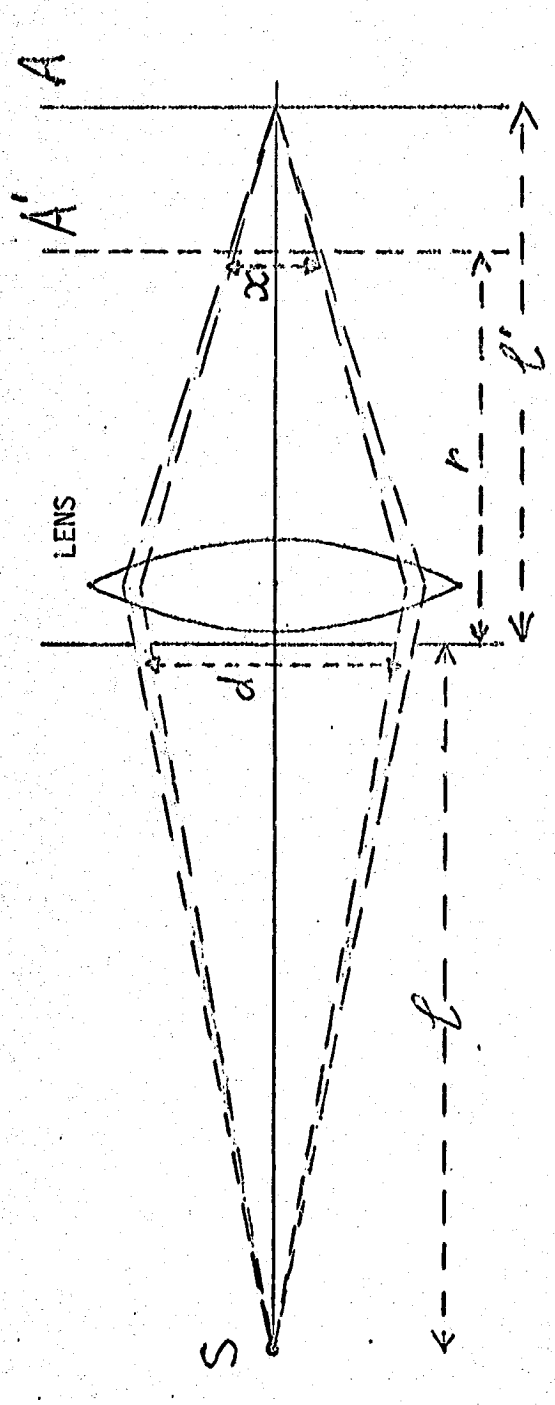

THE SCHEINER PRINCIPLE

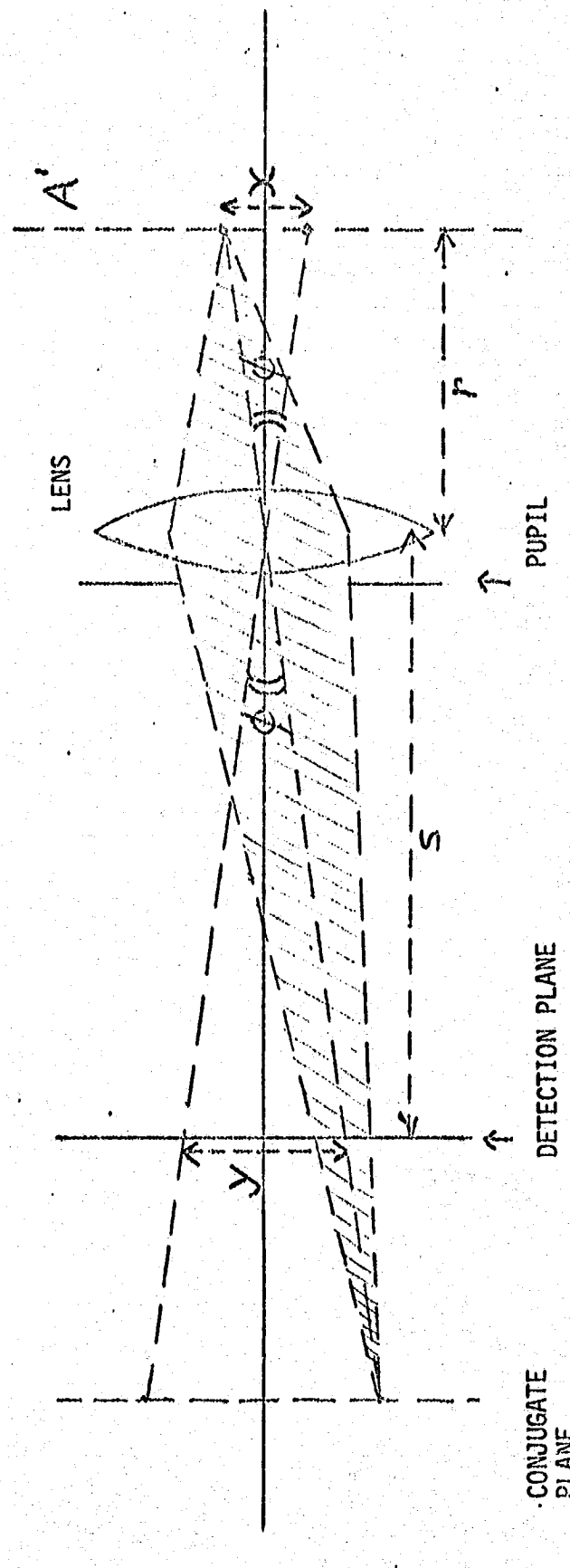

FIGURE 10.1

amount of light contained in the retinal image becomes smaller too, which leads to detection problems. Obviously, a compromise has to be found depending on the particular experimental conditions. Second, the separation of the two images in the double image depends on several factors. Let us assume that in Fig. 10.1 the plane A' is fixed. From the geometry of the figure we find easily:

$$\frac{x}{d} = \frac{l' - r}{l'} = 1 - \frac{r}{l'} \qquad \text{Eq. (10.1)}$$

Expressing the distances r and l' in diopters R and L', respectively, and using the image condition $L' = L + F$ we find:

$$\frac{x}{d} = 1 - \frac{L + F}{R} \qquad \text{Eq. (10.2)}$$

In Eq. (10.2) F is the focal length of the lens in diopters and L is the distance between the light source S and the lens, measured in diopters. Equations (10.1) and (10.2) hold under the assumption that the lens is infinitely thin and that the double-aperture coincides with the lens.

From Eq. (10.2) we can find how the distance x changes with a change of the power F of the lens, by differentiation of x with respect to F

$$\frac{dx}{dF} = -\frac{d}{R} \qquad \text{Eq. (10.3)}$$

This means that if the distance x is used as an indication of the power of the lens, the highest sensitivity is achieved by choosing d as large as possible and R as small as possible.

In the case of the human eye lens we are dealing, of course, with a thick lens and the aperture will not exactly coincide with the lens. But still Eq. (10.3) provides the basic parameters that determine the sensitivity of the method. Furthermore, the plane A' is the retina which means that the distance R is fixed. The maximum distance d is limited by the pupil size and an additional complication is that the pupil diameter varies both with accommodation and retinal illumination. We have to make sure that the distance d falls within the limits of the smallest pupil that occurs under the particular experimental conditions.

In a practical situation d = 4 mm and R = 50 D which makes $\frac{dx}{dF} = -0.02$mm/Diopter.

The wavelength of the light is usually chosen in the infra-red or near infra-red, to avoid pupillary reactions and interference with the normal visual function of the subject.

The next problem is to evaluate the distance x of the retinal double-image in an objective way. Since it is impossible to place light sensitive transducers at the plane of the retina, this retinal double-image has to be re-imaged via the eye-optics and, if necessary, via some additional lenses, in order to obtain a real image of the retinal plane in the "outside world". In the second part of Fig. 10.1 the situation is shown where the retinal plane A' is re-imaged via the eye-optics only (for simplicity represented by a single lens). Usually, the detection plane, where the photosensitive transducers are located, will not coincide with the conjugate plane of the retina. This is simply because the position of this conjugate plane is not constant but depends on the accommodative

state of the eye.

The reflected light rays, coming from one of the retinal double-images, are shown in Fig. 10.1. From the geometry of this figure, it can be derived easily, that for the distance y between the centers of the blurred images in the detection plane the following formula holds as a very good approximation:

$$\frac{y}{s} \approx \tan\phi = \frac{x}{r} \qquad \text{Eq. (10.4)}$$

Using Eq.(10.2) we find for the distance y:

$$y = - sd(L - R + F) \qquad \text{Eq. (10.5)}$$

Note that the quantities L, R and F are defined in connection with Eq. (10.2)

From Eq. (10.5) it follows that again y is a linear function of the lens-power F (in diopters). A measure of the sensitivity is the magnitude of the derivative

$$\frac{dy}{dF} = - sd \qquad \text{Eq. (10.6)}$$

If in Eq. (10.6) d = y mm and S = 100 mm, then,

$$\frac{dy}{df} = - \frac{4}{1000} \times \frac{100}{1000} \text{ meter/diopter} = 0.4 \text{ mm/diopter}$$

The highest sensitivity is achieved again if d is as large as possible and s is as large as possible. However, with this latter condition we have to be careful. As the distance between the conjugate plane and the detection plane increases, the definition of the image decreases (it becomes more and more blurred) and also the illumination of the image per unit area decreases. Here again one has to be cautious with imposing general design criteria on the construction of

an optometer using the Scheiner principle. Often a compromise has to be found depending on specific experimental conditions, such as, for example, the minimum pupil diameter, the area of linear operation of the photosensitive transducer in the detection plane, the light sensitivity of the transducer, etc. Judging from the literature, the following criteria seem to be generally accepted:

1.) Choose the distance d as large as possible under the experimental conditions.

2.) Use a differential method to determine the distance y in the detection plane. The determination of y is not so much affected by the defocussing of the image in the detection plane.

3.) Use near-infra-red or infra-red light.

4.) Interrupt the incoming light beam periodically. This involves the use of a phase and frequency sensitive AC detection method instead of a DC detection method. The obvious advantage is that disturbing signals (light reflections) which are not synchronous with the incoming beam, will not affect the measurement.

In the following paragraphs, the various dynamic optometers based on the Scheiner principle will be discussed briefly.

1. Campbell-Robson Optometer.[10] The optical details of the incoming light paths are shown in the upper part of Fig. 10.2.

- Light source. Two parallel coiled-coil filaments 6 mm long and 3 mm apart, rated each at 36 watt, 24 volt.
- Lens L_1. Produces a double image of the filament at the double aperture (8 cm focal length). An infra-red filter is placed between L_1 and the double aperture, in order to make the measuring light beam invisible for the subject.
- Double aperture. Two rectangular apertures separated by 4 mm fit the shape of the images of the filament. A sector wheel is placed between the double aperture and L_2 (as close to the double aperture as possible) to obtain AC modulation of the two light beams. The double aperture is placed in the focal point of the lens L_2.
- Lens L_2. This lens has a focal length of 12 cm. The light beams emerging from the two openings in the double aperture are transformed in two nearly parallel beams and directed on to the slit diaphragm.
- The slit diaphragm. This is a horizontal slit, 2 cm long and approximately 5 mm wide, placed approximately in the focal point of L_3.

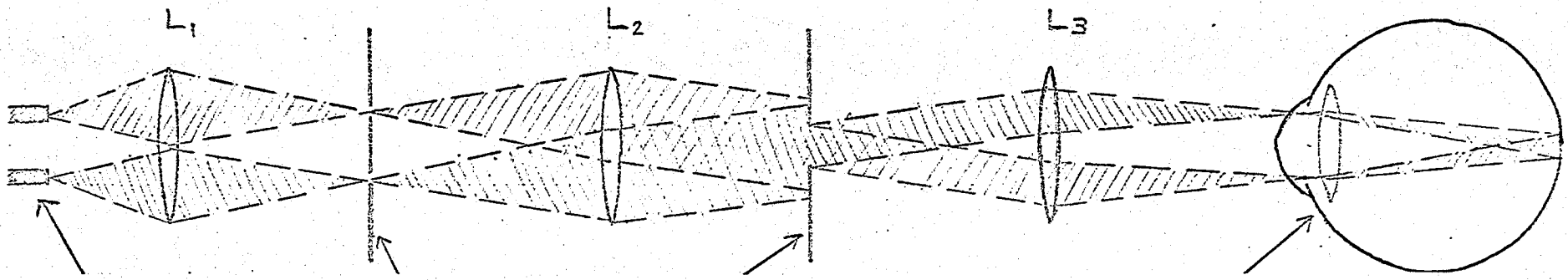

Unaccommodated eye forms sharp single image at the retina of the slit diaphragm
Accommodated eye forms unsharp double image at the retina of the slit diaphragm

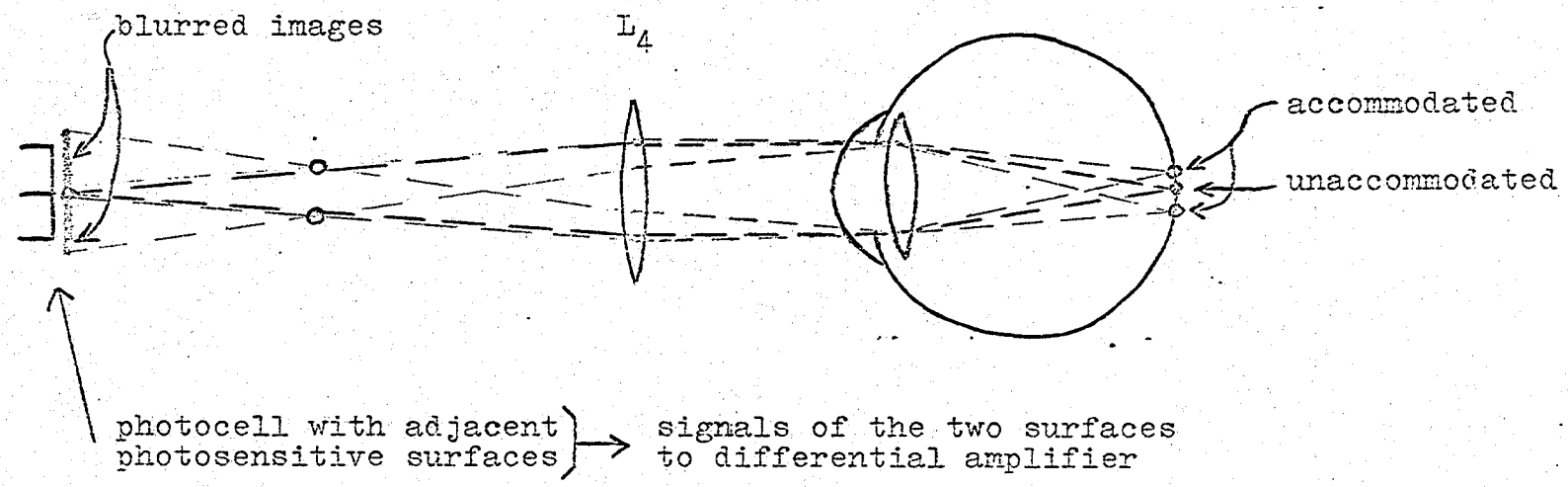

Figure 10.2

"REPRODUCIBILITY OF THE ORIGINAL PAGE IS POOR."

Suppose now that the eye is accommodated at infinity. This means that we have at the retina a single sharp image of the slit diaphragm. This image has a homogeneous illumination, coming from two spatially different light sources, i.e., the two openings in the double aperture. Suppose next that the eye accommodates. The retinal image of the slit diaphragm will become unsharp. But because of the dual illumination a separation of two retinal light distributions can be seen, as shown in Fig. 10.3. The retinal light distribution is reimaged via the eye optics and the lens L_4, and evaluated by two adjacent photosensitive surfaces, as shown in the lower part of Fig. 10.2. After this, a translation of the photocell readings into changes in dioptric power of the eye lens is straightforward.

The human pupil will, of course, limit the maximum separation of the two points where the light beams enter the eye after passing through L_3. Also, the pupil area will determine the amount of light energy falling on the photocell.

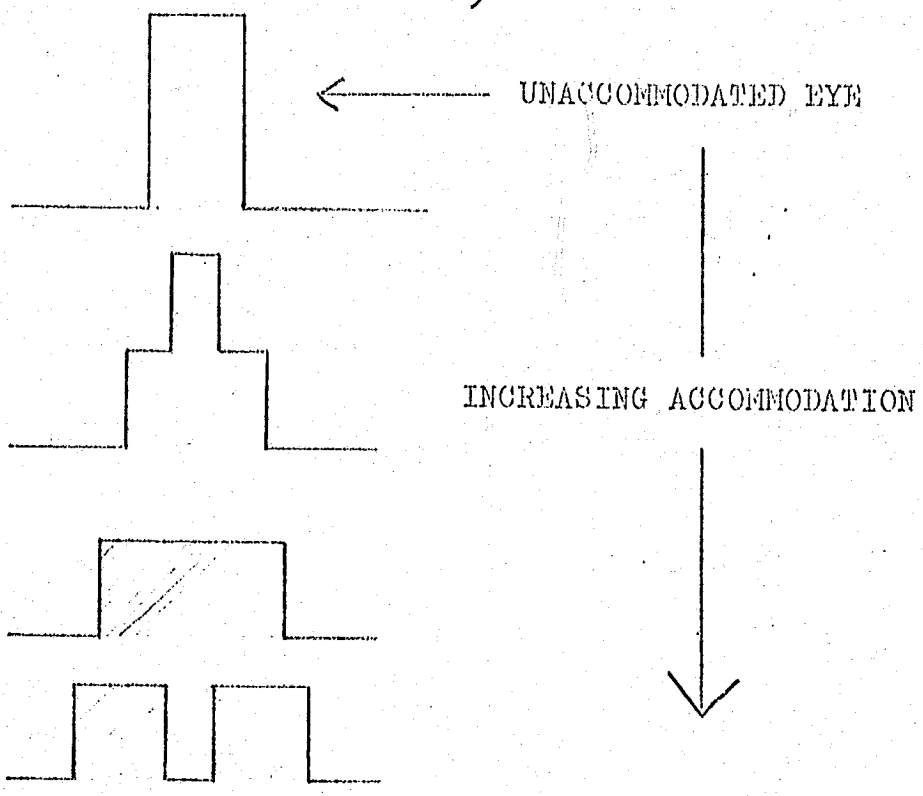

Fig. 10.3

To increase the sensitivity of the instrument, Campbell recommends the use of 1% p-hydroxyamphetamine hydrobromide. This drug takes about 20 to 40 minutes to produce pupil dilation. After this, a period of fixed dilated pupil occurs without noticeable effect on the ciliary muscle.

The equivalent noise of the instrument is about 0.05 diopters for a band-width of 0-5 cps (changes in accommodation). The minimum detectable change in refractive power is about 0.1 diopter, and fixation eye movements of up to $\pm$ 2° do not affect the signal.

2. Allen-Carter Optometer.[6] The incoming light path is shown schematically in the upper part of Fig. 10.4. The light source is imaged in the plane of the pupil by the lens L_1. A diaphragm B is placed between the light

"REPRODUCIBILITY OF THE ORIGINAL PAGE IS POOR."

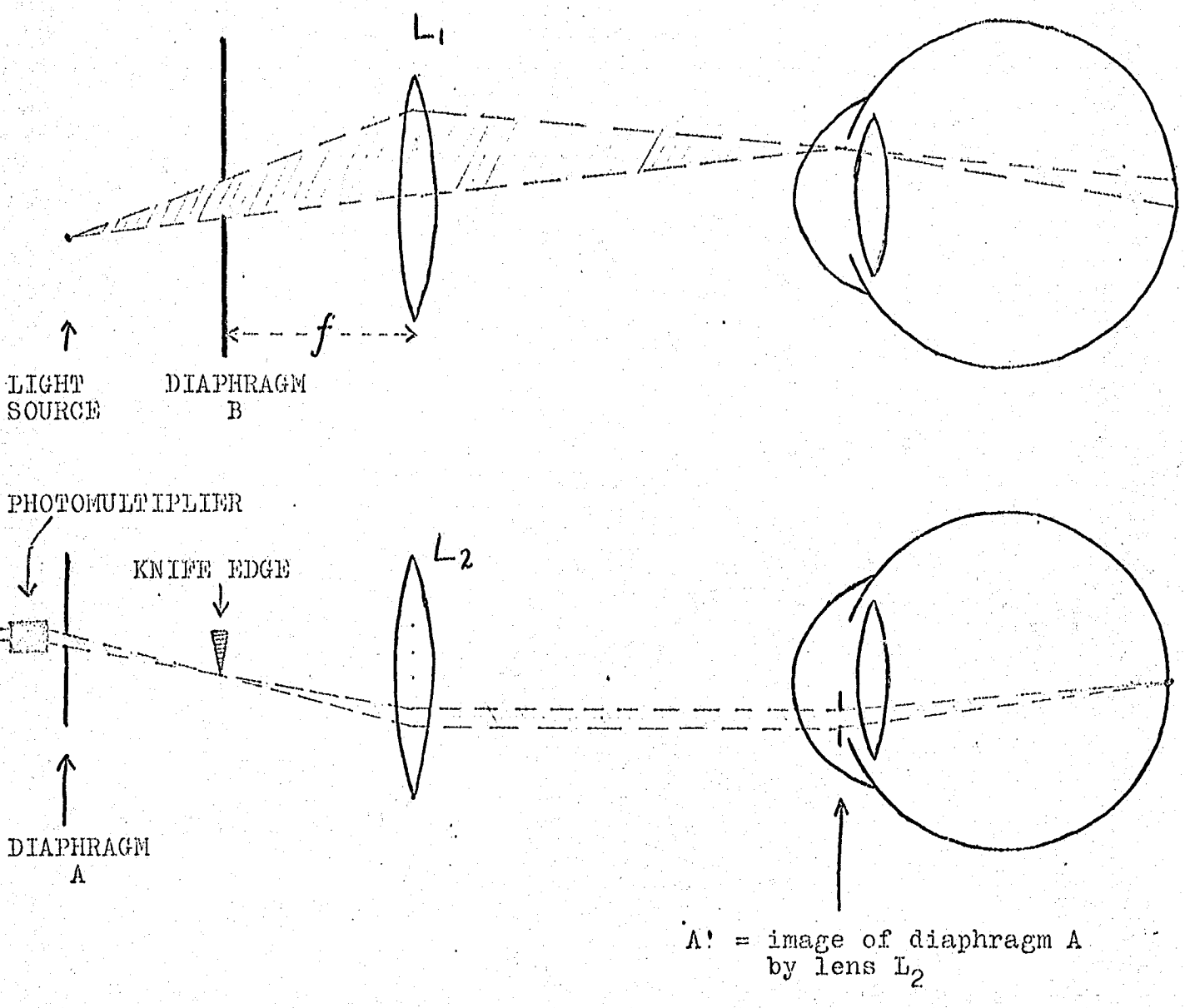

Figure 10.4

source and L_1 in the focal point of L_1. If the eye is unaccommodated, this diaphragm will be imaged in focus on the retina.

An infra-red filter is placed between L_1 and the eye, to make the measuring light beam invisible for the subject. The retinal image is in turn imaged approximately at infinity by the optical system of the eye. It is then brought into focus by the lens L_2 approximately in the plane of the knife edge, as shown in the lower part of Fig. 10.4. A diaphragm A in front of the photomultiplier tube is imaged in the plane of the pupil at A' by the lens L_2. This means that light which leaves the eye by way of area A' will pass through the diaphragm A and enter the photomultiplier tube.

Increased accommodation will bring the retinal image of the diaphragm B out of focus, but also will cause a shift downward of the image due to the excentric entrance of the light beam at the plane of the pupil. This will in turn cause a shift upward of the image on the surface of the knife edge and less light will enter the photomultiplier tube. The arrangement of the entering light beam through one point of the pupil and the outgoing light beam through the diametrically opposite part of the pupil eliminates the possibility that light reflected from the cornea will enter the photomultiplier tube.

Again in this optometer a rotating disc has been placed in the entering light beam between the light source and the diaphragm B, in order to obtain AC modulation of the measuring light beam. The basic difference between this optometer and the Campbell-Robson model can be summarized

as follows.

Instead of a dual light beam entering through two small apertures in the plane of the pupil combined with the use of the entire pupil for the outgoing light beam and a balanced symmetrical detection method, the Allen-Carter model uses one ingoing light beam through a small aperture in the plane of the pupil and one outgoing light beam through another small aperture combined with an asymmetrical detection method.

Although it is impossible to compare the two instruments on a rational basis from the rather superficial data in the literature, it looks as if the light yield and the sensitivity in the Campbell-Robson model will be somewhat higher. Also the balanced detection method looks intuitively more attractive.

3. Roth Optometer.[48] A schematic diagram of the principle underlying this optometer is shown in Fig. 10.5. The upper part of Fig. 10.5 shows a side view of the incoming light beams. Two narrow, parallel light beams form a single image on the retina of an unaccommodated eye. A prism is placed in the upper light beam, so that instead of having two images that fall on top of each other, the eye sees two horizontally displaced images. If the eye is accommodated it will see two blurred images that are vertically displaced as well. The amount of vertical displacement is an indication of the accommodative state of the eye. This displacement is measured by making a real image of the retinal plane outside

"REPRODUCIBILITY OF THE ORIGINAL PAGE IS POOR."

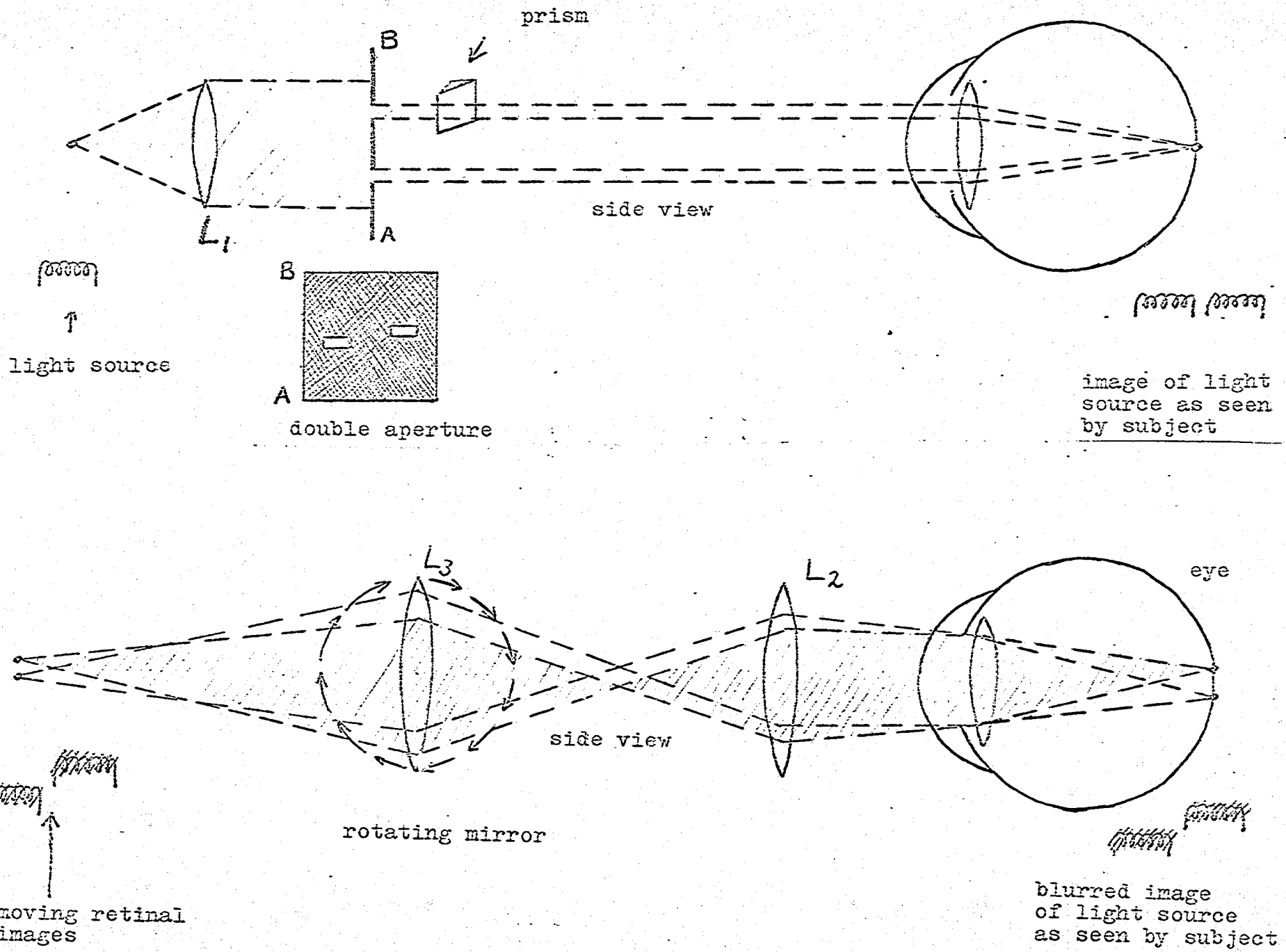

Figure 10.5

the eye with the lenses L_2 and L_3. L_3 is a rotating lens, which makes the retinal images move across a photocell array. Displacement is measured as a phase difference in two electrical signals.

Again, it is impossible to compare this optometer quantitatively with other instruments based on the available data. In an improved version of this instrument,[49] the author claims high resolution without artificial pupil dilation and insensitivity for artifacts such as eye movements, variation in light intensity of the test source, variations in pupil size, and photodetector and amplifier instabilities.

4. Elul Optometer.[20] This optometer does not differ essentially from the optometers described before. The incoming and outgoing light paths are shown in the upper and lower part of Fig. 10.6 respectively. No modulation of the infra-red beam has been used. The author states that the threshold of the system is about 0.01 diopters. However, this figure holds for the eye of the cat where the parameters that determine the sensitivity can be chosen rather favorably. The use of two balanced photocells reduces the effects of fluctuations in source intensity, and of electrical pickup of noise.

5. Warshawsky Optometer.[57] This optometer is a modification of the Campbell-Robson instrument. Photodetectors are placed directly on opposite sides of the exit slit diaphragm (cf. Fig. 10.2).

Whenever the retina and the slit are not optically conjugate, the photocells are illuminated and show a voltage whose magnitude and polarity indicate the degree and direction of the deviation from conjugacy. The slit and photocells are mounted on a carriage which position is moved by a servomotor. The servomotor is controlled by the photodetector signals in such a way that the conjugate position is restored by moving the slit away from or toward the retina. The method is a null-balance method by which the sensitivity and linear operating range are increased. In this mode, the carriage position corresponds to the instantaneous refractive power of the eye. The linear operating range, as quoted by the author, is $\pm$ 3 diopters. Static measurements are accurate to about 0.05 diopters.

b. Non-Scheiner Principle Optometers.

The previous sections have described presently known dynamic optometers using the Scheiner principle. Other optometers have been proposed and constructed that do not employ the Scheiner principle. These devices are, by definition, used to measure the accommodative state and it will be made clear in the text whether or not the optometers are dynamic.

"REPRODUCIBILITY OF THE ORIGINAL PAGE IS POOR."

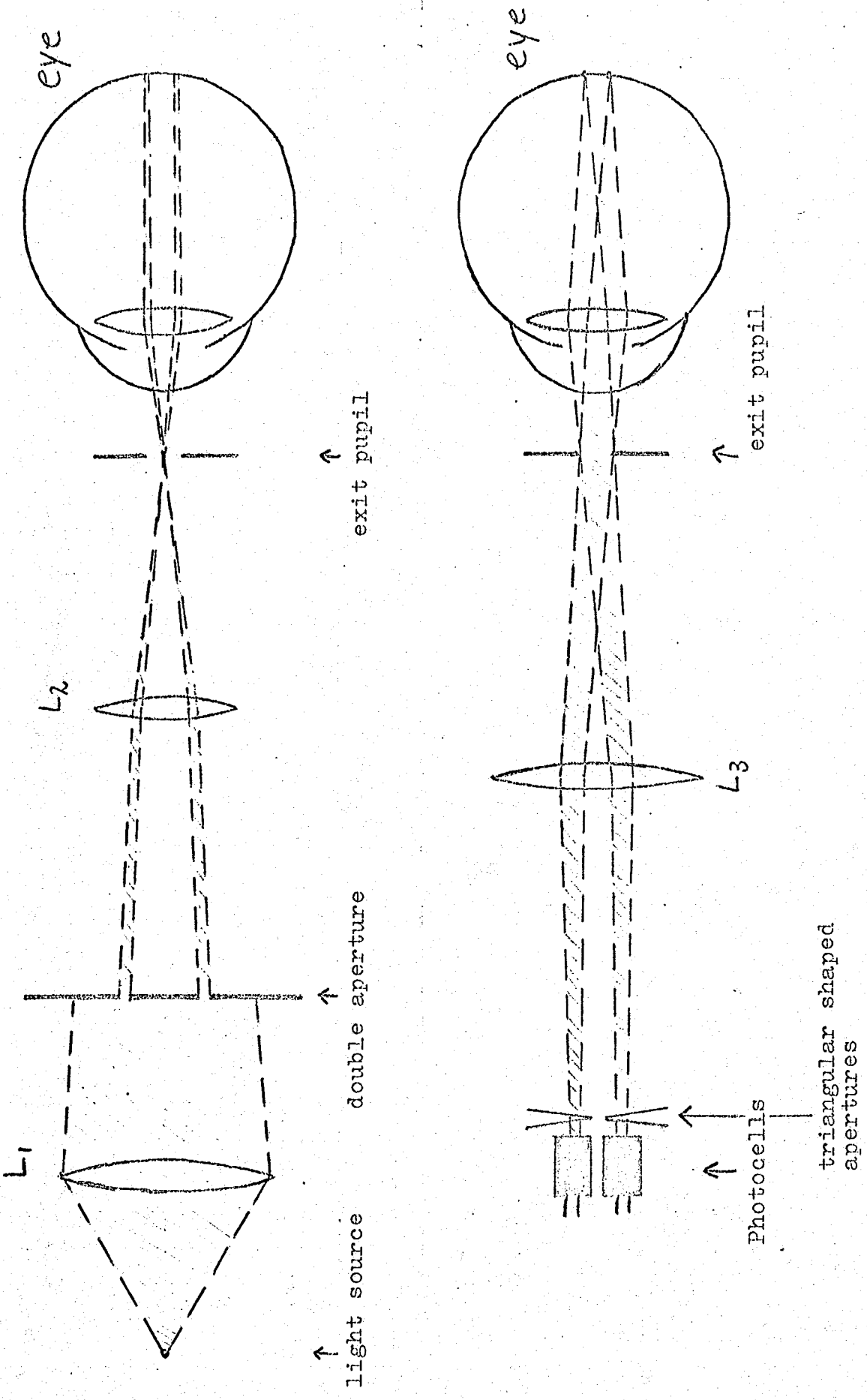

Figure 10.6

"REPRODUCIBILITY OF THE ORIGINAL PAGE IS POOR."

1. Glezer Optometer. [26] This optometer uses the principle of directing a narrow rectangular beam (slit beam) of light through the lens. The slit beam (Fig. 10.7) is aimed at the subject at about 30° horizontally from the visual axis. The magnified image of the dark field (from the front camera) is lighted by the dispersed light of the eye lens and focused on the cathode of the photo-multiplier.

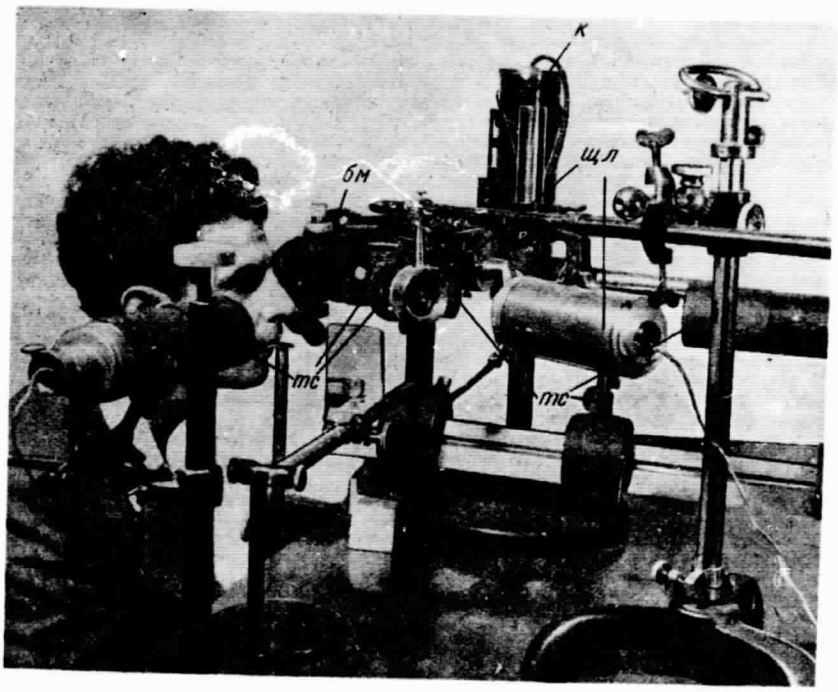

Figure 10.7: Glezer Optometer in Operation. k, photomultiplier; r, slit beam source; mc, target lenses; w, condensing lens; m, microscope.

Figure 10.7

"REPRODUCIBILITY OF THE ORIGINAL PAGE IS POOR."

During increased accommodation the front surface of the lens bulges forward and the lighted area on the photo-multiplier increases. With decreased accommodation, the opposite effect is noted. On the flat surface of the image plane of the photo-multiplier cathode there is a screen containing a slit that is 1/3 the height of the optical system image. The lens motion in the slit is magnified five times so that the proportional changes of the light beam from the lens during accommodation can be detected.

A binocular microscope is used having a working distance of 6.4 mm. One of the eye pieces is used for visual observation and the other transmits the eye lens image to the photo-multiplier. The illuminating lamp consists of a light condenser, diaphragm and moveable slit. The subject's head is fixed with the help of a tooth mold. Figure 10.7 is a photograph of the optometer in operation. Figure 10.8 is a typical response (upper trace) to a 4 diopter change in accommodation (middle trace) and the lower trace represents a 10 HZ sine wave time marking signal.

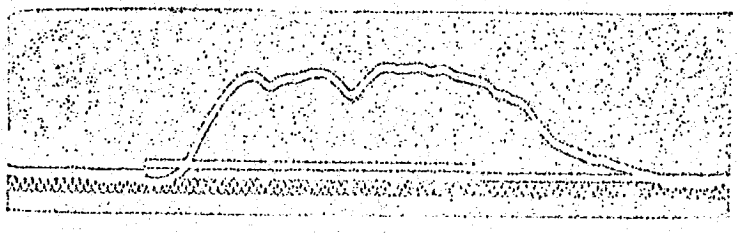

Figure 10.8: Response of Glezer Optometer. Upper trace---Lens Accommodative Response; Center trace---Four Diopter Accommodative Stimulus; Lower trace---10 HZ Sine Wave Time Reference.

No mention is made in the paper of the following points:

a) sensitivity or calibration;

b) noise levels or dynamic response;

c) relationship between output and lens power in diopters.

In view of the sketchy report, it is difficult to compare this optometer, except qualitatively, with the others constructed. In particular, no mention is made of eliminating iris artifacts or the necessity of drugging the subject's pupil reflex system.

2. Haynes, White and Held Method of Dynamic Retinoscopy. 30)

Retinoscopy refers to viewing the retina with an ophthalmoscope. Dynamic retinoscopy is a means of measuring accommodative responses without immobilizing the lenticular system. A sharply focussed spot of light is projected into the subject's eye through the pupil. Modifications in the reflected retina image are used as an index of the refractive state of the eye. These modifications are quantitatively assessed by means of lenses of known power. Refraction is measured while the subject fixates nearby objects and also while he tracks an object moving toward and away from his eye. The accommodative response is measured by briefly introducing lenses of known power in front of the fixating eye. By moving the retinoscope in depth, thereby inducing accommodative tracking, it is then determined what diopter range the subject can maintain accommodation on the target within 0.5 diopters.

Even though this process is called dynamic retinoscopy the response is not the dynamic response of the lens system but merely the lens power at a fixed value of lens accommodation. Additionally, the recording device is the operator's eye so that the measurements are subjective and are not read out on a recording device.

3. Chin and Horn Infra-red Skiascopic Measurements. [12]

The infra-red skiascope is best described with reference to Figure 10.9. The infra-red source A provides infra-red radiation which is reflected by mirror B into the

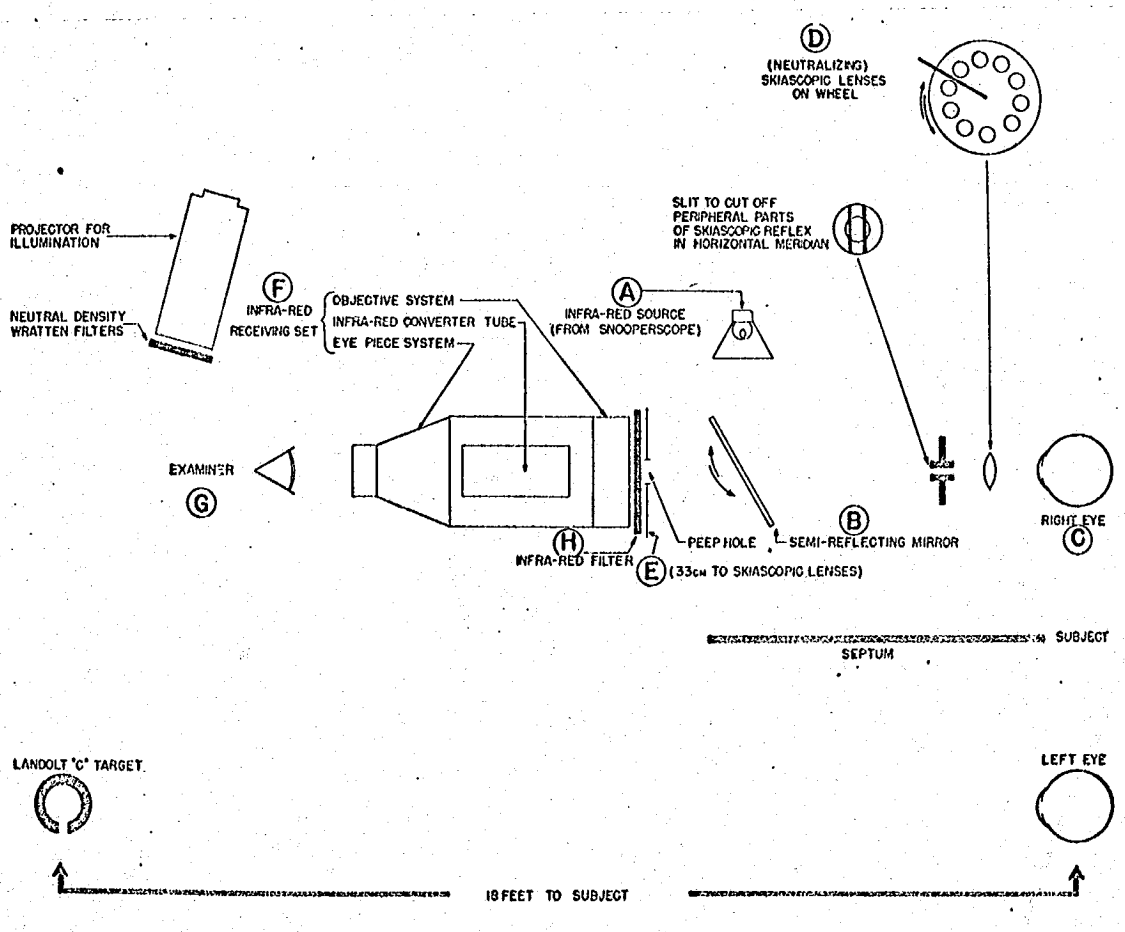

Figure 10.9: Operational schematic of Chin and Horn Skiascope.

Figure 10.9

the subject's right eye C. The retina acts as a secondary source and reflects these rays out through the optical system of the eye forming a focus whose location is dependent upon the refractive state of the eye. The invisible rays are converted by the infra-red receiving set to visible light which is presented to the examiner through the telescope eyepiece. An infra-red filter H is placed over the objective to prevent light leakage from the converter so that no light from the measuring apparatus is seen by the subject. This makes measurements possible at any controlled level of illumination.

If the outcoming focus lies in front on the pinhole E (on the side towards the subject), movement of the mirror, B, will elicit a movement of the retinal image projected at the pupil (skiascopic pupil reflex) opposite to that of the mirror; if behind the pinhole, the pupil reflex moves in the same relative direction; if the focus is at the pinhole there is neither of the above motions. Measurements are made in the horizontal meridian only. Various lenses, set on a wheel, are interposed before the right eye, C, to determine which will set the focus of the outcoming rays exactly at the pinhole. This is the neutralizing lens. The pinhole is 33 cm. from the lens wheel so that 3 diopters is subtracted from the neutralizing lens to obtain the value for correcting the refractive error of the eye. This lens power, called the skiascopic correcting lens, is the value which will

theoretically focus rays from a distant object on the retina. The distance between lens wheel and eye is Z but is a constant factor when refractive changes under various levels are compared.

The image of the retina seen projected at the pupil (skiascopic pupil reflex) is composed of rays which pass through the pupillary opening and whose vergence can be changed by accommodation. The skiascopic pupil reflex can thus be used to determine refractive changes of the eye, as defined.

As can be deduced from the above description, the skiascope is a retinoscope using infra-red light and does not measure dynamic lens motion. The accommodative state is determined subjectively by the observer by manually moving a lens wheel to a nulling lens position. No readout device is employed and the measurements are indirect since the pupil reflex is used as a measure of accommodation.

4. Fincham's Slit Lamp Photography and Coincidence Optometer [23]

In 1937, Edgar Fincham used a prototype slit lamp to photograph the human lens in cross-section. Figure 10.10 illustrates the method he used.

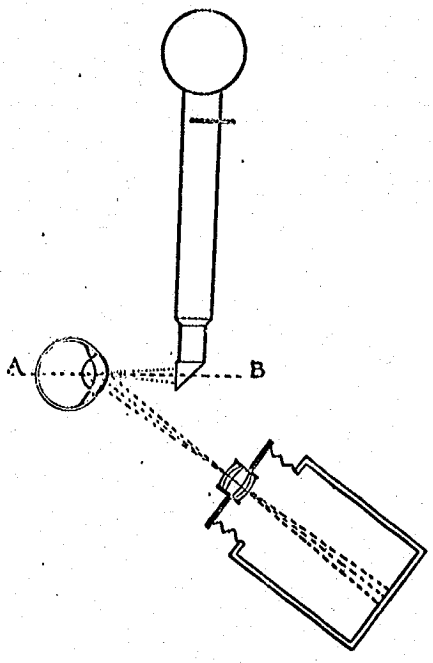

Figure 10.10: Slit Lamp Photography Technique of Fincham.

Figure 10.10

Because the greater horizontal diameter of the cornea exposed more of the interior of the eye in that meridian and also to avoid the eyelids, the photographs were made with a horizontal section of the eye illuminated instead of the usual vertical one. Illumination was made along the visual axis and the camera placed immediately below this axis directed upward to it at an angle of 35°. To have convenient space for the camera, the slit lamp was mounted in a vertical position and the light

reflected into the eye by a prism, B. The slit width was 0.2 mm., its length sufficient to cover the diameter of the cornea. To avoid uncertainty in focusing, the principle of combined focusing was employed. The camera length was fixed and the positions of the slit lamp and camera adjusted and fixed so their axes met at the common focus of the two systems. Exposures of 0.5 seconds were used with reduced camera apertures for sufficient depth of focus.

The photographs (Figure 10.11) typically obtained show the section of the cornea and lens and in the accommodated state, the ciliary processes.

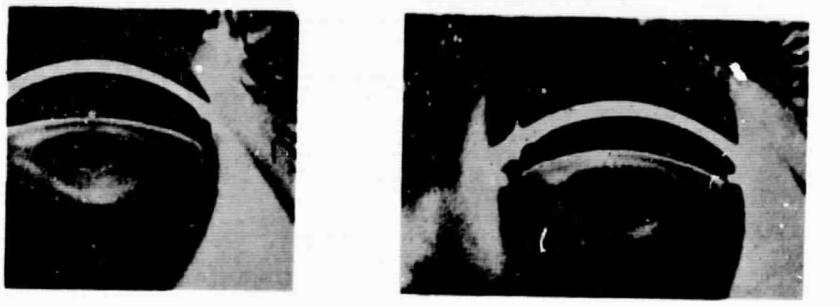

Figure 10.11: Slit lamp photographs of lens at 0 diopters (unaccommodated) and 10 diopters (accommodated).

Figure 10.12: Photograph of image seen through Coincidence Optometer.

Although the results were very helpful in primitive studies of the accommodative system, photographic techniques are limited to static accommodation levels. High speed photography of the refractive lens surfaces has not met with much success.

In addition to slit lamp photography, Fincham also developed a coincidence optometer to measure the lens refraction. By this instrument, the retinal image of a vertical line target is watched throughout an experiment and changes in the refraction of the eye are indicated by a break in the coincidence of the upper and lower halves of the line image (Figure 10.12). When the target is not in a position conjugate to the subject's retina, the retinal image is displaced from the axis. The image is viewed through a system of prisms which divides the field into two and reverses one half, so that when the image is out of alignment the halves of the line image move in opposite directions, and the setting is correct only when an unbroken line is formed. In this system the accuracy of the instrument is doubled, and the most critical method of adjustment is used--that of the alignment of a vernier. An optical fixation target is also incorporated in the instrument for the relaxation and control of accommodation. The photograph shows the appearance of the retinal image when the lens refraction differs from the instrument setting by 0.5 diopter. A difference of 0.1 diopter is discernable and the rate of change as the eye accommodates can be observed. The arrangement of the apparatus is shown in Figure 10.13. The test object O, which is at a distance of 4m. is presented to the eye by reflection at the transparent mirror M attached to the optometer.

"REPRODUCIBILITY OF THE ORIGINAL PAGE IS POOR."

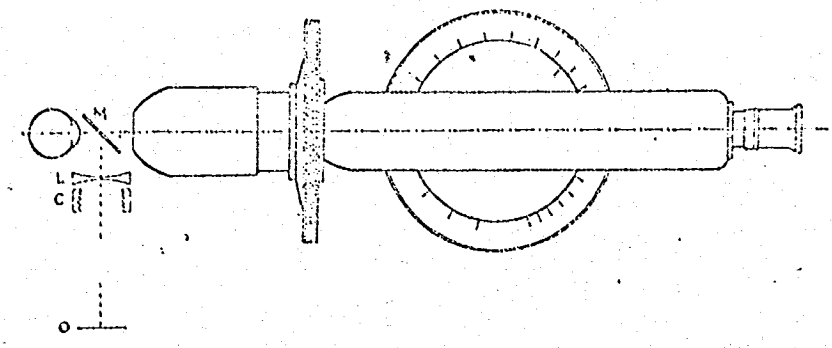

Figure 10.13: Experimental Arrangement of Coincidence Optometer.

The optometer axis is fixed 4° from the subject's visual axis. The object is a diffusely illuminated plate with a series of black dots upon which the subject's eye can focus. The lens refraction is measured about 4° from the visual axis.

The light-vergence from the object is by means of a lens L interposed between object and mirror. The change could be brought about very rapidly, and the lens, being centered on the visual axis, produces no apparent lateral displacement of the object.

No mention is made of the ultimate sensitivity or off axis noise produced by head or eye motion. However, it would appear possible to use the optometer output as a signal to light detection diodes in order to translate the disparity in coincidence into lens diopters. In this way, the coincidence optometer could be adapted to be a dynamic reading optometer. Short of building the instrument it is difficult to say how flexible it would be as a laboratory device.

"REPRODUCIBILITY OF THE ORIGINAL PAGE IS POOR."

5. Coleman and Carlin Ultra Sound Technique [13]

Ultrasonic measurements in the ocular system have been reported at least since the early '60's. The work of Coleman and Carlin is typical of presently operative ultrasonic devices. The method will be explained with reference to Figure 10.14. The system consists of a fluid stand-off column through which both light (for alignment) and sonic waves (for measurement) pass. The optical system is aligned jointly with the sonic system by means of a front surfaced mirror. The center of the optical path is pierced with a 2 mm. hole to allow sonic passage from the 10 mhz. generator and receiver. Alighment can also be checked by substituting a light source for the sonic generator, to assure the 2 mm hole is directly on the optical path.

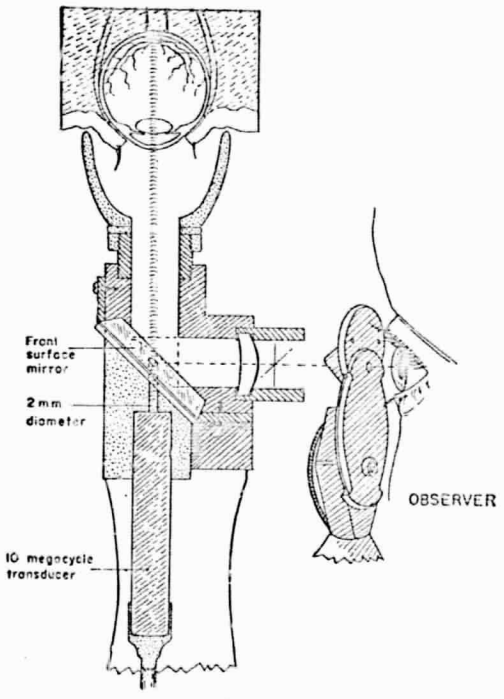

Figure 10.14: Schematic of ultra-sonic intra-ocular measurement experiment.

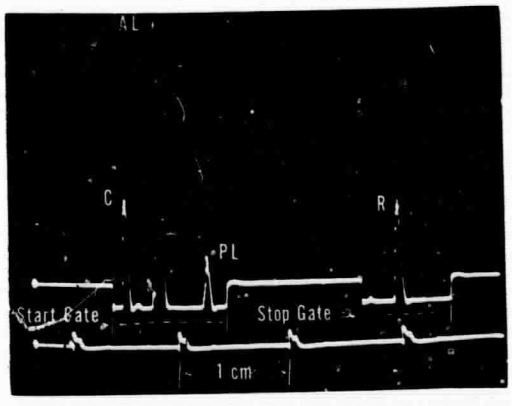

Figure 10.15: Readout trace from ultra-sonic receiver. C, cornea; AL, anterior lens capsule; PL, posterior lens capsule; R, retina.

In operation, the generator is pulsed for 0.1μs and the reflected pulses (echos) detected by the matched receiver. The echos are most pronounced at boundaries having the greatest difference in sonic propagation velocities, viz; the water-cornea and the vitreous-retina interfaces. A notable exception to this (Figure 10.15) is the aqueous-anterior lens surface boundary where the considerable lens capsule elasticity accounts for the high reflection coefficient. The posterior lens surface-vitreous boundary does not enjoy such excellent reflection, its capsule thickness being only $\lambda/70$ versus $\lambda/9$ for the anterior surface. The wavelength λ is 0.15 mm. at 10 mhz.

The display system consists of a commercial stress transducer-CRT unit with electronic clocking and gating to trigger the CRT. Knowing sonic velocities in the various ocular media allows one to calculate the intraocular distances from the velocity-time display. The sonic measurements are accurate to within 0.1 mm- or $2/3\lambda$.

As a dynamic optometer ultra-sonic devices suffer from two serious deficiencies: 1. Necessity of a dense (water or oil) media directly in contact with cornea. This minimizes flexibility and introduces serious errors through orbital deformations. 2. The media in contact with the cornea almost eliminates the 43 diopter refraction of the cornea so that targets are seen by the subject as if they were "under water." In addition, eye motions of any kind almost completely obliterate the return signal.

Presently, the ultra-sonic devices seem to be more valuable in identifying intra-ocular material parameters than detecting dynamic accommodation.

6. Laser Optometers.

With the advent of low power, inexpensive C.W. lasers, there have been recent attempts to use coherent light as a means of measuring accommodation. As outlined in Section 4, the only described modus operandi to date is that of Rigden.[46] However, there seems to be no evident way of making optometry objective. Knoll[35] used the C. W. laser much the same way ordinary retinoscopy is utilized. This means the subject is asked when the reflected light pattern stops moving as various power lenses are interposed between him and an illuminated revolving drum. Consequently the laser optometer is non-dynamic and subjective.

Table 10.1 summarizes the conclusions derived concerning the non-Scheiner optometric methods discussed.

METHOD	RANGE (DIOPTERS)	DYNAMIC	READOUT	CALIBRATION
Slit Lamp Optometers (Glezer)	4	Yes	Oscillograph	None Performed
Dynamic Retinoscopy (Haynes et al)	10	No	None	Known Power Lens Comparison
Skiascopy (Chin and Horn)	10	No	None	Known Power Lens Comparison
Coincidence Optometer (Fincham)	10	Yes	None	Known Power Lens Comparison
Ultrasonics (Coleman and Carlin)	10	No	CRT	Calculation Based on Known Propagation Velocities
Laser Optometer (Knoll)	2	No	None	Subjective

TABLE 10.1

Comparison of Optometric Methods Discussed in the Text.

In summary, the total number of instruments in the U.S.A. to measure dynamic changes in accommodation is of the order of five. Most of these use the Scheiner principle to measure accommodation and are highly specialized laboratory models. This is probably one of the reasons that useful data for analysis of the control aspect of the accommodative system are scarce or not available.

SECTION 11

11. THE MULTIVARIABLE NATURE OF ACCOMMODATIVE TRACKING.

The preceding literature reviews concerning optometers have dealt only with one variable of accommodative tracking viz; changing of the power of the lens. In reality the so-called "near reflex" involves the changing of at least three important analog variables. These are the lens power, the pupil diameter and the vergence rotation of the eye. This section will derive a systems-theoretic model of the eye in accommodative tracking and present the interactions of the three above variables in determining the seeing state. The systems model will show how the previous discussions on ocular physiology, retinal sensitivity, physiological and physical optics enter into controlling the seeing state of the eye.

a. Physical Basis for a Systems Model - The Lens Loop.

The physiological fragmentation of the system has already been presented (see Fig. 5.1 of Section 5). Also, most of the equations and the rationale for a systems model have already been presented. Consequently, in the sequel, detailed derivations will be excluded when they have been previously performed and only the appropriate references made.

As already described, when an object to be kept in focus changes position, three observable analog variables (excluding gross head and body motions) change in order to maintain a sharp image on the most sensitive part of the retina. If the object comes nearer to the person the eyes converge nasally, the pupil becomes smaller (contracts) and the lens changes shape to increase its focusing power. The opposite state pertains when an object recedes. For simplicity in the

following discussion only target (the object to be focused) position changes on the optical axis (a line perpendicular to the cornea and concentric with the pupil) will be considered. This means the accommodatively stimulatedeye maintains a fixed position. Therefore the model will describe the pupil and accommodative state in one eye; that being the one on whose optical axis the target is changing position, and the vergence of the opposite eye. Let D_T be the distance (in diopters) measured from the cornea of the stimulated eye to the target. D_T can take on values from 0; target infinitely far from the eye, to infinity; target right at the cornea. Let D be the instantaneous value of the dioptric power of the lens. It has already been shown (Section 5) that approximately $20 \leq D \leq 30$ diopters so that the dynamic range of D is + 10 diopters. If B represents the diameter in mm. of a uniformly intense blur circle on the retina and P is the diameter of the pupil in mm., then it has been shown (Eq. 4.3, Section 4) that

$$B = 0.018P\ (D_T - D) \qquad \text{Eq. (11.1)}$$

Where D and D_T are in diopters. B is defined as positive when $D_T > D$, i.e., the eye is under accommodated and the image is focused behind the retinal plane and negative for the obvious opposite condition. Equation (11.1) is based on geometrical optics and predicts zero blur when $D_T = D$. In reality experimental evidence shows that $B \neq 0$ when $D = D_T$ but that finite blur occurs from the non-geometrical effects of diffraction and light scattering (see Fig. 7.3, Section 7).

Therefore, Equation 11.1 must be modified to account for actual blur in regions of small $D_T - D$. The amount of non-geometrical blur depends on the pupil size (see Fig. 7.3). It will be assumed that the half power points of the blur distributions in Figure 7.3 serve as an adequate measure of non-geometrical blur. Since 11.1 is a linear equation in $D_T - D$ the non-geometrical blur enters this equation as a dead band (dependent on P) of blur. By considering all of the distributions of Figure 7.3, it can be shown that this dead band, a, depends on P according to

$$a = -0.04\ P + 0.44 \qquad \text{Eq. (11.2)}$$

where a is in diopters for P in mm.[37] It is now possible to construct the first stages of the system. If e_D is the dioptric error with deadband accounted for then B_D, the blur with dead band, will be the output of the block diagram of Figure 11.1.

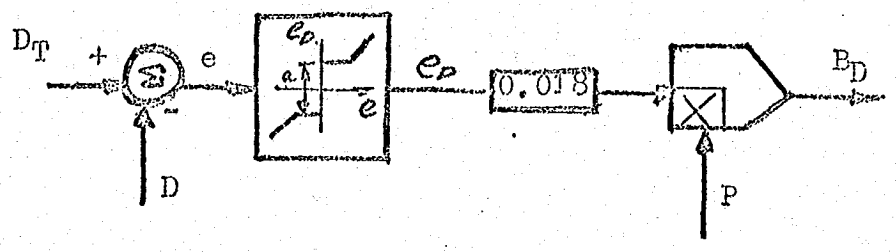

Figure 11.1 Block Diagram Representation of Human Accommodative Tracking System Error Detector.

It was also shown that the retina without additional clues cannot distinguish between positive or negative blur (c.f. even error experiment, ref. 53) so that the multiplier of Figure 10.1

is followed by an absolute value device. (See Figure 11.2). However, because of the multivariable input nature of accommodation, it has been shown (c.f. page 1, section 7) that there are many possible clues the subject may detect, e.g., motion, parallax, aberration, etc. (See Table 7.1, Section 7) that will give him the sign of the blur. These clues usually depend on memory to be effective and are of a reflex nature more than voluntary. In the systems model, any one of these clues can restore the sign to the blur or, equivalently, by-passthe absolute value box in the block diagram. The overall effect of these memory processed clues can be represented functionally in the block diagram as an "or" gate controlling a bypass gate around the absolute value box. An "or" gate is an appropriate representation since astigmatism or motion or any of the clues in Table 7.1 can restore the sign of the blur to the lens controller.

Up to this point, nothing has been said about the predictability of the target motion. Whether or not the subject can gather enough information from past experience to enable him to draw conclusions about the future time course of the target is a very important point in deriving the systems model. If the target motion is a step whose onset is random then experiments show a pure transport delay in the accommodative response. If, on the other hand, the target motion is, for example, a fixed frequency square wave, then experiments show the subject can easily, often in three or four cycles, predict what the future motion will probably be and responds

with zero (or even) negative transport delay.[43] Consequently, the main feedforward path transport delay times are variable depending at least on the past time course of the input signal D_T. Functionally, this feature of the delays can be represented as a memory and input signal controlled transport delay whose numerical delay time is a function of the past input signal time course and memory. Memory as used here denotes any time $t' < t$ where t is the present value of the system independent variable. After passing through the feed forward transport delays, TD_1 and TD_2, the feedforward signals act upon the lens system actuator which is anatomically referred to as the ciliary muscle (See Fig. 11.2). At this point, it is assumed the signals have already been converted from an analog blur circle diameter on the retina to a nerve pulse train whose repetition rate is related to the blur circle diameter. Such an assumption seems reasonable but as yet is not experimentally verified. This conversion process takes place after the absolute value block in the systems model and anatomically is probably performed by the photoreceptors of the retina. Of course, the pulse trains leaving the retina will have been extensively processed by the retina and high visual centers so that the pulses reaching the ciliary muscle are not precisely those leaving the retina. Without going into minute detail, let it be said the ciliary muscle can be considered to be a digital (pulse trains) to analog (muscle tension) converter of a highly nonlinear nature.[43] The non-linearity manifests itself primarily in ciliary muscle damping

"REPRODUCIBILITY OF THE ORIGINAL PAGE IS POOR."

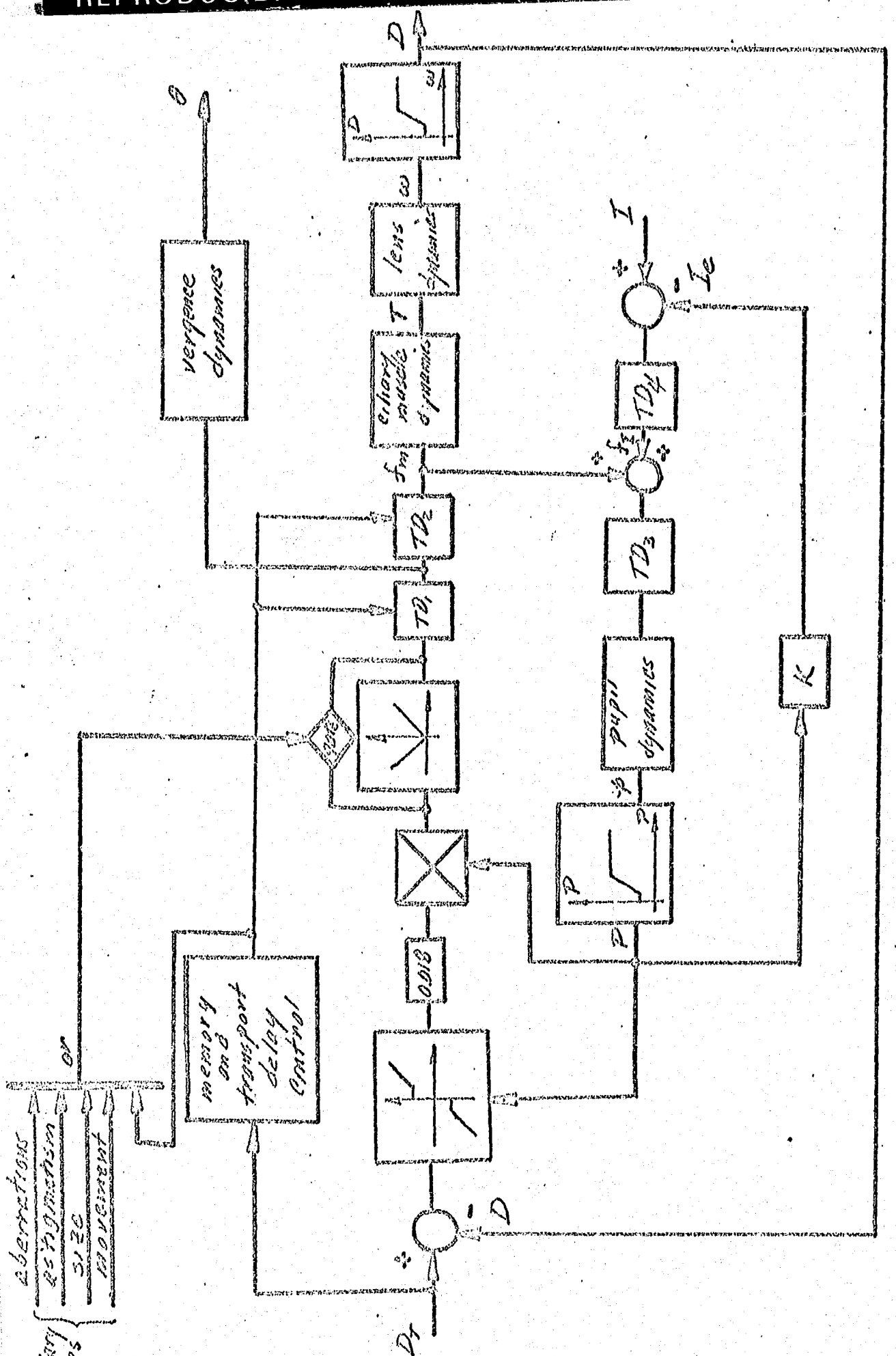

Fig. 11.2

and elasticity. For present purposes the muscle dynamics will be represented as a box with a pulse train input followed by a pulse repetition rate to muscle tension converter. The muscle dynamics are nonlinear, approximately first order and driven by the converter output tension. The muscle tension acts upon the next block which is the lens dynamics. Lens dynamics can also be shown to be approximately first order and nonlinear with the nonlinearity resting primarily in the lens damping.[43] The purpose of the mechanical action of the ciliary muscles on the lens is to change its shape. The relationships between the lens geometrical dimensions and its subjective diopter power is easily measured with a slit lamp optometer. Using the optometer and the theory presented in (42) it can be shown that lens diopters, D, is related to the position of the front surface of the lens w, by

$$D = 16.6\ W + 20$$

when w is measured from the lens anterior surface at 0 diopters and where D is in diopters for w in mm. This relation completes the lens loop begun in Figure 11.1.

b. The Pupil Loop and Variable Interactions.

One of the input variables to the accommodative loop is the pupil diameter P which enters through Equation (11.1). Physically the pupil contracts when one focuses on near objects and dilates for objects more distant. It does this with a transport delay between accommodative stimulus and pupil response which is 100 ms. longer than the accommodative transport

delay. This additional 100 ms. transport time is not changed by other accommodative clues or memory because it represents the pupil acting as a pure reflex system i.e., it cannot be activated voluntarily. Therefore, it is reasonable to take its error signal after the second feedforward transport delay. The pupil diameter also responds to changes in illumination in addition to its accommodatively generated inputs. It does so with a constant transport delay of 280 ms. The illumination induced pupillary response represents a closed control loop within a control loop with pupil diameter, P, as output and illumination level I as one of the controlling inputs. Thus, an additional pupil feedforward transport delay precedes the pupil dynamics. The pupil dynamics arise from the muscles controlling its diameter; the dilator and sphincter pupillae. Being smooth muscle like the ciliary muscle, these pupillae have nonlinear dynamics somewhat similar to the ciliary muscle.[43] The detailed dynamics will not be derived here but suffice it to say theyexhibit nonlinear damping and are second order. The pupil also exhibits a saturating nonlinearity as a function of illumination intensity. This saturation arises because the pupil diameter cannot exceed the range of 2 to 8 mm.

c. Accommodative Convergence - An Open Loop.

When focusing a near object the eyes move nasally in order to keep the target field of interest positioned on the fovea. In the case being considered the target is always on the optical axis of the viewing eye so that this eye need

not converge. The opposite eye does converge, however, and its angle of rotation θ is measured positive nasally from straight ahead gaze. Experimentally, convergence is seen to proceed after a maximum transport delay of 180 ms. Being a voluntary system, the convergence transport delay, like the accommodative delay, is input time history and memory variable. Therefore, its feedforward transport delay is less than that for D and is variable. The muscle dynamics of the convergence system are the same as those used in ordinary horizontal tracking movements since the same muscles are employed. These dynamics have been shown to be nonlinear and fourth order.[14] Unlike the pupil and accommodative systems, however, a definite feedback mechanism has not been firmly established anatomically or functionally for the convergence system. This means the output angle θ of this system has little if any feedback around it for stabilization. Experimentally, it is observed that accommodative convergence, as evidenced by θ, is quite erratic and drift prone almost as though the feedback, if it exists, is intermittant.[43] It should be emphasized, however, that most of the experimental evidence for an open loop convergence system arises from monocular experiments where only one eye is converging. In these experiments, it appears that any system feedback available is A.C. coupled. For systems analysis purposes, the experimental evidence of eye tracking experiments and experiments designed to stimulate the convergence system accommodatively point to an open loop system that is rapid in response, drift prone and very dynamically unilateral.

d. The Block Diagram Representation of the Accommodative, Pupillary and Convergence Systems for On-Axis Stimulation.

We are now prepared to complete the block diagram initiated in Figure 11.1 for the three systems considered. The block diagram illustrates very well the multivariable input and output nature of the overall systems. Figure 11.2 is the block diagram illustrating the systems interconnections and Table 11.1 serves as a legend for interpreting the variables and blocks and gives the probable anatomical location of the blocks The signal processing done by the various parts of the systems model are relatively straightforward except for the memory and transport delay control and the processing performed on the accommodative clues necessary to restore the sign to the blur signal. The memory and transport delay control can be represented functionally as a device capable of extracting from the input signal any low level repetitive behavior and acting upon this information to change the system transport delays. Low level implies the device is limited to recognizing fundamental frequencies in the input signal and using this knowledge to predict future input time behaviour. As an experimental example, subjects have been able to begin tracking a fixed frequency square wave with a transport delay of 280 ms and reduce this delay to zero in 3 or 4 cycles.[43] However, when presented with a frequency modulated square wave no delay reduction is noted.

Block	Input & Output Variables	Variable or Block Definition	Probable Anatomical Location
Memory & Transport Delay Control	D_T, Nerve Firing Rates	Target Position in Diopters	Brain and Retina
"or" Gate	Auxiliary Clues "o" or 1	Described in Fig. 11.2	Brain and Retina
Gate	"0" or "1", "on" or "off"	"on" implies blur sign "off" implies no blur sign	Brain Retina
Convergence Dynamics	Nerve Firing Rates, θ	Angle or Rotation Measured "+" nasally.	Consensual Eye
TD_4	Pulse Trains as Inputs and Outputs. f_I	Transport Delay Constant = 180 ms.	Retina & Pupil Muscles
TD_3	Pulse Trains as Inputs and Outputs	Transport Delay Constant = 100 ms.	Ciliary Ganglion & Pupil Muscles
Pupil Dynamics	Nerve Firing Rates, P	P = non-limited pupil diameter	Dilator and Sphincter Pupillae
Pupil Limiter	p, P	Non-limited and Limited Pupil Diameter	Pupil
K Constant	P, I_e	Pupil Diameter and Illumination Error	Pupil

TABLE 11.1

Block	Input and Output Variables	Variable or Block Definition	Probable Anatomical Location
Dead-Band	From Fig. 11.1 e_1 e_D	Diopter Error, Diopter Error With Deadband	Retina
Multiplier	.018 e_D .018 $e_D^p = B_D$	Diopter Error with Deadband. Pupil Diameter	Retina
Absolute Value	B_D $/B_D/$	Deadband Blur Absolute Value of Deadband Blur	Retina
TD_1	Pulse Trains as Input and Output	Transport Delay (Variable)	Higher Brain Centers
TD_2	Pulse Train Input, Ciliary Muscle Ennervation Rate Output f_m	Transport Delay (Variable)	Ciliary Muscle
Ciliary Muscle Dynamics	f_m T^m	Ciliary Muscle Ennervation Rate. Muscle Tension per Unit Length	Müller's Muscle, radial and meridional fibers.
Lens Dynamics	T, W	Muscle Tension Per Unit Length. Anterior Lens Surface Displacement	Lens
Lens Limiter	W, D	Lens Displacement, Lens Dioptric Power	Lens

TABLE 11.1 Continued

The gate bypassing the absolute value block can be activated by any one or all of the various accommodative clues shown on the memory control. The most dominant auxiliary accommodative clue seems to be change in target size. If the natural blur is accompanied with an increase in size the subject will increase his lens diopters and vice versa. Change in target size alone will not stimulate accommodation. If any one of the auxiliary clues are present the absolute value is bypassed and the blur sign restored.

A detailed analysis of the systems model represented by Figure 11.2 goes beyond the scope of this report; however, its derivation is considered to embody most of the present knowledge concerning the physiological systems involved. In order to test the model, experimental responses from human subjects must be obtained and compared with a computer simulation of the model. Such a procedure would enable one to identify more precisely the various parameters of the interacting loops. In this regard, with an experimental means of measuring 0, P and D experiments could be devised to interrupt certain loops in the system in order to determine accurately individual responses deprived of certain variable interactions. As an example, an artificial pupil could be placed in front of the subject's eye, thereby clamping P at the artificial pupil diameter, and experiments conducted to compare dynamic responses with and without interacting pupil dynamics.

SECTION 12

12. THE NEED FOR AN OPTICAL STATUS TESTER.

Throughout the previous presentation, especially as regards quantitative experimental data, a glaring lack of sufficient instrumentation necessary for developing a realistic model of the System considered is apparent. This is probably because of the passive interest of the engineering society in biomedical engineering until the later half of this decade. The instrumentation answer for the accommodative system, we feel, is embodied in an Optical Status Tester which would fulfill the needs outlined below.

a. Immediate Need.

The systems development embodied in Section 11 is perhaps the most sophisticated and realistic model of the accommodative tracking system presented to date. It illustrates well the multivariable nature of this process and how experimental measurements on only one variable at a time will only suffice to give information about one component of the interacting ocular triad of D,Θ, and P. Such experimental knowledge is of limited practical importance because any conclusions derived are predicted on speculated behavior of the other ocular components. If this quantitative knowledge, such as displayed by the systems block diagram of Figure 11.2 is to be verified while accounting for the known interactions, it is imperative that a device such as an Optical Status Tester be made available. An Optical Status Tester would be a device capable of measuring at least the ocular triad of accommodation, vergence and pupil diameter. Concisely, the immediate needs for an Optical Status Tester are:

1) to perform experiments necessary to verify and identify a systems model derived from physiological, optical and past experimental considerations.
2) to perform experiments on human subjects and compare these results with those of a systems simulation revised on the basis of the experiments in 1).
3) to prepare the way for a more sophisticated Optical Status Tester that would be capable of monitoring the ocular triad for both eyes simultaneously. This would be a significant step toward in-flight Optical Status Monitoring.

b. Future Need.

Presently, there does not exist a commercial supply for one component (the optometer) of an Optical Status Tester; let alone a complete OST itself, although such a device is within the technological abilities of our society. In the future, if some practical engineering knowledge about human optical status is to be gained at least two points must be considered:

1) as outlined in 3) above; ideally the ocular state vector of D, θ and P would be extended in scope to include both eyes in a normal binocular mode of operation. Even more realistically the OST could be used to extend the ocular triad itself. This means the ocular triads would be expanded to include position components that fix the eyes relative to some spatial reference. With a tried and tested monocular OST as a starting point, such extension could be realistically undertaken.

2) In all of the preceding discussion, it has been tacitly assumed that the experimenter would have explicit control of the environmental conditions the subject is placed in. To the present time standard operating procedures call for testing a well-trained subject in normal room conditions. The only significant stimulations are those shown as inputs in Figure 11.2. Realistically, however, the optical status is most important when the subject's present and future environment depends in part on his optical status itself. It is not too unreasonable therefore to envision other inputs than those of Figure 11.2. Considering the system of Figure 11.2 momentarily, it seems quite reasonable to ask how the parameters of this system vary with environmental temperature, G loadings, spin rates, etc. Such questions have not as yet been answered, not because they are not important or have never been asked, but due to a lack of the pertinent instrumentation.

SECTION 13

13. MISSION ORIENTED APPLICATIONS

Mission oriented applications are to be considered under two categories. The first concerns screening and selection procedures of flight personnel under normal test procedure conditions and the second under simulated and actual in-flight conditions.

a. Normal Conditions

Normal conditions imply one g acceleration, room temperature, undrugged subject, zero vibrations and in general the person to be tested is subjected to no extraordinary environmental conditions. Under these conditions the following testing procedures could be performed with an optical status tester (OST):

1. Amplitude Predictable Accommodation Performance

In this test the subject is presented with a target moving randomly on the optical axis of the test eye while the other eye is occluded. The random target motion would be in the form of steps of target position for which the subject would know beforehand the amplitude but not the time of step onset. In this way the subject would not be able to predict when the target was going to move so that the full latency of his accommodation mechanism would be revealed in the (OST) accommodation channel record. It would obviously be necessary to have some standard of latency to which a given subject's performance is to be compared. It would be necessary therefore to test a large group of normal flight personnel to establish this standard. With the OST such a standard could be obtained quite simply. Present standards are found only in research oriented literature covering a very small number of subjects.9,51)

The immediate value of knowing accommodation latency for possible flight personnel is obvious. This number is the minimum amount of time the subject can possibly bring to focus an object that moves in an unpredictable manner. For example, if a pilot is suddenly made aware of another aircraft in his immediate vicinity then we know from the above test procedure the minimum time he would be expected to be able to bring the craft into focus. Apparently it would be desirable to have personnel with minimal accommodative latencies.

2. Sign-Unpredictable Accommodative Performance

It has been shown by several workers that the accommodative system when presented only amplitude changes of accommodative stimulations cannot distinguish in which direction the amplitude has changed.[52] However, there appears to be a tendency for subjects, when deprived of the amplitude sign information, to favor one accommodative level to others.[15,58]

In the proposed test procedure the direction (sign) of the target position change and the time the target position changes will not be known to the subject. All other test conditions are as in 1. above. The target will move in a step-wise fashion but the direction, amplitude and time of movement will be made random. It is immediately obvious from the accommodative records when the subject makes a direction-incorrect accommodation movement of his lens. Based on these records a statistical analysis can produce a probability distribution relating the probability of correct

accommodative movement relative to the amplitude of the stimulus presented. Additionally, the most probable accommodative status during a time of subject confusion will be obtained. This test procedure could also very possibly reveal a correlation to the accommodative level assumed by the subject when presented empty visual fields.[11)]

3. Accommodative Clue Sensitivity

It has been known for several decades that subjects can use clues other than image blur as indications of accommodative stimulation.[21)] How sensitive a subject is to these various clues is a measure of his ability to focus objects that move randomly and present no sign information in their blurred images. It would be advantageous to have flight personnel who could restore the sign information in the blur signal utilizing the minimal amount of auxiliary clues.

To make such a sensitivity test the target stimulus would be varied in the following ways:

1.) Different wavelengths of target illumination--monochromatic cluing.

2.) Off-axis target motion--horizontal motion cluing.

3.) Off-axis target motion--vertical motion cluing.

4.) Target size changes--apparent size cluing.

5.) Variable target illumination intensities--luminosity cluing.

6.) Variable target aberration--aberration cluing.

Each of the above variations would be tested on the subject to determine how long (number of trials) it takes him to utilize the clue (if at all) as a key to correct accommodative effort. In all other respects the test procedures would be as 1.) and 2.) above. In this way one could determine which subject is the most sensitive to the amount of information presented. Presumably the best subject could correctly accommodate with the minimal amount of information concerning the target presented.

4. Relative Pupillary Response Test

In this test both accommodation and pupil diameter of the subject are recorded in response to stimuli of the form presented in test 1.) above. The pupil serves as an accommodative error modulator and can critically alter the rise time of accommodation and even the steady state accommodative amplitude.[43,47]

As has been shown previously (see Section 11) the dead band in accommodation depends critically on the pupil diameter and in general a larger dead-band gives rise to accommodative and pupillary oscillations. These in turn can deteriorate visual acuity especially as pertains visual field details.

5. Near-Reflex Performance Test

This performance test is a relatively routine test to determine the dynamic response of the three ocular variables; vergence, accommodation and pupil diameter. The dynamic responses of a normal test group should be determined a priori

as a standard for latencies, rise-times etc. With this standard the many important variables of the dynamic ocular reflex could be studied quantitatively.

b. Simulated and Actual In-Flight Conditions

The normal conditions-testing procedures produce valuable information concerning the dynamic responses of personnel in a normal environment. As such these tests could be used to select personnel for a variety of duties that would not require of them any above average seeing ability. Of more importance however are quantitative test procedures on personnel of whom it is required to maintain a certain minimal optical status under abnormal conditions; specifically, in-flight conditions.

1) Variable g Conditions Tests

In these tests the acceleration of the subject is varied to simulate the range of g loadings encountered during a particular mission. Typically, this range might be from zero to three or four times g with the direction of the acceleration vector also made variable. Of particular interest is the response of the accommodative system under such conditions. Quantitative test procedures of this system under variable accelerations are almost non-existent and yet there is ample evidence to expect a significant change in performance with variable loading. This is because the lens is an elastic body suspended by an elastic system. The suspensory forces are known to vary from zero to 1.5 grams per mm. circumference during the normal accommodative range.[42)]

When the lens is fully accommodated it is almost a freely floating body and it would be expected to be most susceptible to external loading in this condition.

Ideally the accommodative system should be tested with acceleration an operator-controlled variable both in magnitude and direction. Since the verging consensual eye would also experience the various loadings, it would be possible to simultaneously record its performance under variable acceleration.

The variable acceleration could possibly be obtained both from centrifuges and arcing aircraft which would also necessitate using the OST under these conditions.

2) Vibration Condition and Angular Velocity Tests

If the subject's head and/or body are subject to vibrational movement then the lens and its controlling mechanisms are also. The g loading tests above are an important special case of vibrations. In the vibrations conditions test it would be possible to ascertain the effects of vibration on the suspended lens and also determine the useful function of the systems during external vibrational influences. Just as in the g loading tests, there is sufficient reason to expect significant performance changes in accommodation when external vibrations are applied. In particular, experimental studies have shown the lens dynamics of certain persons to have a resonant frequency of vibration from 1.5 to 4 hertz.[51] When excited at these frequencies the lens can be seen to oscillate with an amplitude that is as much as 35% greater than its excursions at lower frequencies.

Another series of tests of interest would be performed with the subject experiencing angular rotations about his three axes of rotation. It has been known for many years that angular velocities other than zero affect the accommodative system through its interaction with the vestibular control system. [19] The vestibular system maintains the spatial reference of the human being and in so doing probably generates the reference for the accommodative control system. The tests to be undertaken would subject the person under test to constant angular velocities while monitoring the lens, pupil and vergence variables in response to accommodative stimuli. The target to be focused would be moving with the same angular velocity as the subject so that it would always appear to be on his optical axis. Such test conditions simulate to a good approximation the conditions found in a rotating space-craft or airplane with the on-board instruments being represented by the target to be focused.

3) Illumination Test Procedures

The accommodative system has been shown to be of the interacting type. [43] Specifically the iris acts as an error signal modulator where the error signal is the retinal image blur. The iris (or pupil) diameter responds dynamically both to accommodative stimulation and illumination level changes. [55] Therefore the pupil has two dominant inputs in any accommodative experimental situation.

This implies that accommodative performance can be influenced through the pupil system by illumination changes in the environment. To determine a quantitative way these

accommodative influences the subject focuses on a target that is situated on the optical axis of one eye while the other (consensual eye) is stimulated with light of various wavelengths and intensities. Since both pupils respond when either is photically stimulated the pupil of the eye from which the lens is being monitored will dilate or contract in response to the illumination changes. In this way the effect of illumination level on accommodative response can be studied. Such information would be valuable in determining the best accommodative-performance illumination level for in-flight cabins, cockpits or even on-ground work environments requiring good accommodative status. Since the controlling muscles of the lens system are easily fatigued it is important to make the environment (where practical) as conducive as possible to good optical performance. One of the easiest controlled and yet often the most neglected environmental condition is illumination. If the illumination tests show a definite quantitative improvement in accommodative performance, the results certainly would have wide application.

SECTION 14

14. CLINICAL IMPORTANCE OF NEAR REFLEX VARIABLES.

In this section the clinical implications and applications of the ocular reflex variables are outlined in the context of present medical literature. As will become obvious in the text, development of adequate instrumentation for measuring the dynamic near reflex is paramount for utilizing these variables diagnostically.

The three ocular variables of the near reflex are

a) Lens accommodation: Dynamic deformation of the lens as it changes dioptric power to follow target stimuli.

b) Pupil diameter: Dynamic diameter changes of the pupil to either luminance or accommodative stimuli.

c) Consensual vergence: Dynamic angular rotations of the consensual eye to accommodative stimulations.

These variables are strongly dependent on each other, although very little is known about the system relations between the various interactions. Also, the variables depend on other inputs such as illuminance, fused binocular image, etc. The general tendency of these near reflex responses is to optimize the image quality and position on each retina for a wide variety of target positions, so that the subject perceives binocularly a single fused image of minimal blur and sharpest detail.

Clinically, the near reflex variables are of importance because they are ideally suited to serve as performance criteria in testing and monitoring procedures. Numerous defects exist or develop in many persons, and the ophthalmologist or neurologist utilises some of the most advanced physical and engineering principles to establish the exact nature of these

"REPRODUCIBILITY OF THE ORIGINAL PAGE IS POOR."

defects. On the other hand, the development and instrumentation of corrective mechanisms has advanced towards new technical achievements.

We will now give some examples of the clinical importance or utilization of certain aspects of the near reflex variables.

Lens Accommodation

a) Presbyopia is known as the condition in which persons are unable to focus sufficiently to perform normal "near" work. This defect is strongly dependent on the age of a person and becomes increasingly frequent for the older age groups. Some data obtained by Duane [16], using a subjective blur criterion, are shown in Fig. 14.1

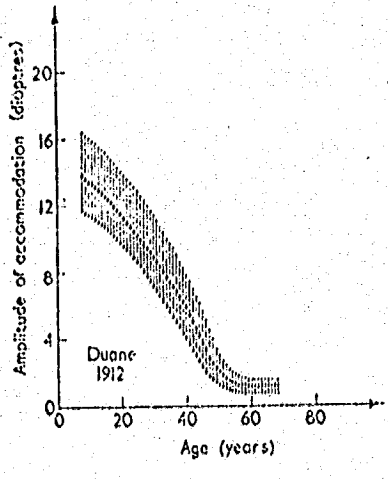

Mean and upper and lower limits of the reciprocal of the near point of accommodation at various ages, according to the measurements of Duane (1912).

Figure 14.1

Since in any subjective blur criterion the depth of focus as experienced by the subject plays an important role, the ordinate of Fig. 14.1 is difficult to relate to amplitude

"REPRODUCIBILITY OF THE ORIGINAL PAGE IS POOR."

of accommodation. Therefore, an objective determination of similar data was given by Hamasaki et al.[29], showing that the amplitude of accommodation for any age group is 1.5-2 diopters smaller than similar values obtained with subjective measurements.

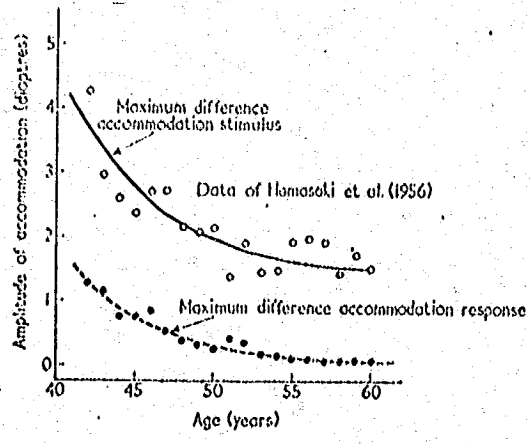

Mean values for the maximum amount the dioptric power of the eye can increase (filled circles) for various ages according to the data of Hamasaki *et al.* (1956). The open circles represent near-point determinations by the push-up method in the same population sample.

Figure 14.2

It is important to note here that what is measured objectively is the static accommodation only. Up to now there is no data available to show how the dynamic accommodation varies with age. One generally assumes that lenticular sclerosis is the main cause for presbyopia. By this is meant the increase in weight, volume, specific gravity, thickness, and rigidity of the lens fibers, and a decrease in elasticity of the lens capsule.

Obviously, presbyopia will change the dynamic equation governing the motion of the lens.

b) Myopia refers to the inability of a person to relax his accommodation enough to focus sharply for "far distance" objects. It can have various causes, like abnormal length of eye axis, high convexity of cornea or lens surfaces, or abnormal index of refraction of some of the eye media. Typically, myopia amounts to 1 diopter but can be as high as 20 diopters in some cases. There again, little is known about associated dynamic defects.

An interesting form of myopia is found under special viewing conditions that may occur frequently during space and flight missions. One form is the empty field myopia which means that persons exert on the average 0.5 diopters of accommodation when viewing an empty visual space; in other words, objects at a distance of 2 meters will be in focus on their retinas (Whiteside [58]). A very similar form of myopia is night myopia, in which case the empty field is produced either by the absence of light or the reduction of the light level to prevent any detail in the visual field to act as an accommodative stimulus. A review of night myopia is given by Knoll [36].

Besides the two deficiencies in accommodation just mentioned, there are numerous other difficulties a person can have (and often has) to obtain a clear and undistorted image on the retina for an appreciable range of object distances (hyperopia, astigmatism, etc.). A vast amount of instruments

have been designed to measure and distinguish the various types of deficiencies, and to correct and restore image quality.

Pupil Diameter

The pupil is an important factor in establishing a certain depth of focus and in maintaining a comfortable retinal illumination. If blur is the error signal to the accommodative control system, the pupil diameter plays a significant role in the determination of the final value of this error signal (Cf. Eq. 4.3, Section 4). However, most ophthalmologists and neurologists are satisfied when the pupils are round and equal, of average size, and show a normal reaction to light and near vision.

The following quotation from a report by Lowenstein[40] illustrates the clinical importance and usefulness of the dynamic pupil reaction to light:

"Pupillary disturbances as found in syphilitic and other infections of the central nervous system, in multiple sclerosis, tumors or traumatism to the brain, in degenerative diseases of the brain, in primary simple glaucoma, or in damage to peripheral pupillary pathways, lead to a large variety of deviations from the normal reflex pattern. They escape observation with the unaided eye but are distinctly characteristic in pupillographic records. Each of the pathological pupillary reflex shapes is the expression of damage at a specific site within the centers or pathways of pupillary control. Therein lies their value for topical diagnosis."

Because the nervous centers and pathways involved in the control of the pupil diameter are fairly well known, abnormalities in the pupillary reaction can often be identified and localized in relation to specific pathological processes. As another practical application, the behavior of the pupil as an aid in determining the depth of narcosis can be mentioned. Also, the pupil diameter depends on psychological influences and can be an indication of fatigue, attention, excitement, mental load, etc. At the moment only qualitative data is available on these influences, but increasing research efforts attempt to relate the data to intelligence, problem difficulty, interest, etc.

The pupil is known to react on accommodation stimuli (Cf. Fig. 11.2) and presently experiments are being carried on to determine the dynamic relation between lens diopters on one side (measured with dynamic optometer) and pupil diameter on the other side.

Consensual Vergence

In its most obvious form, consensual vergence response occurs when a target is moved on the optical axis of one eye, while the other eye is occluded. The occluded eye will rotate inwards or outwards, depending on whether the accommodation is increased or decreased. This rotation is usually referred to as accommodative vergence, and especially the accommodative convergence to accommodation ratio (AC/A) has gained clinical interest and is considered a valuable diagnostic measurement.

"REPRODUCIBILITY OF THE ORIGINAL PAGE IS POOR."

One would like to measure exactly the ratio between the innervations to accommodative convergence and accommodation. At the present time this is not possible with the available techniques. However, Alpern et. al. 7) have shown that under certain conditions a linear relationship exists between accommodation-stimulus, accommodation-response, and accommodation vergence. The AC/A ratio is quantified if, for example, the amount of accommodative convergence associated with a unit change in the refraction of the eye has been determined. This is what is called the response AC/A ratio. Clinically, it is difficult to measure the response AC/A ratio for it needs measuring of the refraction of the eye when the accommodation-stimulus is changed. Therefore, often the amount of change in accommodative convergence per unit change in the accommodation-stimulus is measured, and is referred to as the stimulus AC/A ratio.

Figure 14.3 shows the distribution of the stimulus AC/A ratio in the population, while Figure 14.4 shows that the stimulus AC/A ratio is rather independent of age.

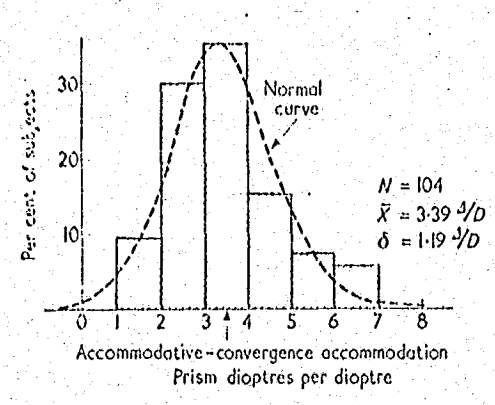

Distribution of stimulus AC/A in the population as measured by fixation disparity methods. (Data from Ogle and Martens, 1957.)

Figure 14.3

"REPRODUCIBILITY OF THE ORIGINAL PAGE IS POOR."

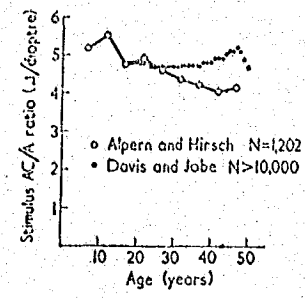

Stimulus AC/A as a function of age as obtained by two different methods. (Alpern and Larson, 1960.)

Figure 14.4

A number of studies have been devoted to the effect of drugs on the AC/A ratio. Figure 14.5 shows an example of the effect of alcohol on the stimulus AC/A ratio.

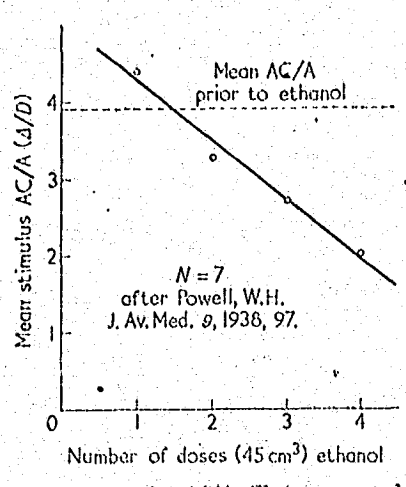

Effect of alcohol on stimulus AC/A (Data computed from the experiments of Powell, 1938.)

Figure 14.5

Summarizing, we can say that the dynamic relation between the various variables in the block diagram of Figure 11.2, are all clinically significant, but only in a limited number of cases do we know anything quantitative about these relationships. This is summarized in Table 14.1.

NEAR -REFLEX VARIABLE	STIMULUS	PRESENT STATUS OF RESEARCH	CLINICAL APPLICATIONS
Pupil	1. Light	1. Has extensively been investigated. Transfer function fairly well known. Ongoing research in nonlinear modelling.	1. Drug influences, Central Nervous System action, Psychological Influences.
	2. Accommodation	2. Presently being investigated and modelled (nonlinear)	2. Unknown
	3. Vergence	3. Presently being investigated and modelled (nonlinear)	3. Unknown
Accommodation	1. Target distance (blur)	1. Has been extensively investigated and modelled (Ref. 51,52,55,15)	1. Corrections for static deficiencies in the accommodation system
	2. Vergence	2. Presently being investigated	2. Unknown
Vergence	1. Accommodation	1. Has been extensively investigated in the static case (AC/A ratio) and the dynamic case (Ref. 8)	1. Static AC/A ratio is clinically an indication of many ocular disorders. Also drug influences. No clinical application of the dynamic accommodation/ vergence relationship at the present time.
	2. Image fusion in binocular vision	2. Has been extensively investigated and modelled (Ref. 45,59)	2. Training procedures (squint, cross-eyed vision)

Table 14.1

REFERENCES

1. Adler - Physiology of the Eye, p. 251, Mosby Co. (1959).

2. Adler - Physiology of the Eye, p. 254, Mosby Co. (1959).

3. Adler - Physiology of the Eye, p. 261, Mosby Co. (1959).

4. Aksola, A. - Observation on the Depth Resolution on Ultrasonic Examination of the Eye, Acta Ophthal., 40, 1962.

5. Allen, M. - American Journal of Optometry, 26, 279, 1949.

6. Allen, M.J. and Carter, J.H. - An Infra-Red Optometer to Study the Accommodative Mechanism, American Journal of Optometry 37, p. 403-407, 1960.

7. Alpern, M.; Kincaid, W.M. and Lubeck, M.J. - Vergence and Accommodation III Proposed Definitions of the AC/A Ratios, American Journal of Ophthalmology 48 (No. 1, pt 2) p 143-148, 1959.

8. Brodkey, J. and Stark, L. - Feedback Control Analysis of Accommodative Convergence, American Journal of Surgery, 114, 1967.

9. Campbell, F.W.; Robson, J.G. and Westheimer, G. - Fluctuation of Accommodation Under Steady Viewing Conditions, Journal of Physiology, 145, p. 579-594, 1959.

10. Campbell, F.W. and Robson, J.G. - High-Speed Infra-Red Optometer, Journal Optical Society of America 49, p. 268-272, 1959.

11. Campbell and Primrose, -The State of Accommodation of the Human Eye in Darkness, Journal of Physiology, 116, 1952.

12. Chin, H.B. and Horn, R.E. - Infra-Red Skiascopic Measurements of Refractive Changes in Dim Illumination and in Darkness, J. Opt. Soc. Am., 46, 1956.

13. Coleman, D. and Carlin, B. - A New System for Visual Axis Measurements in the Human Eye Using Ultra Sound, Archives of Ophthalmology, 77, January, 1967.

14. Cook, G. and Stark, L. - Derivation of a Model for the Human Eye-Positioning Mechanism, Bull. of Math. Biophysics, 29, 153-173, 1967

15. Crane, H.D. - A Theoretical Analysis of the Visual Accommodation System in Humans, NASA Report NAS2-2760, 1966.

16. Duane, A. - Normal Values of the Accommodation at all Ages, trans., Ophth. Amer. Med. Ass., 383-391, 1912.

17. Duke-Elder - System of Ophthalmology, Vol. II, p. 311, Mosby Co., St. Louis (1961).

18. Duke-Elder - System of Ophthalmology, Vol. II, p. 312, Mosby Co., (1961).

19. Duke-Elder - Textbook of Ophthalmology, The Octavus System, Mosby Co., (1949).

20. Elul, R.; Marchiafava, P.L. and Nicotra, L. - Method for Measurement of Accommodation in the Cat, Journal Optical Soc. America, 54, p. 380-386, 1964.

21. Fincham, E.F. - The Mechanism of Accommodation, British J. of Ophthalmology, Supplement VIII, 1937.

22. Fincham, E.F. - The Accommodation Reflex and its Stimulus, British j. of Ophthalmology 35, pp. 381-393, 1951.

23. Fincham, E.F. - The Fincham Coincidence Optometer, British J. of Physiological Optics, 10, p. 179-187, 1937.

24. Fry, G.A. - Blur of the Retinal Image, Ohio State University Press,(1955).

25. Fry, G.A. - The Image-forming Mechanism of the Eye, Handbook of Physiology-Neurophysiology I, p. 659, American Physiological Society,(1959).

26. Glezer, V. - Photoelectrical Recording of the Accommodative Reflex, Fizial, Zhur 41, p. 830-831, 1955.

27. Goldmann, V. Graefes, Arch. Ophth., 122, p. 198 (1929).

28. Gullstrand - Appendices to Part I of Helmholtz -Physiological Optics, Dover Publications (1962).

29. Hamasaki, D.; Ong, J. and Marg, E. - The Amplitude of Accommodation in Presbyopia, Amer. J. of Optometry, 33, 3-14, 1956.

30. Haynes, H.; White, B.; Held, R. - Visual Accommodation in Human Infants, Science, 148, April, 1965.

31. Helmholtz - Physiological Optics (1924), Dover Publications (1962).

32. Hubel, D.H. and Wiesel, T.N. - Receptive Fields, Binocular Interaction and Functional Architecture in the Cat's Visual Cortex, J. Physiol. 160, p. 106-154, 1962.

33. Ivanoff, A. - Les Aberrations de L'Oeil, Revue d'Optique, 1952 (Paris).

34. Jansson, F. - Measurements of Intraocular Distances by Ultra Sound, Acta Ophthal., Supplement 74, 1963.

35. Knoll, H.A. - Measuring Ametropia With a Gas Laser, American J. of Optometry, Vol. 43, p. 415-418, July, 1966.

36. Knoll, H.A. - A Brief History of "Nocturnal Myopia" and Related Phenomena, Amer. J. of Optometry, 29, 69-81, 1952.

37. Krauskopf, J. - Light Distribution in Human Retinal Images, J. Optical Soc. America 52, p. 1046-1050, 1962.

38. Leary, G. - Ultra Sonographic Measurement of the Components of Ocular Refraction in Life: I. Technical Considerations, Vision Research, 3, 1963.

39. Lettvin, J.Y.; Maturana, H.S.; McCulloch, W.S. and Pitts, W.H. - What the Frog's Eye Tells the Frog's Brain, Proc. I.R.E. 47, p. 1940-1951, 1959.

40. Lowenstein, O. - Pupillography, Method and Diagnostic System Exhibit, U.S. Department of Health, Education and Welfare.

41. McCulloch - Trans. Amer. Ophth. Soc., 52, p. 525, 1954.

42. O'Neill, W. and Doyle, J. - A Thin Shell Deformation Analysis of the Human Lens, Vision Research, 1968.

43. O'Neill, W. - An Interacting Control Systems Analysis of the Human Lens Accommodative Controller, Int. Federation on Automatic Control, Erivan, Armenia, U.S.S.R, October, 1968.

44. Polyak, S. - The Vertebrate Visual System, University of Chicago Press (1957).

45. Rashbass, Westheimer - Disjunctive Eye Movements, J. Physiol. 159, p. 149-170, 1961.

46. Rigden, Gordon - The Granularity of Scattered Optical Moser Light, Proc. I.R.E. 50, p. 2367-68, 1962.

47. Ripps, H.; Chin, N.; Siegel, I. and Breinin, G. - The Effect of Pupil Size on Accommodation, Convergence and the AC/A Ratio, Investigative Ophthalmology, February, 1962.

48. Roth, Niles - Recording Infra-Red Coincidence Optometer, Am. J. Optometry 39, p. 356-361, 1962.

49. Roth, Niles:-Automatic Optometer for use with the Undrugged Human Eye, Rev. Scientific Instruments 36, p. 1636-1641, 1965.

50. Salzmann - Anatomy and Histology of the Human Eyeball, translated by E.V.L. Brown, Chicago,(1912).

51. Stark, L.; Takahashi, Y. and Zames, G. - Nonlinear Servoanalysis of Human Lens Accommodation, IEEE Transactions on Systems Science and Cybernetics, Vol. SS C-1, No. 1, 75-83, 1965.

52. Stark, Takahashi - Absence of an Odd-Error Signal Mechanism in Human Accommodation, IEEE Int. Convention Record Part 6, 1965.

53. Stark and Takahashi - Absence of an Odd-Error Signal Mechanism in Human Accommodation, IEEE Transactions on Biomedical Engineering (No. 3-4) p. 138-146, 1965.

54. Stark, Takahashi, Zames - Biological Control Mechanisms: Human Accommodation as an Example of Neurological Servomechanism, in Theoretical and Experimental Biophysics, Vol. 1, p. 129-65, Marcel Dekker, Inc., New York,(1967.

55. Troelstra, Zuber, Miller and Stark - Accommodative Tracking a Trial-and-Error Function, Vision Research, Vol. 4, p. 585-599, 1964.

56. Vos, J.J. - On Mechanisms of Glare, Ph. D. Dissertation, State University, Utrecht, The Netherlands, 1963.

57. Warshawsky, J. - High Resolution Optometer for the Continuous Measurement of Accommodation, J. Optical Soc. America 54, p. 375-379, 1964.

58. Whiteside, T.C. - The Problem of Vision in Flight at High Altitude, Pergamon Press, London,(1957).

59. Zuber, B.L. and Stark, L. - Dynamical Characteristics of the Fusional Vergence Eye Movement System, to be published in IEEE Transactions on System Sciences and Cybernetics.